

UNIVERSITY OF THE  
FREE STATE  
UNIVERSITEIT VAN DIE  
VRYSTAAT  
YUNIVESITHI YA  
FREISTATA



The *in vitro* effects of *Moringa oleifera* on chaperone-mediated autophagy  
in human HepG<sub>2</sub> liver cancer cells

by

Matlola Abel Bopape

Submitted in fulfilment of the requirements for the degree of

Master of Medical Science (Physiology)

in the

Department of Basic Medical Sciences

School of Biomedical Sciences

Faculty of Health Sciences

University of the Free State

Supervisor: Dr Claudia Ntsapi

Co-supervisor: Dr Charlette Tiloke

**Submitted on the 26<sup>th</sup> of July 2023**

## DECLARATION

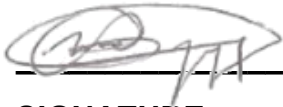
I hereby declare that this work, submitted for the degree Master of Medical Science (Physiology) at the University of the Free State, is my original work and has not previously been submitted to any other institution of higher learning for degree purposes or otherwise. I further declare that all sources cited or quoted are indicated and acknowledged in a comprehensive reference list. Copyright hereby cedes to the University of the Free State.

Matlola A. Bopape

Name and Surname

26/07/2023

Date

A handwritten signature in black ink, appearing to read 'Matlola A. Bopape', is written over a horizontal line.

**SIGNATURE**

## **DEDICATION**

I dedicate this degree to my parents, Anna Bopape and Mashilo Mathew Bopape. No one has supported me more than you have. Even when you didn't fully understand why I wanted to pursue this, you still gave up everything to ensure that I could further my studies. None of this would be possible without you. This degree is my thank you note to you.

## TABLE OF CONTENTS

	Page
DECLARATION	i
DEDICATION	ii
ACKNOWLEDGEMENTS	vii
PUBLICATION	viii
PRESENTATIONS	ix
LIST OF FIGURES	x
LIST OF TABLES	xiii
LIST OF ABBREVIATIONS	xiv
ABSTRACT	xix
INTRODUCTION	1
CHAPTER 1: Introduction	1
1.1. Arrangement of the thesis	1
1.2. Introduction	2
1.3. Problem statement	5
1.4. Research rationale	7
1.5. Aim of the study	8
1.6. Research study questions	8
1.7. Objectives of the study	8
1.8. Methodology	9
1.9. Value of the study	10
CHAPTER 2: Literature review	12
2.1. Hepatocellular carcinoma	12
2.2. HCC in sub-Saharan African countries	12

<b>2.3. HCC risk factors</b>	<b>13</b>
<b>2.4. The molecular mechanisms implicated in HCC progression</b>	<b>15</b>
2.4.1. Autophagy pathways	16
2.4.2. The CMA pathway	18
2.4.2.1. <i>The regulation of LAMP2A dynamics at the lysosomal membrane</i>	20
2.4.2.2. <i>The role of the lysosomal mTORC2/PHLPP1/Akt signalling axis in CMA</i>	21
2.4.2.3. <i>The dual role of CMA</i>	23
2.4.2.4. <i>Modulators of CMA activity</i>	26
2.4.2.5. <i>Chemical modulators of CMA activity</i>	27
2.4.2.6. <i>Chemical modulation of CMA by retinoic acid derivatives</i>	28
2.4.3 The effects of ATRA on cancerous cells	29
2.4.3.1. <i>The effects of ATRA in HCC</i>	30
2.4.4. The role of CMA in HCC	32
<b>2.5. Treatment options for HCC</b>	<b>33</b>
<b>2.6. The use of <i>Moringa oleifera</i> in HCC treatment</b>	<b>36</b>
2.6.1. Apoptosis	40
<b>CHAPTER 3: Materials and Methods</b>	<b>46</b>
<b>3.1. Description of study design</b>	<b>46</b>
<b>3.2. Materials</b>	<b>47</b>
<b>3.3. Procedures and experimental techniques</b>	<b>47</b>
3.3.1. Culturing of human HepG <sub>2</sub> cancer cells	47
3.3.2. <i>Moringa oleifera</i> aqueous leaf extract preparation	48
3.3.3. Inhibition of CMA activity	50
3.3.3.1 ATRA preparation	50
3.3.4. Assessment of cell viability	50

3.3.5. Human HepG <sub>2</sub> cell experimental treatment groups	52
3.3.6. Assessment of apoptosis markers	53
3.3.7. Assessment of CMA markers	54
<b>3.4. Statistical analysis</b>	<b>63</b>
<b>CHAPTER 4: Results</b>	<b>64</b>
4.1. Introduction to results	64
4.2. Cell viability	64
4.3. The assessment of cell death markers	67
4.4. The evaluation of basal CMA activity	69
4.5. The assessment of basal CMA markers by western blotting	70
4.5.1. Preliminary western blot results	71
<b>CHAPTER 5: Discussion</b>	<b>74</b>
5.1. Introduction to discussion	74
5.2. Discussion	76
<b>CHAPTER 6: Study conclusions, limitations, and future recommendations</b>	<b>86</b>
6.1. Introduction	86
6.2. Conclusion	86
6.3. Recommendations	89
6.4. Limitations	91
<b>References</b>	<b>93</b>
<b>Appendices</b>	<b>118</b>
<b>Appendix A</b>	<b>118</b>
<b>Appendix B</b>	<b>122</b>
<b>Appendix C</b>	<b>129</b>
<b>Appendix D</b>	<b>131</b>

**Appendix E**

**134**

**Appendix F**

**136**

## **ACKNOWLEDGEMENTS**

I would like to acknowledge the following people that have helped me complete this project:

**My parents:** Thank you for all you have sacrificed for me to further my studies. Your undying support and patience as I went through this journey have motivated me immensely. Thank you.

**My supervisory team:** Dr Claudia Ntsapi and Dr Charlette Tiloke. Thank you for being patient and present from the beginning to the end. You have not only taken the time and energy to equip me with the skills required to complete the project, but you have also helped me develop myself beyond this degree. Thank you.

**My peers:** Mr Songezo Vazi and Ms Mbasakazi Saki. Your undying support, encouragement and assistance are one of the main reasons I completed this project. Thank you.

**The Department of Basic Medical Science, University of the Free State:** Thank you for all the support and assistance offered during the course of the project.

**The Department of Human Molecular Biology, Department of Chemical Pathology, and the Department of Haematology and Cell Biology:** Thank you for allowing me to use your facilities.

**Funders:** The National Research Foundation (NRF), Avacare Health and the UFS First-Year Research Master's Bursary. Thank you for the financial support that has made it possible for me to further my studies. Mr Gerhard van Deventer, thank you for the lab coat. Your kindness and generosity are something I aim to pay forward one day.

A special thank you to Khomotso Maake. Thank you for all your support and encouragement even before I began this degree.

## PUBLICATION

Literature review manuscript:

**Bopape, M.**, Tiloke, C., Ntsapi, C. 2023. *Moringa oleifera* and autophagy: Evidence from *in vitro* studies on chaperone-mediated autophagy in HepG<sub>2</sub> cancer cells.

In production - accepted for publication in the journal of Nutrition and Cancer on 23-Aug-2023 (Manuscript ID: N&C-11-22-6324.R4) (see Appendix F for confirmation of acceptance email).

## **PRESENTATIONS**

- 1) Presented at the Department of Human Molecular Biology Unit – Haematology and Cell Biology (University of the Free State, Faculty of Health Sciences) Student and Staff Academic Forum Meeting (on the 18<sup>th</sup> of July 2023).
- 2) Presented at the Department of Basic Medical Sciences (University of the Free State, Faculty of Health Sciences) Medical Talks meeting (on the 8<sup>th</sup> of September 2023).
- 3) Presented at the University of the Free State Faculty of Health Sciences Three Minute Thesis Competition (on the 18<sup>th</sup> of September 2023).

## LIST OF FIGURES

FIGURE 2.1:	<b>The three major autophagic pathways</b>	<b>17</b>
FIGURE 2.2:	<b>The stepwise chaperone-mediated autophagy process</b>	<b>19</b>
FIGURE 2.3:	<b>The regulation of CMA activity by mTORC2/PHLPP1/Akt</b>	<b>23</b>
FIGURE 2.4:	<b>The Barcelona Clinic Liver Cancer Treatment Strategy</b>	<b>35</b>
FIGURE 2.5:	<b><i>Moringa oleifera</i> leaves</b>	<b>38</b>
FIGURE 2.6:	<b>The caspase-mediated apoptotic pathway</b>	<b>42</b>
FIGURE 4.2.1:	<b>The concentration-dependent effects of ATRA on HepG<sub>2</sub> cancer cell viability</b>	<b>65</b>
FIGURE 4.2.2:	<b>The concentration-dependent effects of MO aqueous leaf extract on HepG<sub>2</sub> cancer cell viability</b>	<b>66</b>
FIGURE 4.3.1:	<b>Caspase-9 activity in HepG<sub>2</sub> cancer cells following treatment exposure to ATRA, MO and ATRA+MO combination treatment groups</b>	<b>68</b>
FIGURE 4.3.2:	<b>Caspase-3/7 enzyme activity in HepG<sub>2</sub> cancer cells following treatment exposure to ATRA, MO and ATRA+MO combination treatment groups</b>	<b>69</b>
FIGURE 4.4:	<b>CMA-selective LAMP2A ELISA assay results. LAMP2A activity following 24-hour ATRA, MO, and ATRA+MO combination treatment (p &gt; 0.05)</b>	<b>70</b>
FIGURE 4.5.1:	<b>LAMP2A expression in HepG<sub>2</sub> cancer cells following treatment exposure to ATRA, MO and ATRA+MO combination treatment groups. Protein expression densitometric analysis (A)</b>	<b>72</b>

	and representative western blot (B) for LAMP2A protein expression is shown	
FIGURE 4.5.2:	HK2 expression in HepG <sub>2</sub> cancer cells following treatment exposure to ATRA, MO and ATRA+MO combination treatment groups. Protein expression densitometric analysis relative to the control (A) and representative western blot (B) for LAMP2A protein expression is shown	73
FIGURE 6:	Diagram depicting this study's main findings	89
FIGURE A1:	Initial ethical clearance letter	118
FIGURE A2:	Subsequent ethical clearance letter following the request to obtain the human HepG <sub>2</sub> cancer cells from the University of KwaZulu-Natal	119
FIGURE A3:	Ethical clearance extension letter for 2023	120
FIGURE A4:	<i>Moringa oleifera</i> certificate of authenticity issued by the KwaZulu-Natal Herbarium (NH)	121
FIGURE B1:	Illustration of the preparation of the Human LAMP2A ELISA standards serial dilution	125
FIGURE B2:	Standard curve of collated repeats for LAMP2A ELISA.	125
FIGURE B3:	Standard curve of collated repeats for BCA protein quantification assay	126
FIGURE C1:	Morphological characterisation of human HepG <sub>2</sub> cells in response to 24-hour treatment	129
FIGURE C2:	Cell count and viability of human HepG <sub>2</sub> cells in	130

**response to 24-hour treatment**

<b>FIGURE D:</b>	<b>Fluorescent micrograph confirming the absence of mycoplasma in the human HepG<sub>2</sub> cells used for this study</b>	<b>133</b>
<b>FIGURE E1:</b>	<b>Declaration from language practitioner</b>	<b>134</b>
<b>FIGURE E2:</b>	<b>Turnitin similarity summary report</b>	<b>135</b>
<b>FIGURE F:</b>	<b>Manuscript confirmation of acceptance email from the Journal of Nutrition and Cancer</b>	<b>136</b>

## LIST OF TABLES

TABLE 2.1: <b>Cell-specific chemical modulators of CMA activity.</b>	<b>28</b>
TABLE 3.1: <b>Experimental groups.</b>	<b>53</b>
TABLE 3.2: <b>Precast gel arrangement of wells (loading sequence).</b>	<b>59</b>
TABLE 3.3: <b>Primary antibody preparations.</b>	<b>61</b>
TABLE B1: <b>DMSO percentages for ATRA concentration range used to determine the IC<sub>50</sub></b>	<b>121</b>
TABLE B2: <b>Dilution scheme for standard test tube protocol adapted from the manufacturer's protocol.</b>	<b>126</b>

## LIST OF ABBREVIATIONS

### Common abbreviations

ABTS	2,20-azinobis-(3-ethylbenzthiazoline-6-sulfonic acid)
ADCD	Autophagy-dependent cell death
Akt	Protein kinase B
ANOVA	One-Way Analysis of Variance
Apaf-1	Apoptotic protease activating factor 1
APL	Acute promyelocytic leukaemia
ATRA	All-trans-retinoic acid
Bag-1	B-cell lymphoma 2-associated athanogene
BCA	Bicinchoninic acid
BCLTS	Barcelona Clinic Liver Treatment Strategy
Bcl-2	B-cell lymphoma 2
CCM	Complete culture media
CMA	Chaperone-mediated autophagy
CO <sub>2</sub>	Carbon dioxide
Covid-19	Coronavirus diseases of 2019
CYP2E1	Cytochrome P450 family 2 subfamily E member 1
DCIS	Ductal carcinoma cells in situ
dH <sub>2</sub> O	Distilled water
DISC	Death-indicating signalling complex
DMSO	Dimethyl sulfoxide
DNA	Deoxyribonucleic acid
DPPH	2,2-diphenyl-1-picrylhydrazyl
ECM	Extracellular matrix

EF1 $\alpha$	Elongation factor 1 $\alpha$
ELISA	Enzyme-linked immunosorbent assay
EMEM	Eagle's minimum essential medium
FADD	Fas-associated protein with death domain
Fas	CD96 trans-membrane death receptor
GFAP	Glial fibrillary acidic protein
GTP	Guanosine triphosphate
HBV	Hepatitis B virus
HCC	Hepatocellular carcinoma
HCV	Hepatitis C virus
Hip	Heat shock protein 70-organising protein
HIV	Human immunodeficiency virus
HK2	Hexokinase II
Hop	HSP70-HSP90 organising protein
HRP	Horseradish peroxidase
HSC70	Heat shock cognate 71 kDa protein
HSP90	Heat shock protein 90
IC <sub>50</sub>	Inhibition concentration 50
KFERQ	Lysine (K)-Phenylalanine (F)-Glutamic Acid (E)-Arginine (R)-Glutamine (Q)
LAMP2A	Lysosome-associated membrane protein type 2A
LDAC	Low-dose cytosine arabinoside
Lys-HSC70	Lysosomal resident variant of heat shock cognate 71 kDa protein
MEPM	Mouse embryonic palatal mesenchymal
MO	<i>Moringa oleifera</i>
mRNA	Messenger ribonucleic acid

mTOR	Mammalian target of rapamycin
mTORC	Mammalian target of rapamycin complex
mTORC1	Mammalian target of rapamycin complex 1
mTORC2	Mammalian target of rapamycin complex 2
MWM	Molecular weight marker
p53	Tumour protein 53
PBS	Phosphate buffered saline
PEI	Percutaneous ethanol injection
pGFAP	Phosphorylated variant of glial fibrillary acidic protein
PHLPP1	Pleckstrin homology domain, leucine-rich repeat protein phosphatase 1
PVDF	Polyvinylidene fluoride
RA	Retinoic acid
Rac1	Rat sarcoma virus-related C3 botulinum toxin substrate 1
RAR	Retinoic acid receptor
RAR $\alpha$	Retinoic acid receptor alpha
RB1	Retinoblastoma 1
RFA	Radiofrequency ablation
RNA	Ribonucleic acid
ROS	Reactive oxygen species
RT	Room temperature
SA	South Africa
SDS-PAGE	Sodium Dodecyl Sulfate-Polyacrylamide Gel Electrophoresis
SEM	Standard error of the mean
SSA	Sub-Saharan Africa
T25	25 cm <sup>3</sup> filter capped cell culture flask

T75	75 cm <sup>3</sup> filter capped cell culture flask
TACE	Trans-arterial chemoembolization
TBST	Tris-buffered saline and Tween 20
TFEB	Transcription factor EB
TGF- $\beta$	Transforming growth factor-beta
Wnt	Wingless/int-1
WR	Working reagent
WST-1	2-(4-iodophenyl)-3-(4-nitrophenyl)-5-(2,4-disulfophenyl)-2H-tetrazolium, monosodium salt
UFS	University of the Free State

### Measuring units and symbols

1°	Primary
2°	Secondary
°C	Degrees Celsius
$\mu\text{g/mL}$	Microgram(s) per millilitre
$\mu\text{L}$	Microlitre
$\mu\text{M}$	Micromolar
%	Percent
~	Approximately
A	Ampere
Abs	Absorbance
a.u.	Arbitrary units
cm <sup>3</sup>	Cubic centimetre(s)
kDa	Kilodalton(s)

mg	Milligram(s)
mg/mL	Milligram per millilitre
mL	Millilitre(s)
mM	Millimolar
ng/mL	Nanogram(s) per millilitre
nm	Nanometres
RLU	Relative light units
rpm	Revolutions per minute
V	Voltage

## ABSTRACT

**Introduction:** The impact of hepatocellular carcinoma (HCC) is most significant in developing countries, including South Africa. Emerging evidence suggests that the cell survival mechanism, chaperone-mediated autophagy (CMA), promotes HCC tumour progression and chemotherapeutic drug resistance. Current treatment approach for HCC is guided by the Barcelona Clinic Liver Treatment Strategy (BCLTS), which recommends different treatment approaches depending on the level of tumour progression. Despite their efficacy, currently available chemotherapeutic options have numerous limitations such as acquired resistance, recurrence, and hypertension. To address these limitations, phytochemical extracts are increasingly being investigated for the anti-cancer potential. The phytochemical extracts of the medicinal plant, *Moringa oleifera* (MO) have been shown to induce apoptosis of HCC cells. MO leaves have the greatest abundance of phytochemicals displaying anticancer potential. Investigating the interplay between all-trans-retinoic acid (ATRA), a potential inhibitor of CMA, and MO regarding their effects on CMA holds potential in identifying adjuvant therapeutic approaches for treatment modalities for HCC.

**Aim:** This study aimed to investigate the *in vitro* effects of MO aqueous leaf extract on CMA activity in human HepG<sub>2</sub> cancer cells.

**Methods:** HepG<sub>2</sub> cells were cultured and exposed to MO and ATRA for 24 hours. Thereafter, a cell viability assay was performed and an inhibition concentration 50 (IC<sub>50</sub>) was determined which was used for all subsequent experiments. The cells were allocated to three treatment groups: MO, ATRA and a combination group of MO and ATRA. A Caspase-Glo™ cell death assay and western blot analysis were also conducted to

evaluate changes in lysosome-associated membrane protein type 2A (LAMP2A) and hexokinase II (HK2) protein expression levels.

**Results:** The cell viability assay results displayed a concentration-dependent decline in reductive capacity following MO and ATRA exposures. An IC<sub>50</sub> of 1415 µM (ATRA) and 2198 µg/mL (MO) were observed. The cell death assay revealed decreased caspase-9 activity following the respective treatment exposures. There was a corresponding decline in caspase-3/7 activity following respective treatment exposures, except for MO, where an increase in caspase-3/7 activity was observed. Western blot analysis showed a decline in the expression of LAMP2A and a corresponding increase in the expression of the CMA cargo protein HK2.

**Conclusion:** The results revealed that MO and ATRA could inhibit the growth and proliferation of HCC cells, offering a promising adjuvant therapeutic approach against HCC. Further investigation into these compounds and their underlying mechanisms of action may contribute to developing novel treatment modalities for HCC.

**Keywords:** All-trans-retinoic acid; apoptosis; cancer therapeutics; chaperone-mediated autophagy; hepatocellular carcinoma; HepG<sub>2</sub> cancer cells; *Moringa oleifera*

## CHAPTER 1

### 1.1. Arrangement of the thesis

**Chapter 1:** Introduction. This chapter introduced the thesis and provided a brief overview of its content. It set the stage for the subsequent chapters by outlining the research topic, objectives, and significance of the study.

**Chapter 2:** Literature review. This chapter describes HCC and explores the role of CMA in the progression of this disease. It also describes MO, explaining its potential and anti-HCC potential. Emphasis is placed on the existing knowledge gap regarding the interaction between CMA and MO in the context of HCC progression.

**Chapter 3:** Methodology. This chapter outlines the methodology employed in the study, detailing the various techniques used to address the research questions. This chapter also clearly describes the methods used to collect data and perform analyses, ensuring reproducibility and validity.

**Chapter 4:** Results. This chapter describes the findings and observations obtained from this study. It includes a comprehensive report on the experimental findings, including the statistical analyses conducted.

**Chapter 5:** Discussion. This chapter thoroughly discusses the observed results by relating them to relevant published literature and expanding on their implication.

**Chapter 6:** Study conclusions, limitations, and future recommendations. This chapter presents the final conclusions of the study, summarising the 'take-home' message of

the results and whether the research questions were answered, and objectives were achieved. This chapter also acknowledges the study's limitations and how they can be addressed in later studies. Future recommendations are provided to guide subsequent studies and enhance the understanding of the study findings.

**References:** Comprises a comprehensive list of all literature consulted in the thesis's writing.

**Appendices:** The appendices include supplementary materials and a list of all additional information used for the study but not included in the main body of the thesis. This includes detailed methodologies or supporting documentation that may be relevant for understanding the core results' content.

## **1.2. Introduction**

Cancer is the second leading cause of death globally (Boukes et al., 2017). Although liver cancer is only the sixth most common type, it was reported as the second largest contributor to cancer-related deaths in 2020 (Boukes et al., 2017; Sung et al., 2021). Hepatocellular carcinoma (HCC) is the most prevalent type of primary liver cancer in sub-Saharan African (SSA) countries, including South Africa (SA) (Kew, 2013; Liu et al., 2015). HCC is typically initiated by extensive liver damage-induced epigenetic changes such as DNA methylation and histone modifications that progressively lead to liver fibrosis and, ultimately, cirrhosis (Aravalli et al., 2008; He and Tang, 2020). Risk factors for HCC include chronic hepatitis, alcohol-induced liver damage, obesity, human immunodeficiency virus (HIV) and type II diabetes mellitus (He and Tang, 2020; Pinheiro et al., 2019; Tang et al., 2018).

The treatment of HCC depends on numerous factors, such as the stage of the tumour progression. It thus requires a patient-tailored approach (Liu et al., 2015). The Barcelona Clinic Liver Treatment Strategy (BCLTS) summarised the approved treatment strategies for the various stages of HCC development (Garancini et al., 2016). For the early stage of HCC, local therapeutic strategies such as the surgical removal of the tumour remain the most preferred treatment strategy (Garancini et al., 2016; Liu et al., 2015). However, particular challenges (e.g., limited access to diagnostic tools in developing countries such as SA) often result in this treatment method not being timeously administered (Lemoine et al., 2013; Liu et al., 2015). HCC is often accompanied by cirrhosis, necessitating the patient to receive a liver transplant (Fattovich et al., 2004; Lee et al., 2017). However, the scarcity of liver donors remains a significant challenge (Lee et al., 2017; Waller et al., 2015). Loco-regional treatments, such as trans-arterial chemoembolization, are often administered to reduce or prevent the progression of HCC while patients await their donated livers. However, should the HCC progress to the advanced stage, chemotherapy becomes the only effective treatment strategy for those affected (Garancini et al., 2016; Liu et al., 2015). The chemotherapeutic drug treatment of HCC belongs to a class of medications called multi-kinase inhibitors (Liu et al. 2015; Waller 2015). From this class of kinase inhibitors, Sorafenib (Nexavar®) is the only drug exclusively used for the treatment of HCC, followed up by the use of Regorafenib (Stivarga®) (Lemoine et al., 2013; Liu et al., 2015). However, there are still challenges with the current therapeutic options, such as the high risk of relapses and cancer recurrence (Lemoine et al., 2013; Liu et al., 2015), as evidenced by the 5% survival rate reported for advanced HCC patients (Yang et al., 2019).

Given the limitations of current HCC therapeutics, there is an increasing need for alternative adjuvant therapeutic options (Ahmed et al., 2020). Amongst the various molecular mechanisms identified to date, the autophagy pathway has gained significant interest as a potential adjuvant therapeutic target in HCC treatment (Aravalli et al., 2008; Ding et al., 2016; Kon et al., 2011). Autophagy is an inherent cell pathway targeting sequestration and transporting defective and toxic cytoplasmic components to the lysosome for subsequent degradation (Mizushima and Komatsu, 2011). There are three main types of autophagy: macroautophagy, microautophagy, and chaperone-mediated autophagy (CMA) (Levy et al., 2017; Mizushima and Komatsu, 2011; Mowers et al., 2017). Of these pathways, the upregulation of CMA has been extensively described in various types of cancer cells, including the human hepatoma cancer cell line (HepG<sub>2</sub>) (Choi, 2012; Ding et al., 2016; Kon et al., 2011). The CMA pathway involves a chaperone complex that recognises, targets and 'chaperones' specific cytoplasmic proteins to the lysosomal membrane for subsequent degradation and recycling (Juste and Cuervo, 2019). The specific proteins targeted for CMA degradation contain the prerequisite Lysine (K) - Phenylalanine (F) - Glutamic Acid (E) - Arginine (R) - Glutamine (Q) (KFERQ) pentapeptide sequence (Parzych and Klionsky, 2014). CMA has been shown to participate in cellular metabolism and aids in the protection of the cell against the accumulation of toxic proteins and carcinogenesis (Gomes et al., 2017; Kaushik and Cuervo, 2018; Tang et al., 2017). However, CMA also supports HCC tumour growth and chemotherapeutic drug resistance, thus contributing to HCC tumorigenesis (Ding et al., 2008; Guo et al., 2017; Kon et al., 2011). The modulation of CMA, therefore, serves as a promising adjuvant target for current HCC therapeutic strategies (Ding et al., 2016; Kon et al., 2011).

Plant-derived extracts are increasingly being explored as alternative HCC anti-cancer therapeutics (Ahmed et al., 2020; Elsayed et al., 2015). Phytochemical extracts primarily found in the medicinal plant, *Moringa oleifera* (MO) proved effective against numerous diseases, including HCC (Abd-Rabou et al., 2017; Ahmed et al., 2020; Kerdsomboon et al., 2020; Tiloke et al., 2018). MO leaves have the greatest abundance of phytochemicals (Ahmed et al., 2020; Tiloke et al., 2018). The MO leaf extracts have been shown to have anti-cancer properties against HCC, which include inducing apoptosis and reducing the viability of human HepG<sub>2</sub> cancer cells (Ahmed et al., 2020; Charoensin, 2014; Tiloke et al., 2019). However, the interaction between the anti-tumour effects of MO aqueous leaf extract and the tumour-supportive role of CMA has not been assessed in an *in vitro* model of HCC. Therefore, this study explored the effect of MO aqueous leaf extract on CMA activity in human HepG<sub>2</sub> cancer cells.

### **1.3. Problem statement**

The effective, long-term treatment of HCC remains an unmet clinical challenge (Khor et al., 2018). This is partly due to the high cost of specialised healthcare and the lack of readily available, long-term effective treatment options, which are easily accessible to most low-income households representing most of the South African population (Khor et al., 2018). Even following the administration of Sorafenib, the only approved HCC first-line drug, a minor three- to five-month increase in overall patient survival has been reported, especially in the advanced stages of HCC (Anwanwan et al., 2020). Treatment challenges are further compounded by the various Sorafenib-associated side effects, such as dermatologic complications, hypertension, neuropathy, and the development of leukopenia in some patients (Anwanwan et al., 2020; Zhu et al., 2017).

Thus, there is an increasing need for adjuvant HCC treatment options, which may improve the efficacy of current therapeutic strategies (Elsayed et al., 2015).

Plant-derived adjuvant treatment options are increasingly explored to address the HCC therapeutic shortcomings (Ahmed et al., 2020; Charoensin, 2014; Elsayed et al., 2015; Khor et al., 2018). The use of the MO medicinal plant has been recognised for its anti-cancer effects on numerous cancer cells, such as the A549 lung adenocarcinoma cells, K562 leukaemia, human HepG<sub>2</sub> cancer cells and the HCC tumour cells (Jung, 2014; Tiloke et al., 2019). Studies have shown that the MO aqueous leaf extract exerts an apoptotic effect following exposure in human HepG<sub>2</sub> cancer cells (Abd-Rabou et al., 2017; Tiloke et al., 2019). The hepatotoxicant galactosamine found in MO leaves is highly effective against the proliferation of human HepG<sub>2</sub> cancer cells (Abd-Rabou et al., 2017; Khatun et al., 2007). MO leaf extract also inhibits normal liver cell-to-carcinogenic cell transformation by reducing the formation and accumulation of free radicals (Khor et al., 2018). In contrast, enhanced CMA activity plays a crucial role in promoting the survival of cancerous cells (Janser et al., 2019; Kaushik and Cuervo, 2018; Kon et al., 2011; Majeski and Dice, 2004). Furthermore, CMA contributes to HCC chemotherapeutic cell resistance – one of the prominent long-term effects of Sorafenib treatment (Guo et al., 2017; Zhu et al., 2017). Given the established apoptotic effect of MO and the pro-survival effect of CMA in human HepG<sub>2</sub> cancer cells, elucidating the effect of MO leaf extract on CMA activity could provide novel insight into MO's potential modulation of CMA activity as an adjuvant therapeutic target for HCC. However, the *in vitro* effects of MO aqueous leaf extract on CMA activity in human liver HepG<sub>2</sub> cancer cells remain unclear.

#### **1.4. Research rationale**

As the most common type of primary liver cancer, HCC remains a significant healthcare challenge (Ghafouri-Fard et al., 2021; Sung et al., 2021; Villani et al., 2019). Despite the many advances made in HCC therapeutics, ongoing obstacles continue to hinder the early diagnosis of HCC (Liu et al., 2015). These obstacles include limited access to appropriate healthcare facilities, the exorbitant cost of specialised HCC treatment, the high rate of tumour recurrence, the side effects associated with Sorafenib treatment (e.g., hypertension and dermal complications), and the development of Sorafenib drug resistance (Aravalli et al., 2008; Hwang et al., 2015; Liu et al., 2015; Oishi and Wang, 2011). Plant-derived HCC adjuvant treatment alternatives have emerged as a promising addition to current treatment options to address the above concerns (Ahmed et al., 2020; Charoensin, 2014; Elsayed et al., 2015; Khor et al., 2018). MO is a medicinal plant containing polyphenols and polyflavonoids that have anti-cancer effects (Ahmed et al., 2020; Tiloke et al., 2018). The MO leaves contain the greatest abundance of these phytochemicals (Ahmed et al., 2020). Tiloke and colleagues found these MO-derived phytochemicals to be effective as a significant induction of apoptosis in human HepG<sub>2</sub> cancer cells following MO aqueous leaf extract treatment was observed (Tiloke et al., 2019).

Strong evidence suggests that autophagy-related pathways such as CMA may contribute to the survival of HCC cells in a time- and tumour-stage-dependent manner, as shown by the significant increase in lysosome-associated membrane protein type 2A (LAMP2A) expression in the HCC Huh-7 liver cancer cell line (Chava et al., 2017; Ding et al., 2016; Kon et al., 2011). However, the effect of MO aqueous leaf extract on CMA activity remains unclear in an *in vitro* model system using the HCC HepG<sub>2</sub> cell

line. The therapeutic potential of CMA blockage has been demonstrated using small interfering RNA silencing of the LAMP2A gene in multiple cancer cell lines (Kon et al., 2011). However, no *in vitro* assessments to date demonstrate the influence of MO aqueous leaf extract on the CMA surrogate marker, LAMP2A, in human HepG<sub>2</sub> cancer cells. Therefore, the effect of MO aqueous leaf extract was evaluated for its potential effect on CMA activity following exposure in human HepG<sub>2</sub> cancer cells.

### **1.5. Aim of the study**

This study aimed to investigate the *in vitro* effects of MO aqueous leaf extract on CMA activity in human HepG<sub>2</sub> cancer cells over a pre-determined time.

### **1.6. Research study questions**

The following overarching research questions guided this study:

- 1) What role does CMA play in human HepG<sub>2</sub> liver cancer cell viability?
- 2) How does 24-hour MO aqueous leaf extract treatment affect activity in human HepG<sub>2</sub> cancer cells?

### **1.7. Objectives of the study**

In order to achieve the aim of this study, the following objectives were pursued using the human HepG<sub>2</sub> cancer cells as the *in vitro* HCC model system:

- 1) Assessment of the concentration-dependent effects of 24-hour MO aqueous leaf extract exposure on cell viability using a 2-(4-iodophenyl)-3-(4-nitrophenyl)-5-(2,4-disulfophenyl)-2H-tetrazolium, monosodium salt (WST-1) assay.

- 2) Assessment of the concentration-dependent effects of 24-hour all-*trans*-retinoic acid (ATRA), LAMP2A-inhibitory compound, exposure on cell viability using a WST-1 assay.
- 3) Assessment of the effects of 24-hour exposure to ATRA and MO combination treatment on cell viability using a WST-1 assay.
- 4) Assessment of LAMP2A, heat shock protein 90 (HSC90), and pro-oncogenic protein, hexokinase II (HK2) expression following 24-hour exposure to ATRA, MO, and a combination of ATRA and MO aqueous leaf extract using western blot analysis.
- 5) Quantification of LAMP2A expression following 24-hour exposure to ATRA, MO leaf aqueous extract, and a combination of ATRA and MO aqueous leaf extract using the human LAMP2A enzyme-linked immunosorbent assay (ELISA) Kit.
- 6) Assessment of the initiation (caspase-9 activity) and execution (caspase-3/7 activity) of apoptosis following 24-hour exposure to ATRA, MO aqueous leaf extract, and a combination of ATRA and MO aqueous leaf extract using the Caspase-Glo™ 9 and Caspase-Glo™ 3/7 Assay Kit, respectively.

## **1.8. Methodology**

Ding and colleagues found a significant difference in the level of CMA activity between different human HCC cell lines when compared to the level of CMA activity reported in the control human hepatic cell line L-02 (Ding et al., 2016). Therefore, the human HepG<sub>2</sub> cancer cells were used as an *in vitro* model of HCC. MO aqueous leaf extract and ATRA were prepared and exposed to human HepG<sub>2</sub> cancer cells. ATRA allows for assessing cell viability following the potential inhibition of CMA surrogate marker LAMP2A. Cells were cultured and allocated to four treatment groups: (1) control, (2)

ATRA, (3) MO, (4) and a combination of ATRA and MO treatment over 24 hours. The 24-hour assessment time point is well-established for optimal CMA activity. A cell proliferation assay assessed cell viability following a concentration-dependent exposure to MO aqueous leaf extract and ATRA. Western blot analysis determined LAMP2A, HSC90, and HK2 protein expression. The ELISA Kit was used to quantify LAMP2A expression. The initiation and execution of apoptosis were assessed using appropriate Caspase Glo™ Assay Kits to quantify the activity of caspase-3/7 and -9. All experimental procedures complied with the national COVID-19 regulations, which were adhered to by the Department of Basic Medical Sciences at the University of the Free State's (UFS) Faculty of Health Sciences.

The primary researcher at the UFS Faculty of Health Science's Department of Basic Medical Sciences, Department of Human Molecular Biology, and Department of Haematology and Cell Biology conducted all the experimental procedures. The respective departments all have a well-ventilated sterile laboratory environment which permitted a 2-metre working distance under the guidance of one study supervisor.

### **1.9. Value of the study**

The MO aqueous leaf extract has been shown to induce cell death in human HepG<sub>2</sub> cancer cells. The pro-tumour role of enhanced CMA activity has been documented in multiple cancer cells and associated tissues. This study characterised the possible interaction between MO and CMA activity, determining if that interaction can potentially be therapeutically exploited to favour cell death onset in the human HepG<sub>2</sub> cancer cells. The outcomes of these experiments will provide insight into the effects of MO aqueous leaf extract to potentially modulate CMA activity in favour of apoptosis,

which may allow for its potential use as an adjuvant target to improve the efficacy of current HCC therapeutics. Given the poor prognosis of HCC, the associated healthcare limitations, and ineffective HCC management strategies, an urgent need exists for novel adjuvant treatment targets. It is envisioned that the knowledge gained from this study will provide better insights into the anti-cancer role of MO aqueous leaf extract in targeting CMA activity, which is well-established for its tumour-supportive effect in cancerous cells. Due to the MO plant being readily accessible and its ease of growth in most household gardens, it is a promising adjuvant treatment option that is affordable for most South Africans with limited access to costly healthcare treatment options. The results from this study may also contribute to the scientific and clinical knowledge about the therapeutic exploitation of molecular pathways, such as CMA, to potentially improve the efficacy of HCC chemotherapeutics and ultimately translate into better HCC patient prognosis.

## CHAPTER 2

### LITERATURE REVIEW

#### **2.1. Hepatocellular carcinoma**

Globally, cancer is the second leading cause of death, accounting for approximately 8.2 million deaths in 2012 and 8.8 million in 2015 (Boukes et al., 2017). In 2020, 19.3 million new cancer cases and ten million cancer-related deaths were recorded worldwide (Sung et al., 2021). New cancer cases are predicted to rise to more than twenty-three million by the end of this decade (Twilley et al., 2020). African countries account for an estimated 60% of all new cancer cases worldwide (Boukes et al., 2017). Amongst the thirty-six common types of cancer worldwide, primary liver cancer was reportedly the sixth most common type and the second largest contributor to cancer-related mortalities (830 000 deaths) in 2020 (Sung et al., 2021). Hepatocellular carcinoma (HCC) is the most common type of primary liver cancer, accounting for 75% to 90% of all liver cancer cases (Liu et al., 2015). In 2010, HCC alone was responsible for approximately 1 million deaths (Gillman et al., 2021; He and Tang, 2020). Although HCC is the fifth most common type of cancer in men and only the seventh most frequent form of cancer in women, it currently serves as the third leading cause of cancer-related deaths owing to the poor clinical outcomes associated with this disease (Ghafouri-Fard et al., 2021; Liu et al., 2015; Villani et al., 2019).

#### **2.2. HCC in sub-Saharan African countries**

The regions with the highest incidence of liver cancer include East Asia, sub-Saharan Africa (SSA), and Northern and Eastern European countries (Liu et al., 2015; Tang et al., 2018). HCC affects developed countries. However, this disease remains more

prominent in developing countries (Liu et al., 2015; Sung et al., 2021; Tang et al., 2018). SSA is the most cancer-affected region, particularly by HCC (Kew, 2013). In 2018, African countries collectively recorded 64 779 new HCC cases, with 43 530 of these cases being male (67%) and accounting for a cumulative 63 562 deaths (98% mortality) (Ndom, 2019). The regional incidence rate of HCC is amongst the highest in South Africa (SA) and its neighbouring countries (Kew, 2013). A total of 2 710 of the 64 799 new HCC cases in Africa were from Southern Africa, resulting in 2 597 deaths (95% mortality) (Ndom, 2019). Socioeconomic factors also significantly influence the incidence of HCC, with low-income households residing in rural areas at a higher risk (Tang et al., 2018). However, due to the healthcare challenges that continue to impede early-stage HCC detection, current epidemiological data in SSA are thought to be an underestimation of the true scale of prevalence and impact of HCC (Kew, 2013). Early-stage HCCs are usually undetectable using conventional clinical diagnostic tools (e.g., serum markers and radiography), thus making disease diagnosis difficult at this stage (Sakamoto, 2009). As in many SSA countries, early-stage HCC diagnostic challenges in SA are also compounded by healthcare resource limitations (Kew, 2013; Lemoine et al., 2013). In contrast to developed countries, most South African public hospitals have limited diagnostic resources, which include a lack of imaging technologies used in the identification of early-stage HCC progression, an insufficient number of HCC healthcare specialists, and ill-equipped medical infrastructure and diagnostic laboratories (Lemoine et al., 2013).

### **2.3. HCC risk factors**

The initiation and development of HCC is a complex process that involves numerous genetic and epigenetic events (Aravalli et al., 2008). These events are often hallmarks

of conditions that promote the proliferation of cancer cells while concurrently inhibiting apoptosis (programmed cell death) (Aravalli et al., 2008). Liver diseases and conditions such as chronic hepatitis and alcohol-induced liver damage cause liver fibrosis through epigenetic changes (Aravalli et al., 2008; He and Tang, 2020; Liu et al., 2015; Pinheiro et al., 2019). Epigenetic events associated with hepatocarcinogenesis include DNA methylation and histone modifications (Aravalli et al., 2008; He and Tang, 2020). Irregular DNA methylation associated with HCC development results in changes in signalling pathways that play a critical role in the regulation of cell cycle progression and cell death, such as the retinoblastoma 1 (RB1), tumour protein 53 (p53) and wingless/int-1 (Wnt) pathways, a reduction in DNA repair and efficacy, and interruptions of interferon-alpha signalling (Herceg and Paliwal, 2011). The histone modifications include an increase in histone deacetylation activity, changes in cellular gene expression, and the downregulation of cytochrome P450 family 2 subfamily E member 1 (CYP2E1), a drug-metabolising enzyme that is primarily expressed in hepatocytes (Herceg and Paliwal, 2011; Lu and Cederbaum, 2008). Herceg and Paliwal found that RNA interferences may also be associated with HCC development (Herceg and Paliwal, 2011). The epigenetic changes eventually develop into cirrhosis, the most common precursor for HCC (Aravalli et al., 2008; He and Tang, 2020; Herceg and Paliwal, 2011); cirrhosis results from late-stage liver disease and its associated complications (He and Tang, 2020). Hepatitis B virus (HBV) and hepatitis C virus (HCV) have also been found to be major contributors to the high incidence of HCC, with HBV being the primary underlying cause for an estimated 60% of all HCC cases in developing countries (Liu et al., 2015; Waller et al., 2015). Other significant contributors to primary liver cancer include obesity, type II diabetes mellitus, alcohol-related liver disease, and non-alcoholic fatty liver disease (Liu et al., 2015;

Pinheiro et al., 2019; Tang et al., 2018; Waller et al., 2015). The human immunodeficiency virus (HIV), of which SA has the highest number of cases worldwide, is also considered a prominent risk factor for developing HCC (Jewkes et al., 2009; Tang et al., 2018). Additional risk factors include liver metastasis, ethnicity, age, diet, gender, and geographic location (Aravalli et al., 2008; Kew, 2013; Liu et al., 2016; Pinheiro et al., 2019). The varying HCC epidemiological disparities across different world regions are further observed between populations within the same region (Aravalli et al., 2008; Pinheiro et al., 2019).

#### **2.4. The molecular mechanisms implicated in HCC progression**

Selective cell signalling pathways, crucial in maintaining cellular homeostasis, have been identified as promising adjuvant therapeutic targets in treating HCC (Aravalli et al., 2008). However, much remains unclear about the complex molecular mechanisms involved in hepatocarcinogenesis (Aravalli et al., 2008). The autophagy pathways, which have been implicated in various human diseases, including age-associated neurodegenerative diseases, cardiovascular diseases, and liver disorders, have also been implicated in the pathogenesis of HCC (Cuervo, 2009; Kon et al., 2011; Levine and Kroemer, 2008; Saha et al., 2018; Shintani and Klionsky, 2004). Under physiological conditions, autophagy is a cell survival mechanism that delivers cytoplasmic components, including damaged organelles and aggregated and superfluous proteins, to the lysosome for subsequent degradation (Mizushima and Komatsu, 2011). Autophagy is considered a stress-response mechanism crucial in maintaining overall cell health and homeostasis in both the absence and presence of various stress conditions (Galluzzi et al., 2017; Zhang and Cuervo, 2008). Under physiological conditions, cytoplasmic components, including mitochondria and

proteins, become damaged and aggregate over time, thus necessitating their removal (Kimmelman, 2011). The continuous removal of defective and toxic cytoplasmic components by the distinct types of autophagy pathways prevents the accumulation thereof, thus averting the development of various diseases and ensuring that these cytoplasmic materials are recycled for reuse by the cell (Glick et al., 2010; Levine and Kroemer, 2008).

#### 2.4.1. *Autophagy pathways*

Autophagy can be sub-classified into three major pathways: microautophagy, macroautophagy, and chaperone-mediated autophagy (CMA) (Figure 2.1) (Levy et al., 2017; Mizushima and Komatsu, 2011; Mowers et al., 2017). Microautophagy involves engulfing cytosolic components through the direct lysosomal membrane invagination of cytoplasmic material (Galluzzi et al., 2017; Mizushima and Komatsu, 2011). Macroautophagy involves the formation of a specialised double-membrane vesicle called an autophagosome (Hollenstein and Kraft, 2020). This specialised structure surrounds and engulfs cytoplasmic material for subsequent trafficking and degradation following the fusion of autophagosomes with lysosomes (Mizushima, 2018; Morishita and Mizushima, 2019). Unlike micro- and macroautophagy, the CMA pathway involves chaperone proteins that selectively recognise, bind, and transport specific cytosolic proteins to the lysosome for subsequent degradation (Juste and Cuervo, 2019).

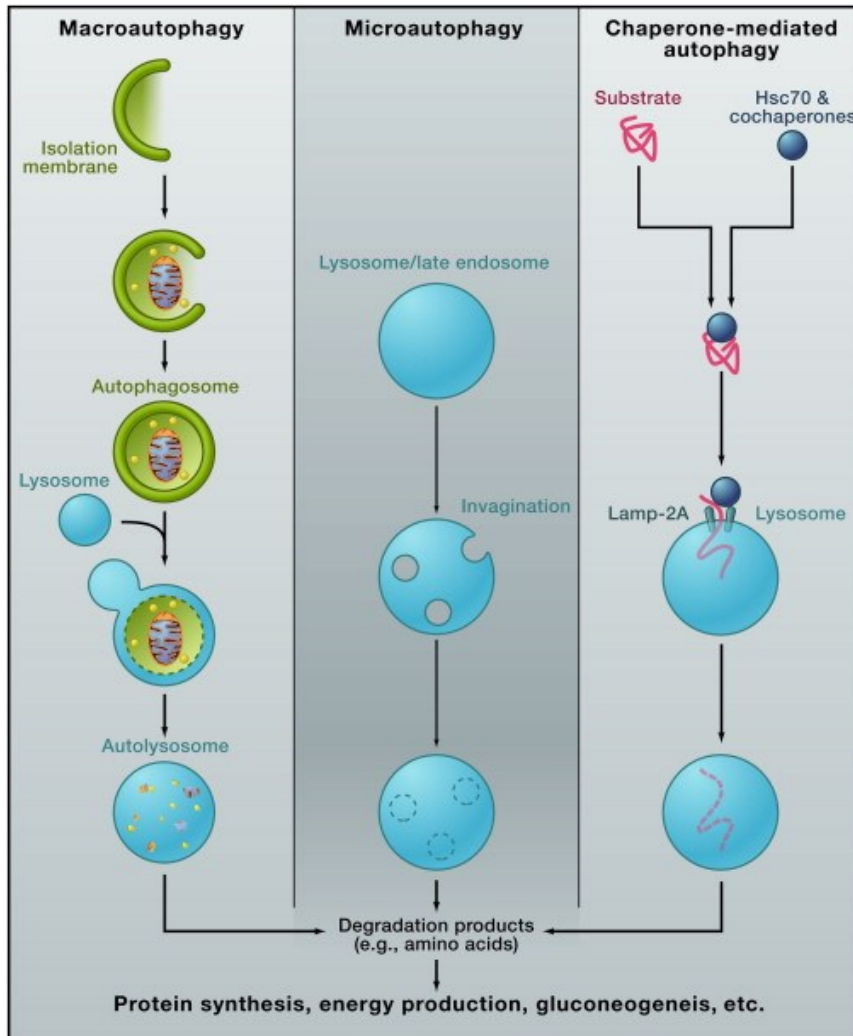


**Figure 2.1: The three major autophagic pathways.** Abbreviations: HSC70, heat shock cognate 71 kDa protein; LAMP2A; lysosome-associated membrane protein type 2A (Mizushima and Komatsu, 2011).

CMA activity is upregulated in response to prolonged starvation conditions, thus ensuring the continuous degradation of nonessential proteins, providing nutrient reserves for the cell, and preserving key proteins (Cuervo, 2009). Of the three autophagy pathways, the upregulation of CMA has been extensively described in different cancer cells, such as skin, lung, and liver (Choi, 2012; Kon et al., 2011). In particular, the increased expression of the CMA-specific receptor, lysosome-associated membrane protein type 2 (LAMP2A), has been shown to augment HCC tumour growth and enhance tumour recurrence (Ding et al., 2016). This suggests that

elevated levels of key CMA markers may be associated with a worse prognosis for HCC patients (Chava et al., 2017; Ding et al., 2016). Therefore, it is plausible that the downregulation of CMA activity may be exploited as an adjuvant target in HCC therapeutic strategies.

#### 2.4.2. *The CMA pathway*

The CMA pathway employs a recognition system that allows specific proteins to be 'chaperoned' by a cytosolic chaperone complex to the lysosomal membrane for subsequent degradation (Majeski and Dice, 2004). The CMA pathway specifically targets and degrades cytosolic proteins containing the Lysine (K)-Phenylalanine (F)-Glutamic Acid (E)-Arginine (R)-Glutamine (Q) (KFERQ) pentapeptide sequence (Parzych and Klionsky, 2014). Such proteins constitute approximately 30% of all cytosolic proteins (Kaushik et al., 2011). In immunochemistry studies, the KFERQ pentapeptide sequence within these substrate proteins is constantly exposed, making it easily accessible for recognition and binding (Majeski and Dice, 2004). The KFERQ-harbouring protein is recognised and bound by the heat shock cognate 71 kDa protein (HSC70), which forms part of a chaperone complex (Kaushik et al., 2011; Majeski and Dice, 2004; Parzych and Klionsky, 2014). The chaperone complex also consists of heat shock protein 40, heat shock protein 90 (HSP90), heat shock protein 70-organising protein (hip), HSP70-HSP90 organising protein (hop), and B-cell lymphoma 2-associated athanogene (bag-1) (Kaushik et al., 2011; Majeski and Dice, 2004). Once bound, the cargo protein (i.e., the targeted KFERQ-harbouring protein) is transported by the chaperone complex and delivered to the lysosomal membrane (Majeski and Dice, 2004; Parzych and Klionsky, 2014). Subsequently, the chaperone complex binds to the cytosolic tail of LAMP2A, triggering the unfolding of the cargo protein and aiding

in the protein's translocation across the lysosomal membrane (Kaushik et al., 2011; Majeski and Dice, 2004; Parzych and Klionsky, 2014). During this translocation process, an HSC70-associated chaperone protein, HSP90, helps to keep the LAMP2A-protein interaction stable (Parzych and Klionsky, 2014). HSC70 then facilitates the disassembly of the chaperone complex once the translocation process is completed, allowing LAMP2A to return to its natural monomeric state (Parzych and Klionsky, 2014). The translocation of the substrate protein into the lysosomal lumen is further aided by the lysosomal resident variant of HSC70 (lys-HSC70), which is necessary for complete substrate translocation (Figure 2.2) (Parzych and Klionsky, 2014). The degradation and organisation (assembly and disassembly) of LAMP2A at the lysosomal membrane determines how much viable LAMP2A is available for additional substrate protein binding (Parzych and Klionsky, 2014). Therefore, the binding of LAMP2A to the substrate protein is defined as the rate-limiting step for CMA, with the expression levels of LAMP2A at the lysosomal membrane being directly correlated with the level of CMA activity (Cuervo and Dice, 2000a, 2000b).

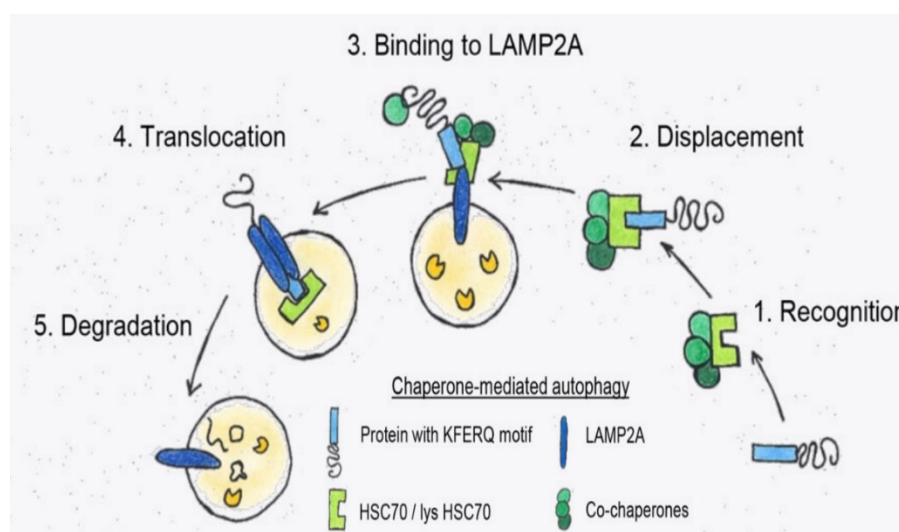


**Figure 2.2: The stepwise chaperone-mediated autophagy process.** Abbreviations: HSC70, heat shock cognate 71 kDa protein; LAMP2A; lysosome-associated membrane protein type 2A; lys-HSC70, a lysosomal resident variant of HSC70 (Janser et al., 2019)

#### 2.4.2.1. *The regulation of LAMP2A dynamics at the lysosomal membrane*

Lysosomes are a vital single-membraned organelle that digests and recycles delivered potentially toxic materials such as bacteria and damaged organelles (Yang and Wang, 2021). Lysosome biogenesis is triggered by numerous factors and is mainly regulated by the transcription factor EB (TFEB) (Franco-Juárez et al. 2022; Yang and Wang, 2021). Once activated, TFEB up-regulates the biogenesis of lysosomes and autophagic flux, enhancing substrate clearance (Zhang et al., 2020). The binding of the chaperone complex with the cytosolic tail of LAMP2A triggers the multimerization of LAMP2A, forming a multimeric complex that mediates the translocation of the substrate protein into the lysosome (Arias, 2015; Dash et al., 2019). The stability of the LAMP2A multimeric complex is regulated by two proteins in a guanosine triphosphate (GTP)-dependent manner: glial fibrillary acidic protein (GFAP) and elongation factor 1 $\alpha$  (EF1 $\alpha$ ) (Bandyopadhyay et al., 2010). The multimerization of LAMP2A triggers a series of events at the lysosomal membrane: (1) GFAP transiently binds with LAMP2A, stabilising it in its multimeric conformation, and (2) the second regulatory protein, EF1 $\alpha$ , binds to a phosphorylated variant of GFAP (pGFAP) that is also present at the lysosomal membrane (Arias, 2015; Dash et al., 2019; Li et al., 2011). Following the successful translocation of the substrate protein and the presence of GTP, the lysosomal membrane releases EF1 $\alpha$  from pGFAP, thus exposing the pGFAP binding site (Arias et al., 2015; Catarino et al., 2017). GFAP has a stronger affinity for pGFAP than it does to LAMP2A; the release of EF1 $\alpha$ , therefore, causes GFAP to unbind with the multimeric LAMP2A and bind to pGFAP instead (Arias et al., 2015; Catarino et al., 2017; Li et al., 2011). The release of GFAP from the multimeric LAMP2A-chaperone complex destabilises LAMP2A, causing it to revert to its monomeric confirmation (Arias et al., 2015; Dash et al., 2019). This causes a

decrease in CMA activity, allowing the cycle to be repeated (Arias, 2015; Catarino et al., 2017).

#### 2.4.2.2. *The role of the lysosomal mTORC2/PHLPP1/Akt signalling axis in CMA*

One of the mechanisms through which cells regulate metabolism and evaluate the cell's nutritional status is primarily through the activity of the 289 kDa serine/threonine-protein kinase, mammalian target of rapamycin (mTOR), which senses and integrates different nutritional inputs, including cellular stress, amino acids, and energy levels (Arias, 2015; Fu and Hall, 2020). There are two main mTOR complexes: mTOR complex 1 (mTORC1) and mTOR complex 2 (mTORC2) (Arias, 2015; Fu and Hall, 2020). While the activation of mTORC1 results in the inhibition of macroautophagy activity, mTORC2 and its effector protein kinase B (Akt), specifically Akt1, is almost exclusively detected in CMA-competent lysosomes where they negatively regulate the assembly of LAMP2A into the CMA translocation complex (Arias, 2015; Arias et al., 2015). Under basal CMA activity, mTORC2 phosphorylates Akt1, which phosphorylates GFAP at the lysosomal membrane (Catarino et al., 2017; Kaushik and Cuervo, 2018). According to Catarino and colleagues, Akt activity, which is activated by mTORC2, controls the level of pGFAP (Catarino et al., 2017). The continuous activity of mTORC2/Akt1 represses CMA activation by negatively regulating the assembly of LAMP2A into the translocation complex and thereby contributing to the relatively low levels of CMA activity (Arias, 2015; Arias et al., 2015). However, under cellular stress conditions, when the upregulation of CMA activity is required, the activity of mTORC2 is opposed by the recruitment of pleckstrin homology domain and leucine-rich repeat protein phosphatase 1 (PHLPP1) to the lysosomal membrane (Arias, 2015; Catarino et al., 2017; Dash et al., 2019; Kaushik and Cuervo, 2018). At

the lysosomal membrane, PHLPP1 is stabilised by the GTPase rat sarcoma virus-related C3 botulinum toxin substrate 1 (Rac1) (Arias, 2015). PHLPP1 is responsible for dephosphorylating Akt1; the deactivation of Akt1 activity increases the pool of non-phosphorylated GFAP, thus favouring the formation of the CMA translocation complex (Arias, 2015; Catarino et al., 2017; Dash et al., 2019; Kaushik and Cuervo, 2018). The mTORC2/PHLPP1/Akt signalling axis regulates CMA activity through its activity on the CMA translocation complex at the lysosomal membrane (Figure 2.3) (Arias, 2015; Dash et al., 2019).

Bandyopadhyay and colleagues found that mechanistically, the inhibition of CMA by GTP is through its effect on EF1 $\alpha$  (Bandyopadhyay et al., 2010). GTP induces the release of EF1 $\alpha$  from its complex with pGFAP at the lysosomal membrane, subsequently causing GFAP to be released from LAMP2A (Bandyopadhyay et al., 2010; Catarino et al., 2017). Catarino and colleagues also highlighted the role of GTP in CMA regulation. They found that GTP inhibited both the recruitment of PHLPP1 to the lysosomal membrane and the stabilisation of PHLPP1 by Rac1 (Catarino et al., 2017).

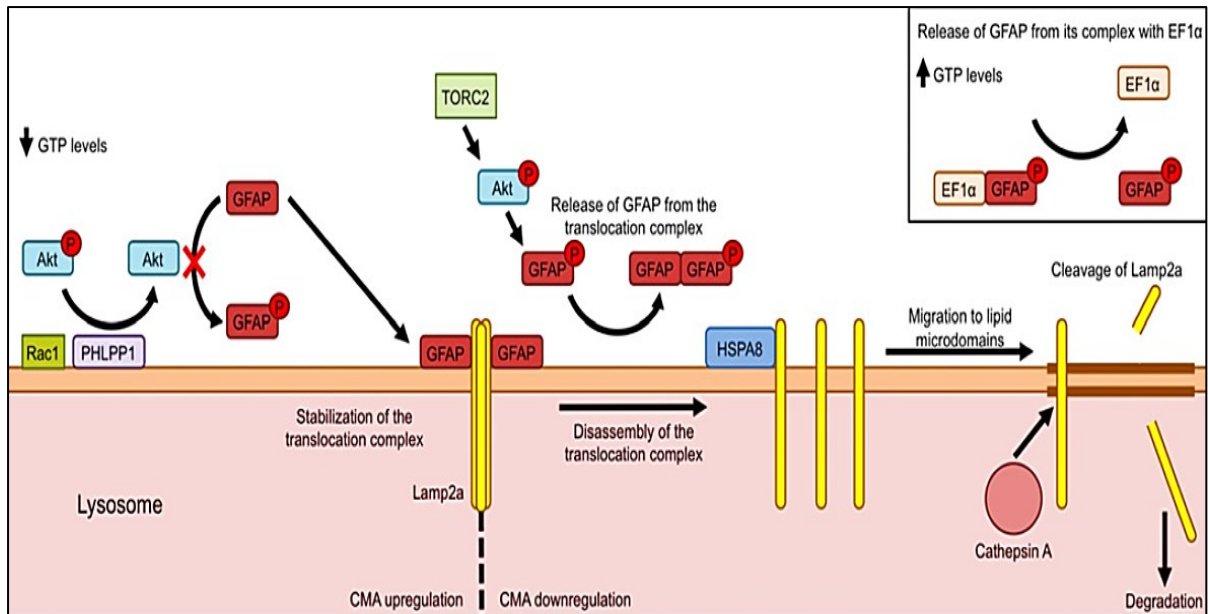


**Figure 2.3: The regulation of CMA activity by mTORC2/PHLPP1/Akt.** Abbreviations: Akt, Protein kinase B; EF1 $\alpha$ , Elongation factor 1 $\alpha$ ; GFAP, Glial fibrillary acidic protein; GTP, Guanosine triphosphate; HSPA8, Heat shock protein family A member 8 / HSC70 chaperone-substrate complex; PHLPP1, Pleckstrin homology domain and leucine-rich repeat protein phosphatase 1; Rac1, Rat sarcoma virus-related C3 botulinum toxin substrate 1; TORC2, Target of rapamycin complex 2 (in mammals: mammalian target of rapamycin complex 2, mTORC2) (Catarino et al., 2017).

#### 2.4.2.3 *The dual role of CMA*

CMA's primary role involves maintaining cellular quality control by regulating cellular metabolism (Gomes et al., 2017; Liao et al., 2021). Through its function, CMA contributes to preventing malignant cell transformation in untransformed cells (Gomes et al., 2017). However, it also promotes cancer cell proliferation (Gomes et al., 2017; Kon et al., 2011). CMA has recently also been shown to play a continuous role in the cell cycle process through actions such as the regulation of DNA repair (Arias and Cuervo, 2020). Basal CMA activity levels are elevated in organs with higher gluconeogenesis rates, such as the liver (Kaushik and Cuervo, 2018). According to Kaushik and Cuervo, despite the compensatory role of other autophagy pathways

such as macroautophagy, ageing and cellular stressors (e.g., oxidative stress), it still results in proteotoxicity due to the aggregation of damaged proteins in CMA-compromised tissues (Kaushik and Cuervo, 2018). In an earlier study, Tang and colleagues also demonstrated that the selective activation of CMA promotes cancer cell death by targeting and removing specific oncogenic proteins (Tang et al., 2017). Consistent with these findings, in 2015, Galan-Acosta and colleagues first reported the role of hexokinase II (HK2) as a CMA amiable target (Galan-Acosta et al., 2015). HK2 acts as both a glycolytic enzyme and an oncogenic kinase. It is overexpressed in cells with a relatively high glucose metabolism rate, indicative of numerous cancer cell types (Ciscato et al., 2020; Galan-Acosta et al., 2015; Patra and Hay, 2013). Under physiological conditions, HK2 plays a key role in the first committed step of glycolysis (glucose metabolism) by catalysing the phosphorylation of glucose (Galan-Acosta et al., 2015; Patra and Hay, 2013). Due to its oncogenic kinase function, HK2 promotes glycolytic activity in cancer cells, contributing to the initiation and survival of several cancerous tumours, including breast and lung cancer (Galan-Acosta et al., 2015; Patra and Hay, 2013; Xia et al., 2015). The overexpression of this protein has been associated with the ability of cancer cells to maintain growth factor-independent glucose metabolism and avoid cell death without growth factors (Galan-Acosta et al., 2015). In addition, HK2 expression in HCC tumours has been associated with worse patient outcomes (Guo et al., 2015; Kwee et al., 2012). The ability of CMA to target and degrade HK2, and the role of HK2 in cancerous cells, suggest that CMA can potentially be manipulated and adapted to promote cancer cell death (Galan-Acosta et al., 2015).

CMA has also been shown to have a cancer-suppressive effect under physiological conditions (Liao et al., 2021), as evidenced by previous reports revealing the removal

and degradation of selective proto-oncogenic proteins, including p53, misfolded nuclear co-repressor proteins epidermal growth factor receptor pathway substrate 8, mouse double-minute 2 homolog, and the translationally controlled tumour-associated protein (Bonhoure et al., 2017; Liao et al., 2021; Lu et al., 2010). These findings suggest that the impairment of CMA could lead to accumulation of these tumour-inducing proteins, subsequently favouring pro-cancer conditions.

Although CMA has a well-established physiological role, most studies indicate that CMA activity is elevated and adopts a pro-survival role in most cancer cells studied to date (Gunduz et al., 2020; Kon et al., 2011). A decrease in cancerous cell growth has been reported following the concentration-dependent inhibition of CMA activity in response to retinoic acid (RA) treatment, as evidenced in leukaemia, breast, and liver cancer cells (Anguiano et al., 2013; Qin et al., 2018; Wu et al., 1997). Kon and colleagues found a significant increase in CMA activity in multiple human primary tumour tissues compared to their respective normal tissues (Kon et al., 2011). This finding was verified by the noticeable increase in LAMP2A expression in various tumour tissues *in vivo* (Kon et al., 2011). The study also revealed that inhibition of CMA significantly reduced cancer cell proliferation, as demonstrated by the decreased cancer cell growth in human lung cells, in which LAMP2A had been knocked down (Kon et al., 2011). More recently, Arias and Cuervo (2020) extensively reviewed the pro-cancer role of CMA and its potential to promote the survival of cancer cells. Their review highlighted how CMA permits human lung cancer and melanoma cells to maintain the Warburg effect, which is characterised by the preference of nearly all cancer cells to anaerobically metabolise glucose, resulting in high glucose uptake and lactate release even in the presence of oxygen (Arias and Cuervo, 2020; Kon et al.,

2011). Suzuki and colleagues also explored the role of CMA in cancer survival, revealing that CMA inhibits the degradation of Myeloid leukaemia 1 (a key cancer pro-survival protein), stabilising this protein in non-small-cell lung cancer cells (Suzuki et al., 2017). Furthermore, CMA has been reported to contribute to both cancer cell resistance to stress and resistance to cancer cell treatment (Arias and Cuervo, 2020). These findings reinforce the role of CMA in cancer cell proliferation.

#### 2.4.2.4. *Modulators of CMA activity*

Under physiological conditions, CMA activity remains relatively low in most cell types, including hepatocytes (Arias, 2015; Arias et al., 2015). According to Rodriguez-Navarro and colleagues, under basal CMA activity, LAMP2A is mobilised to specific lipid microdomains on the lysosomal membrane, where it is cleaved upon binding (Rodriguez-Navarro et al., 2012). The dynamic interaction between LAMP2A and the lipid microdomains regulates the distribution of LAMP2A on the lysosomal membrane and ensures that CMA activity remains at basal activity levels under physiological conditions (Li et al., 2011; Rodriguez-Navarro et al., 2012).

However, under stress conditions such as prolonged starvation, CMA activity is upregulated above basal levels in a cell-specific manner (Catarino et al., 2017). The elevated levels of LAMP2A multimerization during substrate translocation ensures that most proteins are excluded from the microdomains (Rodriguez-Navarro et al., 2012). Additional cellular stressors that have also been shown to elevate the level of CMA activity include oxidative stress, lipotoxicity and proteotoxicity (Arias, 2015; Arias et al., 2015; Patel and Cuervo, 2015). External factors such as age may also alter the cell-dependent levels of basal CMA activity, as it decreases with increasing age in

most cells (Patel and Cuervo, 2015; Rodriguez-Navarro et al., 2012). Changes in the dynamic degradation of LAMP2A at the lipid microdomains are the main contributor to the age-related decline in CMA activity (Rodriguez-Navarro et al., 2012). Other mechanisms, such as the mobilisation of LAMP2A in the lysosomal lumen to the lysosomal membrane, the degradation of LAMP2A and the synthesis of LAMP2A proteins, also modulate the cellular level of CMA activity (Rodriguez-Navarro et al., 2012).

#### 2.4.2.5. *Chemical modulators of CMA activity*

Due to its dual role in cancer progression, the ability to selectively target CMA on a cellular level could be a promising adjuvant therapeutic strategy (Robert et al., 2019). To this end, the selective modulation of CMA activity using various chemical compounds has increasingly become a topic of research interest (Robert et al., 2019). Table 2.1 summarises the chemical modulators that selectively modulate CMA activity in various cell types.

**Table 2.1: Cell-specific chemical modulators of CMA activity** (Robert et al., 2019).

Compounds	Target	Effect on CMA
Cycloheximide	Protein synthesis inhibitor	Inhibition
Anisomycin	Protein synthesis inhibitor	Inhibition
SB230580	P38 MAPK inhibitor	Inhibition
Geldanamycin	HSP90 inhibitor	Activation
17-AAG/DCA	HSP90 inhibitor + PDK1 inhibitor	Activation
6-aminonicotinamide	G6PDH inhibitor	Activation
Synthetic ATRA derivatives	RAR-alpha inhibitor	Activation
Torin	TORC2 inhibitor	Activation
TAK165/AC220	MA inhibitor + FLT3 Inhibitor	Activation
Spautin/AC220	MA inhibitor + FLT3 inhibitor	Activation

#### 2.4.2.6. *Chemical modulation of CMA by retinoic acid derivatives*

Retinoic acids have shown significant promise in the selective modulation of CMA activity when compared to other chemical modulators in numerous cancerous cells assessed to date (Anguiano et al., 2013; Robert et al., 2019). The molecular mechanism through which RA inhibits cancerous cell growth involves the retinoic acid receptor alpha (RAR $\alpha$ ) mediated signal transduction (Zhang et al., 1992). The RAR $\alpha$  pathway is the only ubiquitous RAR pathway in mammalian cells successfully exploited for its selective inhibition of the CMA pathway (Anguiano et al., 2013; Robert et al., 2019). Thus, the RAR $\alpha$  activator, all-trans-retinoic acid (ATRA), has been therapeutically exploited to target the RAR $\alpha$  pathway (Anguiano et al., 2013). Lee and colleagues found that ATRA activate mTORC2 and its effector protein kinase, Akt1, which has been previously shown to inhibit CMA activity (Arias, 2015; Lee et al., 2017). ATRA thus serves as a promising compound to investigate the cellular effects of CMA inhibition.

#### 2.4.3. The effects of ATRA on cancerous cells

Reportedly, retinoic acid derivatives influence cellular differentiation, cellular growth, and apoptosis (Zhu et al., 2019). In cancerous cells, ATRA and its derivatives (retinoids) have shown promising anti-cancer effects and displayed anti-proliferative, antioxidant and cytotoxic traits that influence cell differentiation and induce apoptotic effects through the nuclear retinoic acid receptors, including RAR $\alpha$  apoptosis (Zhu et al., 2019). Studies suggest that a lack of oxygen in the tumour microenvironment may be associated with a more aggressive tumour and an increased ability of the cancerous cells to invade nearby tissues (Al-Qassab et al., 2018). Al-Qassab and colleagues investigated the effects of ATRA on breast cancer using non-invasive ductal carcinoma cells *in situ* (DCIS) under hypoxic conditions (Al-Qassab et al., 2018). Their study revealed that ATRA eliminated the effects of hypoxia, prevented epithelial-to-mesenchymal cell transformation, and prevented malignancy of the DCIS cells, which is usually associated with a hypoxic microenvironment (Al-Qassab et al., 2018).

However, ATRA's efficacy against cancerous cells is not limited to breast cancer. According to Ni and colleagues, ATRA also induces differentiation of acute promyelocytic leukaemia (APL) tumour cells, thereby significantly increasing the remission rate of APL-affected patients (Ni et al., 2019). Interestingly, clinical examination following the administration of ATRA revealed the potential ability of this compound to reverse an otherwise fatal APL case into one that is highly treatable in selective cases (Ni et al., 2019). ATRA has also shown therapeutic potential to improve the efficacy of other available leukaemia therapeutics (Schenk et al., 2014). This was evidenced by the improved survival of acute myeloid leukaemia patients over

the age of 60 who were treated with a combination of low-dose cytosine arabinoside (LDAC) and ATRA compared to LDAC treatment alone (Schenk et al., 2014). Furthermore, children with high-risk neuroblastoma treated with 13-*cis*-retinoic acid (an ATRA derivative) had an improved survival rate following high-dose chemotherapy and stem cell transplantation (Schenk et al., 2014). Other forms of cancer where ATRA activity has shown efficacy include kidney, lung, cervical and liver cancer (Liu et al., 2016; Zhu et al., 2019).

However, there are several challenges with the clinical application of ATRA. For example, ATRA promotes angiogenesis within the tumour by upregulating the transcription of the vascular endothelial growth factor gene (Liu et al., 2016). Moreover, ATRA is a highly toxic compound that may become ineffective due to the high probability of tumour cells developing resistance to it (Liu et al., 2016). Some isomers and derivatives of ATRA are more effective when administered in combination with chemotherapeutic drugs compared to combination treatment using other isoforms of ATRA in selective types of cancer (Ni et al., 2019).

#### 2.4.3.1. *The effects of ATRA in HCC*

Clinical and *in vitro* studies have shown that ATRA affects HCC progression (Burley and Roth, 2007; Liu et al., 2016; Wang et al., 2013; Zhu et al., 2019). These studies indicated that ATRA influences the transcriptional response and cell differentiation process of human HepG<sub>2</sub> cancer cells (Burley and Roth, 2007). A separate study conducted by Wang and colleagues (2013) revealed that ATRA may promote the survival of various HCC cells, including HepG<sub>2</sub> cancer cells. They assessed the effects of ATRA treatment on HepG<sub>2</sub>, Hep3B and Huh7 liver cancer cells cultured without

serum, revealing that ATRA treatment enabled these cells to evade starvation-induced apoptosis (Wang et al., 2013). ATRA treatment also promoted the proliferation and invasion of HCC cells into the interstitial connective tissue under serum starvation conditions (Wang et al., 2013). Furthermore, ATRA treatment upregulated the cellular extracellular matrix (ECM) genes, ultimately resulting in HCC ECM remodelling and thus promoting the survival of the HCC cells (Wang et al., 2013). In contrast to the above findings, Wang and colleagues reported the anti-cancer properties of ATRA treatment in HCC, highlighting a potential dual role of ATRA in HCC (Wang et al., 2013). The above findings revealed that ATRA may improve the prognosis of HCC patients and potentially influence the survival period of patients with advanced-stage HCC (Wang et al., 2013).

Findings from an increasing number of studies agree with the above hypothesis that ATRA may also exhibit HCC anti-cancer properties (Liu et al., 2016; Yoon et al., 2004; Zhu et al., 2019). A clinical study by Zhu and colleagues showed that combination chemotherapeutic treatment, including ATRA inhibited the development of secondary cancers in patients with early-stage HCC (Zhu et al., 2019). Consistent with these findings, *in vitro* studies have also shown ATRA's anti-cancer effects, including ATRA-induced inhibition of HCC cell growth (Liu et al., 2016; Zhu et al., 2019). Liu and colleagues found that ATRA treatment inhibits the proliferation of HepG<sub>2</sub> cancer cells by increasing the expression of tumour suppressor protein, p53 (Liu et al., 2016). In line with these findings, Wei and colleagues also highlighted the anti-cancer effects of ATRA on HepG<sub>2</sub> cancer cells by demonstrating that ATRA had a time- and concentration-dependent apoptotic effect on these cells (Wei et al., 2014). An earlier study by Yoon and colleagues revealed that ATRA could also hinder the expression

of Vimentin (a growth-related gene) mRNA in Hep3B HCC cells (Yoon et al., 2004). Vimentin is associated with the progression of carcinomas (i.e., increased motility and invasive ability of the cancer cells), evasiveness of tumours against treatment and worse patient prognosis (Yoon et al., 2004). The overexpression of this gene has been associated with the metastasis of various tumour types, including HCC tumours (Hu et al., 2004; Park et al., 2007; Yoon et al., 2004). Yoon and colleagues reported that ATRA reduced the motility and invasion of the Hep3B cells by inhibiting Vimentin expression (Yoon et al., 2004).

Aside from its various effects on HCC, ATRA treatment has also been shown to have a variety of physiological functions within the liver (Burley and Roth, 2007). These functions include hepatic protein metabolism, cell differentiation, and the production of albumin and urea (Burley and Roth, 2007).

#### 2.4.4. The Role of CMA in HCC

According to Li and colleagues, CMA promotes HBV and HCV replication, thus accelerating its carcinogenic effects on the liver (Li et al., 2017). Ding and colleagues assessed CMA activity in different human HCC cell lines, including the HepG<sub>2</sub>, Hep<sub>3</sub>B, Huh7, MHCC97L, MHCC97H and HCCLM3, further comparing their findings to the level of CMA activity in the normal human hepatic cell line L-02 (Ding et al., 2016). Their study revealed that a high LAMP2A expression was not only associated with larger HCC tumour size and improved overall tumour survival, but it was also associated with a higher rate of tumour recurrence (3-, 5- and 7-year cumulative recurrence rates) in HCC patients (Ding et al., 2016). Additionally, the inhibition of LAMP2A in HCC tumours decreased tumour cell viability and proliferation under

stressful conditions (Ding et al., 2016). These findings suggest that the long-term survival of HCC tumour cells may depend, at least in part, on the presence of a high level of CMA activity. CMA has also been shown to contribute to the development of chemotherapeutic resistance in HCC cells (Guo et al., 2017), as evidenced by the reduction of cyclin D1 expression, a protein that was previously shown to interact with tumour-suppressor proteins in response to increased CMA activity (Guo et al., 2017), thus reducing HCC cell apoptosis. These findings provide compelling evidence for the pro-cancer role in the presence of enhanced CMA activity, suggesting that CMA may be a potential target for novel HCC therapeutics (Ding et al., 2016; Kon et al., 2011).

## **2.5. Treatment options for HCC**

The treatment of HCC depends on numerous factors, including the stage of tumour progression and the existence of patient co-morbidities, which may require a tailored management and treatment strategy (Liu et al., 2015). Local therapeutic strategies remain the gold standard for treating early-stage HCC (Charoensin, 2014; Liu et al., 2015; Oishi and Wang, 2011). Surgical tumour removal is the most effective approach for HCC patients (Aravalli et al., 2008). Patients with early-stage HCC may undergo a partial liver resection provided there is only an isolated lesion(s), their liver function is retained, and no cirrhosis is observed (Liu et al., 2015; Waller et al., 2015). HCC is often accompanied by cirrhosis, making liver transplants the most promising treatment option (Lee et al., 2017). However, due to the scarcity of donors, a liver transplant may not be immediately available for HCC patients (Lee et al., 2017; Waller et al., 2015). According to Burley and Roth, bioartificial liver support is sometimes used to temporarily assist the damaged liver while the patient awaits a liver transplant (Burley and Roth, 2007). However, due to the difficulty of hepatocyte isolation and *in vitro*

culturing, bioartificial liver support is far inferior to the normal liver and is also not considered a permanent solution (Burley and Roth, 2007). Patients on the waiting lists for liver transplants often remain there for a significant length of time, sometimes more than a year, and risk being removed from the list if their conditions progress past the requirements of the Milan criteria (Bruix et al., 2015; Waller et al., 2015). The Milan criteria require that the tumour growth falls within the following categories: (a) an isolated malignancy that is no greater than 5 cm, (b) 2-3 tumours that are smaller than 3 cm, and (c) exclusively restricted to the liver tissue (Waller et al., 2015). In order to reduce or prevent the progression of HCC while patients await a liver donor, locoregional treatments (i.e., trans-arterial chemoembolization (TACE), radiofrequency ablation (RFA), and percutaneous ethanol injection (PEI)) are often administered (Cescon et al., 2013; Lee et al., 2017; Li et al., 2014; Waller et al., 2015). These locoregional treatments, alone or in combination, may be a more promising option against early, unresectable HCC cases (Chen et al., 2014).

Chemotherapy is administered orally and serves as the only medical treatment option for HCC that does not include the physical infiltration of body tissues (Chen et al., 2014; Kane et al., 2006). Sorafenib (Nexavar<sup>®</sup>) is to date the only chemotherapeutic drug approved by the Food and Drug Administration for exclusive use in the treatment of HCC (Chen et al., 2014; Gillman et al., 2021; D. Li et al., 2014). Sorafenib is a multiple kinase inhibitor administered as a first-line chemotherapeutic drug, followed by Regorafenib (Stivarga<sup>®</sup>) (Gillman et al., 2021; Liu et al., 2015). However, these drugs have limitations, including numerous adverse side effects such as dermal and cardiovascular complications (Tang et al., 2020). An increase in the development of Sorafenib drug resistance was also reported in patients in the advanced stages of

HCC progression (Gillman et al., 2021; Liu et al., 2015; Tang et al., 2020). Figure 2.4 illustrates the approved treatment strategy for different stages of HCC tumour progression, described as the Barcelona Clinic Liver Treatment Strategy (BCLTS) (Garancini et al., 2016).

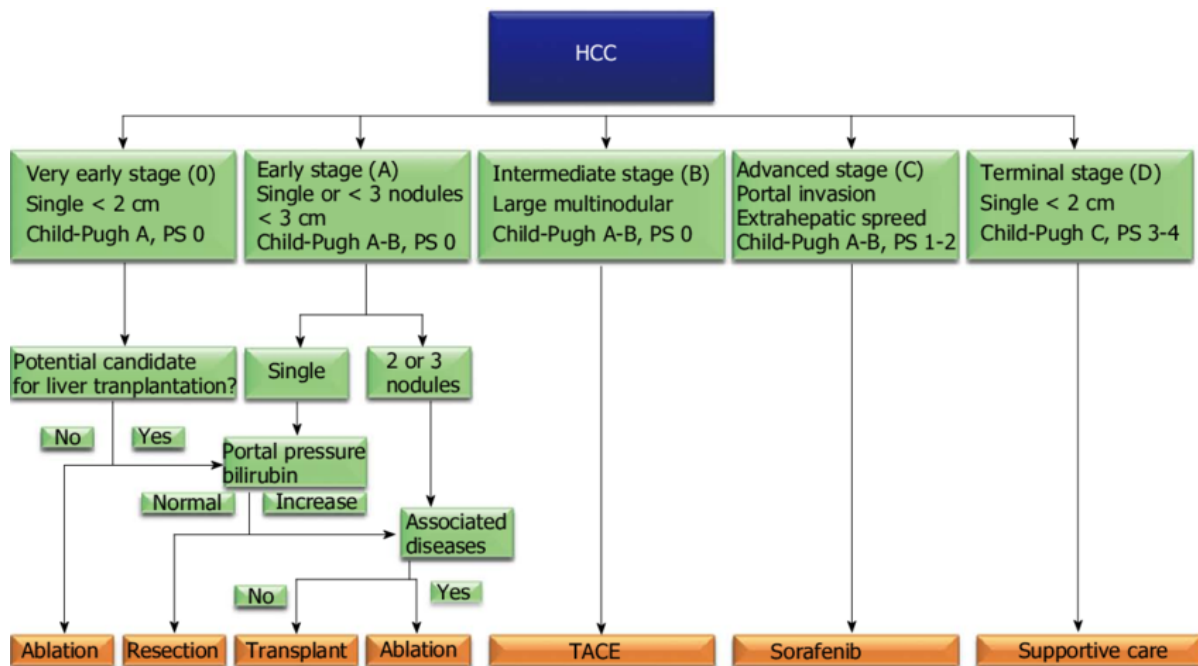


**Figure 2.4: The Barcelona Clinic Liver Cancer Treatment Strategy.** Abbreviations: TACE, trans-arterial chemoembolization; RFA, radiofrequency ablation; PEI, percutaneous ethanol injection (Garancini et al., 2016).

Despite the medical advancements made to date towards the treatment of HCC, relapses, the prevention of metastasis, and the recurrence of cancer continue to pose a significant clinical challenge (Oishi and Wang, 2011). The risk of tumour recurrence continues to pose an obstacle in the treatment of HCC and has been observed in nearly 70% of all patients within the first five years of having received treatment (Aravalli et al., 2008; Hwang et al., 2015; Liu et al., 2015). Advanced-stage HCC is typically incurable, and this late-stage diagnosis worsens the prognosis for the majority of HCC patients (Liu et al., 2015). Consequently, advanced HCC patients only have a

5% survival rate, highlighting the importance of exploring alternative adjuvant therapies and therapeutic targets (He and Tang, 2020; Yang et al., 2019).

The efficacy of current chemotherapeutics is further hampered by their inability to selectively target cancer cells without impacting the healthy cells (Abd-Rabou et al., 2017). Given the above limitations with current HCC therapeutics, plant-derived extracts are increasingly being explored as an alternative adjuvant anti-cancer therapeutic (Ahmed et al., 2020; Elsayed et al., 2015). Approximately 60% of all current anti-tumour therapeutics derive from naturally sourced plant components (Twilley et al., 2020). Exploiting naturally sourced medicinal plant materials with HCC anti-tumour properties may provide adjuvant treatment solutions (Ahmed et al., 2020). Such adjuvant therapeutics could have significantly fewer side effects and be more affordable for most South Africans (Ahmed et al., 2020; Khor et al., 2018). Therefore, there is an increased interest in the research and the potential use of medicinal plant-derived anti-tumour components as adjuvant therapy in treating various liver cancers, including HCC (Charoensin, 2014; Elsayed et al., 2015). Subsequently, the MO plant has been extensively investigated for its anti-cancer properties and has shown therapeutic potential in HepG<sub>2</sub> cancer cells (Abd-Rabou et al., 2017; Charoensin, 2014; Khalafalla et al., 2010; Tiloke et al., 2019).

## **2.6. The use of *Moringa oleifera* in HCC treatment**

The MO plant, called the 'drumstick tree', belongs to the family *Moringaceae* (Anand et al., 2015; Kerdsomboon et al., 2020). MO is native to the sub-Himalayan Indian subcontinent; however, Indian migrants spread it to other tropical and subtropical parts of the world, including SA (Abd-Rabou et al., 2017; Kerdsomboon et al., 2020; Khor et

al., 2018). This plant was initially consumed as a vegetable. However, its numerous health benefits were soon recognised and are now being exploited in various traditional treatments and healthcare practices (Ahmed et al., 2020; Charoensin, 2014). Different parts of the MO plant contain numerous phytochemicals (e.g., nutrients, amino acids, and carotenoids) proven to have anti-inflammatory, hepatoprotective, neuroprotective, antioxidant, immunity-enhancing, and anti-cancer properties (Abd-Rabou et al., 2017; Ahmed et al., 2020; Anand et al., 2015; Elsayed et al., 2015; Kerdsomboon et al., 2020).

Despite all parts of the MO plant containing several bioactive compounds, the leaves (see Figure 2.5) have an abundance of polyphenols and polyflavonoids with antioxidant and anti-cancer properties (Ahmed et al., 2020; Tiloke et al., 2018). The phytochemicals present in the MO leaf extracts have been found to display anti-cancer properties by reducing the formation of free radicals (Khor et al., 2018). Free radicals are formed under oxidative stress conditions, and the failure to control this production contributes to cancer development (Khor et al., 2018). According to a recent study by Wu and colleagues, MO leaf extracts have high concentrations of gallic acid, orientin, quercetin, kaempferol and catechin, all potent antioxidants (Wu et al., 2020). In a more recent study, Xu and colleagues identified kaempferol 3-*O*-rutinoside, kaempferol 3-*O*-glucoside, quercetin 3-*O*-(6'-malonyl-glucoside), and quercetin derivatives as compounds within MO leaf extracts that exhibited the strongest antioxidant activity (Xu et al., 2020). Xu and colleagues further reported that these compounds showed strong free radical scavenging capacity as determined by both 2,2-diphenyl-1-picrylhydrazyl (DPPH) and 2,20-azinobis-(3-ethylbenzthiazoline-6-sulfonic acid) (ABTS) antioxidant determination assays (Xu et al., 2020).



**Figure 2.5: *Moringa oleifera* leaves** (Mahfuz and Piao, 2019).

Sreelatha and colleagues reported on the anti-cancer potential of MO by showing concentration-dependent morphological changes in human KB tumour cells, such as cytoplasmic membrane shrinkage, following MO leaf extract treatment (Sreelatha et al., 2011). Barhoi and colleagues also reported on the anti-cancer potential of MO leaf extract treatment. They showed a significant dose- and time-dependent decrease in Ehrlich ascites carcinoma cells (EAC) solid tumour volume and weight following MO aqueous leaf extract treatment (Barhoi et al., 2021), concluding that MO leaf treatment increases the tissue restoration and survival of tumour-bearing rats (Barhoi et al., 2021). Furthermore, the normal physiology of the tumour-less rats was not affected by the MO leaf extract treatment, suggesting that its cytotoxicity is selective towards the cancerous cells (Barhoi et al., 2021). Patel and colleagues added that the MO leaf extract was significantly less cytotoxic towards the VERO African green monkey's kidney cells (normal control cells) compared to various cancer cell lines, such as MCF-7 breast cancer cells, K562 leukaemia cells, DU145 prostate cancer cells, and HCT15 colon cancer cells (Patel et al., 2018). For Al-Asmari and colleagues, MO leaf extracts had the highest anti-cancer potential compared to extracts from other parts of the plant (Al-Asmari et al., 2015), showing a 90% decrease in breast cancer cells (MDA-MB-

231) and colorectal cancer cells (HCT-8) motility following MO leaf extract treatment compared to a 50% decrease that followed MO bark extract treatment (Al-Asmari et al., 2015). They further reported that MO leaf extract treatment had the highest apoptotic potential, as evidenced by a 19% increase in apoptotic cells compared to a 2% increase following MO bark extract treatment of MDA-MB-231 and HCT-8 cells (Al-Asmari et al., 2015).

Most cancer treatment strategies (e.g., chemotherapeutics and radiation) aim to induce apoptosis in cancer tumour cells (Bold et al., 1997; Wong, 2011). Bioactive compounds found in MO leaves have shown to be a viable adjuvant therapeutic option to current HCC chemotherapeutics (Ahmed et al., 2020) due to the proven ability of these bioactive compounds to induce apoptosis in various cancerous cells (e.g., breast cancer cells, colon cancer cells and human liver cancer cells) and their overall efficacy in improving immune system responses (Ahmed et al., 2020). Understanding the mechanism of MO-induced apoptosis is necessary to develop novel treatment strategies (Blank and Shiloh, 2007). Studies revealed that MO leaf extract can induce apoptosis through numerous apoptosis-triggering events such as an up-regulation of the apoptosis genes (e.g., p53 and B-cell lymphoma 2 (Bcl-2) family of genes members) induction of DNA fragmentation, and the suppression of angiogenesis and metastasis in different cancer cell lines (e.g., MCF-7 breast cancer cells, Caco2, Pac-1, p34, and HepG<sub>2</sub> cells) (Ahmed et al., 2020; Berkovich et al., 2013; García-Beltrán et al., 2020; Karim et al., 2016).

### 2.6.1. Apoptosis

Apoptosis is programmed cell death in multicellular organisms (Blank and Shiloh, 2007). It is observed as cell death due to the shrinking of the cell and its nucleus (Blank and Shiloh, 2007; Hotchkiss et al., 2009). The cell's shrinkage during apoptosis is a result of the collapse of intracellular structures due to the cleavage of their cytoskeleton, nuclear membrane disruption, and chromatin condensation (Hongmei, 2012; Hotchkiss et al., 2009).

Apoptosis is a trigger-stimulated mechanism that regulates cellular self-destruction (Fuchs and Steller, 2011). This mechanism systematically eliminates damaged, irregular, or excess cells in response to stimuli or to maintain homeostasis (Fuchs and Steller, 2011). Apoptosis is governed by proteins called caspases, which ensure the cell is fragmented systemically (Blank and Shiloh, 2007; Hongmei, 2012). Caspases are a family of cysteine proteases synthesised as catalytically inactive zymogens in cells and facilitate apoptosis activation (Li et al., 2015a; Porter and Jänicke, 1999; Salvesen and Dixit, 1997). In mammalian cells, caspases are classified into initiator and effector caspases (Shi, 2004). The initiator caspases (caspase-8 and -9) interact with upstream molecules that trigger the apoptotic process, and upstream initiator caspases activate the effector caspases (caspase-3 and -7) and are responsible for the downstream events such as the cleaving of intracellular components (Li and Yuan, 2008; Shi, 2004). Initiator caspases occur in inactive cell states as monomeric zymogens (Boatright and Salvesen, 2003). Activation of initiator caspases involves the recruitment of the caspase into a multiprotein activating complex, resulting in the dimerization of the caspase (Boatright and Salvesen, 2003). The activating complex

could either be intrinsic or extrinsic, depending on the origin of the death stimulator (Blank and Shiloh, 2007; Boatright and Salvesen, 2003).

The extrinsic pathway occurs via caspase-8 initiator caspase as follows: a compound with a cell death ligand such as cytokines, drugs, hormones, pathogens, and native activity compounds such as vitamin 3 and Lycopene bind with the transmembrane death receptor, CD95 (Fas) (Blank and Shiloh, 2007; Boatright and Salvesen, 2003; Hongmei, 2012; Hotchkiss et al., 2009). Following this ligation, Fas recruits a Fas-associated protein with death domain (FADD), which, in turn, recruits caspase-8 (Boatright and Salvesen, 2003). The resulting complex is known as a death-inducing signalling complex (DISC) (Boatright and Salvesen, 2003; Peter and Krammer, 2003). Caspase-8 is activated within this DISC, and the Fas/FADD/caspase-8 DISC activates caspase-3 (see Figure 2.6) (Boatright and Salvesen, 2003). The intrinsic pathway occurs via the caspase-9 initiator caspase as follows: intracellular stressors such as DNA damage, oxidative stress, endoplasmic reticulum stress and growth factor withdrawal alter the permeability of the mitochondrial outer membrane (Blank and Shiloh, 2007; Boatright and Salvesen, 2003; Hongmei, 2012). Mitochondrial outer membrane permeabilization releases cytochrome c (Blank and Shiloh, 2007; Boatright and Salvesen, 2003; Fulda and Debatin, 2006). Cytochrome c binds with apoptotic protease activating factor 1 (Apaf-1) within the cytosol, forming a complex that recruits caspase-9 to form an apoptosome, which is a large protein formed during apoptosis (Boatright and Salvesen, 2003; Li and Yuan, 2008).

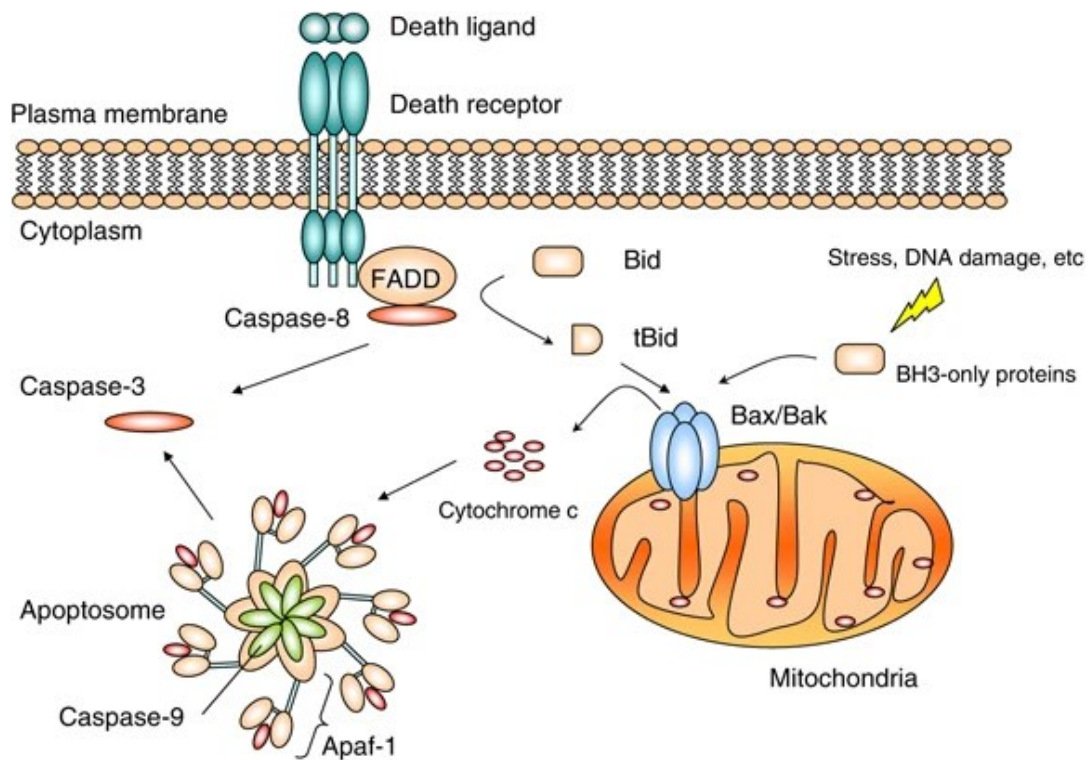


**Figure 2.6: The caspase-mediated apoptotic pathway.** Abbreviations: Apaf-1, apoptotic protease activating factor; Bak, B-cell lymphoma 2 (Bcl-2) killer; Bax, Bcl-2 is a protein in humans; Bid, BH3 interacting-domain; BH3, Bcl-2 homology domain 3; FADD, Fas-associated protein with death domain; tBid, cleaved Bid (Li and Yuan, 2008).

Caspase-9 is activated within the apoptosome, and the cytochrome c/Apaf-1/caspase-9 apoptosome complex activates caspase-3 (see Figure 2.6) (Boatright and Salvesen, 2003; Fulda and Debatin, 2006). Executioner caspases (caspase-3 and -7) are dimers in their inactivated state (Boatright and Salvesen, 2003). Caspase-8 and -9 activate executioner caspases by breaking down the links between their domains (Blank and Shiloh, 2007; Boatright and Salvesen, 2003). Once activated, caspase-3 cleaves numerous intracellular components, resulting in apoptosis (Fulda and Debatin, 2006). Increased caspase activity indicates increased apoptosis (Ahmed et al., 2020; Shi, 2004).

A recent study by Ahmed and colleagues revealed the anti-cancer effects of MO leaf extract as evidenced by a concentration-dependent increase in caspase activity (Ahmed et al., 2020). Importantly, the disruption of apoptosis contributes to the progression of tumorigenesis (Pfeffer and Singh, 2018). For example, the loss of apoptosis control has been found to promote the prolonged proliferation of transformed cells, providing more time for accumulating cellular mutations and increasing tumour cell invasiveness and metastasis (Pfeffer and Singh, 2018).

Several studies have shown that MO leaf extract has cytotoxic effects against selective cancer cell lines, including human HepG<sub>2</sub> cancer cells (Ahmed et al., 2020; Khalafalla et al., 2010; Khor et al., 2018; Tiloke et al., 2019). The human HepG<sub>2</sub> liver cancer cell line is hypersensitive to galactosamine, a hepatotoxicant phytochemical found in MO leaves (Abd-Rabou et al., 2017; Khatun et al., 2007).

Studies have also shown that MO leaf extract exerts a concentration-dependent reduction in the cell viability of human HepG<sub>2</sub> cancer cells (Abd-Rabou et al., 2017; Charoensin, 2014; Khor et al., 2018; Tiloke et al., 2019). Consistent with these findings, Abd-Rabou and colleagues reported a 68% reduction in the human HepG<sub>2</sub> liver cancer cell viability following MO leaf extract treatment (Abd-Rabou et al., 2017), revealing a concentration-dependent decrease in the ATP levels in human HepG<sub>2</sub> cancer cells accompanied by cell death, with the lowest ATP levels observed at the highest dosage of MO leaf extract treatment (Abd-Rabou et al., 2017). However, it was not clear whether the cytotoxicity of the MO leaf extract was responsible for the ATP disruption, thus leading to apoptosis, or if it directly induced apoptosis, which, in turn, resulted in ATP disruption (Abd-Rabou et al., 2017). A separate study revealed that

MO leaf extract helps the liver to evade the effects of diethylnitrosamine – a compound that causes severe liver damage, often resulting in hepatocarcinogenesis, even in low concentrations (Susanto et al., 2021; Tolba et al., 2015). Susanto and colleagues discovered that the MO leaf extract has concentration-dependent inhibitory effect on the transforming growth factor-beta (TGF- $\beta$ ) expression and its signalling pathway (Susanto et al., 2021). TGF- $\beta$  is a hallmark of liver fibrosis, an HCC risk factor (Susanto et al., 2021).

In recent years, valuable insight has been provided into the pro-cancer role of enhanced CMA activity in multiple cancerous cells. However, no *in vitro* studies have assessed the effects of MO aqueous leaf extract on CMA activity in an *in vitro* model of HCC. Investigating the interaction between MO and CMA in HCC cells could provide valuable insights into the potential therapeutic implications of MO in modulating CMA activity, thus contributing to the understanding of alternative approaches for HCC treatment. This research study, therefore, aimed to investigate the effects of MO aqueous leaf extract on CMA activity in human HepG<sub>2</sub> cancer cells.

### **Summary**

Primary liver cancer is the third-largest contributor to cancer-related deaths, with HCC the most common type of liver cancer. Developing countries in SSA remain the most affected by this disease, as the diagnosis and treatment of HCC remain a significant challenge, especially in countries such as SA. The CMA pathway has been shown to contribute to the survival of HCC. Studies have consistently shown increased CMA activity in HCC tumours, as evidenced by an elevated expression of LAMP2A. Due to

its dual role in cancer progression, CMA is considered a potentially promising adjuvant therapeutic target.

Owing to the challenges associated with HCC treatment, plant-derived extracts are increasingly explored as alternative adjuvant anti-cancer therapeutics. For example, the medicinal plant MO leaf extracts contain bioactive compounds that display anti-cancer properties. A concentration-dependent increase in caspase activity (indicative of apoptosis) has been shown following MO leaf extract treatment of numerous cancer cells, including human HepG<sub>2</sub> cells. There is compelling evidence of the pro-cancer role of CMA and the anti-cancer role of MO aqueous leaf extract. However, to date, no *in vitro* studies have investigated the effects of MO aqueous leaf extract on CMA activity. Thus, the aim of this study was to investigate the effects of MO aqueous leaf extract on CMA activity in human HepG<sub>2</sub> cancer cells, over a pre-determined time (24-hours). To achieve this aim, the concentration-dependent effects of 24-hour exposure to MO aqueous leaf extract and ATRA on cell viability were assessed. This was followed by the assessment of caspase-3/7 and -9 activity and the assessment of the of LAMP2A and HK2 following 24-hour exposure to ATRA, MO leaf aqueous extract, and a combination of ATRA and MO aqueous leaf extract.

## CHAPTER 3

### MATERIALS AND METHODS

#### 3.1. Description of study design

This study was a laboratory-based intervention study conducted at the University of the Free State, Faculty of Health Science, Department of Basic Medical Sciences, Department of Chemical Pathology, Department of Human Molecular Biology, and the Department of Haematology and Cell Biology research laboratory facilities. The study was conducted using human HepG<sub>2</sub> cancer cells. Ethical clearance was received from the University of the Free State (UFS) Health Science Research Ethics Committee (Ethics clearance number: UFS-HSD2021/1629-0003) (see Appendix A). This study followed the government's COVID-19 regulations, which were strictly adhered to by the Department of Basic Medical Sciences, Department of Human Molecular Biology, and Department of Haematology and Cell Biology in the Faculty of Health Sciences at the University of the Free State.

Human HepG<sub>2</sub> cancer cells were used as an *in vitro* model system for HCC. These cells were cultured and allocated to four groups to perform all experimental protocols. These groups included a control group, a MO aqueous leaf extract exposure group, an ATRA treatment exposure group, and a combination exposure treatment group consisting of both MO aqueous leaf extract and ATRA. The cells were subjected to a treatment exposure time of 24 hours. The treatment effects for each treatment group were assessed using various molecular techniques. The data obtained from these assessments were analysed using appropriate statistical tests to determine the statistical significance of the observed changes. In order to ensure the reliability of the

results, the experiments were conducted in triplicate and repeated three times, thus ensuring robustness and minimising experimental variability.

### **3.2. Materials**

*Moringa oleifera* leaves were obtained from Durban, KwaZulu-Natal (SA), and verified by a herbarium (NH) (Accession number: 151125) (see Appendix A, Figure A4 for certification). All-trans-retinoic acid (ATRA, R2625) was purchased from Sigma-Aldrich (SA). Human HepG<sub>2</sub> cancer cells were purchased from Sigma-Aldrich (SA) [hepatocyte carcinoma (85011430-1V)] and donated by the Department of Medical Biochemistry and Chemical Pathology at the University of KwaZulu-Natal (SA). Cell culture consumables were purchased from Bio Smart Scientific (Cape Town, SA), Thermo Fisher Scientific Inc (Randburg, SA), Whitehead Scientific (Winelands, SA), and SPL Life Sciences (South Korea, online SA supplier).

### **3.3. Procedures and experimental techniques**

#### **3.3.1. Culturing human HepG<sub>2</sub> cancer cells**

Human hepatocellular carcinoma cells (Sigma-Aldrich, 85011430-1V), HepG<sub>2</sub> cells, were immortalised cells derived from a liver biopsy of a 15-year-old Caucasian male. These cells are routinely used as an *in vitro* model to study various aspects of liver biology, including liver metabolism, drug metabolism, hepatotoxicity, and liver diseases, and to determine the effects of bioactive compounds on the progression of HCC (Martín-Renedo et al., 2008; Tabboon et al., 2016; Tiloke et al., 2019). The human HepG<sub>2</sub> cancer cells were cultured, as described by Tiloke and colleagues (Tiloke et al., 2019). The cells were received in a cryovial tube containing approximately  $1 \times 10^6$  HepG<sub>2</sub> cells and stored at -80°C until ready to use. Complete

culture media (CCM) consisting of Eagle's minimum essential medium (EMEM) (Sigma-Aldrich, 51416C), 10% foetal bovine serum (Life Cell Technology, LS-1012), 1% L-glutamine (ThermoFisher Scientific, 25030149), and 1% penicillin streptomycin-fungizone (Sigma-Aldrich, P4333) was prepared. The CCM was aliquoted into 50 mL conical tubes (SPL Life Sciences, 50050) and stored at 4°C until ready to be used. The CCM was pre-warmed to 37°C using a Dri-Block® (Techne®, DB200/3) for 20 minutes before being used. Pre-warmed CCM (15 mL) was added to a 75 cm<sup>3</sup> filter-capped cell culture flask (T75) (SPL Life Sciences, 70075). The cell suspension was rapidly thawed at room temperature (RT) before gently adding it to the T75 flask containing the pre-warmed CCM. The cells were placed in a humidified incubator (Heal Force, HF240) at 37°C with 5% CO<sub>2</sub> for 24 hours. Following the 24-hour cell attachment period, CCM was removed from the flask using a 10 mL serological pipette, and 5 mL of pre-warmed phosphate-buffered saline (PBS) was added to the flask (ThermoFisher Scientific, 10010049). The flask containing the PBS was gently swirled for one minute to rinse the flask surface. The PBS was removed using a 10 mL serological pipette before adding 5 mL fresh pre-warmed PBS to the flask. This rinsing step was repeated three times. Following the final rinse step, the PBS was removed, and 10 mL pre-warmed CCM was added to the flask. The flask was placed in a humidified incubator at 37°C with 5% CO<sub>2</sub>. The rinsing process was repeated, and the CCM was replaced every 2 to 3 days until the cells reached 80% confluency.

### 3.3.2. *Moringa oleifera* aqueous leaf extract preparation

The verified MO leaves were air-dried and crushed into a fine powder using a pestle and mortar. The primary researcher weighed 10 g of the MO leaf powder using an Adam Equipment (HCB 123) scale in a 100 mL beaker. Following this, 100 mL of

distilled water (dH<sub>2</sub>O), purified using the Labotec (PTY) LTD Water Puri System, was added to the beaker. The mixture was boiled using a magnetic heating stirrer (Heidolph, MR2002) at 100°C at 750 revolutions per minute (rpm) for 20 minutes. The mixture was then transferred into 50 mL conical tubes. The conical tubes containing the MO leaf powder and dH<sub>2</sub>O mixture were centrifuged (Hermle Labortechnik GmbH, Z 32 HK) at RT for 10 minutes at 2000 rpm. The supernatant was transferred into 15 mL conical tubes (SPL Life Sciences, 50015) (2 mL of the supernatant was added to each conical tube) and stored at -20°C, at a 45° angle, on a plastic 15 mL conical tube rack, until completely frozen. The supernatant was lyophilised as follows: the benchtop freeze-drying system (VirTis, 2KBTXL) attached to the freeze-drying pump (Telstar®, 2F10) was allowed to acclimatise to the desired freeze-drying conditions (-75°C to -79°C, and 10 mTorr vacuum pressure). The lid of each conical tube was replaced with a perforated aluminium foil to expose the tubes' contents to freeze-drying conditions while simultaneously preventing the contents from being expelled from the tubes. The tubes were placed into the freeze-drying machine. The contents of the tubes were lyophilised under the above-stated conditions for 24 hours. Subsequently, the MO aqueous leaf extract powder containing tubes was retrieved, the aluminium foil was replaced with the original tube lids, wrapped with parafilm, and the tubes were stored at 4°C until ready to use. To prepare the MO aqueous treatment solution, 40 mg of the MO aqueous leaf extract powder was diluted with 4 mL pre-warmed CCM to form a 10 mg/mL stock solution. This solution was then filter-sterilised using a Zhejiang Ini Medical Devices (HSCS500) 5 mL syringe attached to a 0.22 µm Bio Smart Scientific CA syringe filter (FBS25CA022S). The stock solution was added and passed through the filter at 1 mL intervals. Once filtered, the solution was adjusted to its desired

concentration by diluting it with pre-warmed CCM using the following equation:

$$\frac{\text{Treatment concentration} \times \text{Treatment media volume}}{\text{concentration of stock solution}}.$$

### 3.3.3. Inhibition of CMA activity

According to previous studies, the mechanism of CMA inhibition involves the activation of the RAR $\alpha$  by ATRA, inhibiting CMA activity by altering LAMP2A expression at the lysosomal membrane (Anguiano et al., 2013; Nguyen et al., 2019; Robert et al., 2019). Studies have shown that increased levels of LAMP2A expression are associated with enhanced CMA activity. When CMA is upregulated, more LAMP2A receptors are available on the lysosomal membrane, allowing for increased targeting and degradation of CMA-specific proteins (Patel and Cuervo, 2015).

#### 3.3.3.1. *ATRA preparation*

ATRA was purchased in powder form from Sigma-Aldrich (R2625) as a 100 mg ampule. The 100 mg ATRA powder was dissolved in 6658  $\mu$ L dimethyl sulfoxide (DMSO) (Sigma-Aldrich, D2650) to produce a 50 mM stock solution. The stock solution was aliquoted into 2 mL microcentrifuge tubes (LightSafe<sup>®</sup>) and stored them at -20°C until ready to use. For experiments, the ATRA solution was adjusted to the desired concentration with pre-warmed CCM using the following equation:

$$\frac{\text{Treatment concentration} \times \text{Treatment media volume}}{\text{concentration of stock solution}}.$$

### 3.3.4. Assessment of cell viability

The inhibition concentration 50 (IC<sub>50</sub>) of ATRA and MO aqueous leaf extract was determined by assessing the cytotoxicity of the respective agents (MO and ATRA) on

HepG<sub>2</sub> cancer cells using the 2-(4-iodophenyl)-3-(4-nitrophenyl)-5-(2,4-disulfophenyl)-2H-tetrazolium, monosodium salt (WST-1) Cell Proliferation Assay (ab155902). The WST-1 assay is a well-established calorimetric assay used to measure cell viability and proliferation (Peskin and Winterbourn, 2000; Ranke et al., 2004). This assay is based on the cleavage of the tetrazolium salt, WST-1, to produce formazan by various mitochondrial dehydrogenase enzymes in metabolically active cells (Peskin and Winterbourn, 2000). The assay indirectly measures cell viability by assessing the activity of cellular enzymes involved in mitochondrial electron transport, with an increase in metabolically healthy cells typically accompanied by an increased absorbance signal detected at a wavelength of 450 nm (Ranke et al., 2004).

The assay was conducted as per the manufacturer's instructions (ab155902). Cultured cells were seeded into a 96-well clear microplate and incubated for 24 hours in a humidified incubator at 37°C with 5% CO<sub>2</sub>. The cells were seeded as follows: 15 000 cells per well were suspended in 150 µL pre-warmed CCM. A total of 30 wells were prepared for MO and ATRA treatments (control and 9 variable concentrations in triplicate). Following the 24-hour incubation, CCM was removed, and each well was rinsed with 100 µL of pre-warmed PBS. The PBS was removed, and the rinse step was repeated 2 times. After the final rinse, the PBS was removed, and the plate was inverted and tapped gently on a sterile paper towel to remove the residual PBS. The cells were treated as follows: for MO aqueous leaf extract, the treatment concentrations ranged from 0 to 10,000 µg/mL, including 100, 500, 1000, 1500, 2000, 2500, 5000, 7500, and 10000 µg/mL. For ATRA, the treatment concentrations ranged from 0 to 500 µM, including 100, 150, 200, 250, 300, 350, 400, 450, and 500 µM. All the treatment concentrations were prepared in CCM, adding 200 µL of each treatment

concentration to their respective wells in triplicate. The 96-well plate was then incubated for 24 hours in a humidified incubator at 37°C with 5% CO<sub>2</sub>. Following the 24-hour incubation, the plates were rinsed 3 times with pre-warmed PBS, as described above. Following the final rinse, 200 µL of pre-warmed CCM and 10 µL of WST-1 reagent at RT was added to each well. The 96-well plate was covered with aluminium foil and gently shaken for 5 minutes on an IKA® VRX basic Vibrax® orbital shaker (IKA 2819001). The plate was incubated for 2 hours in a humidified incubator at 37°C with 5% CO<sub>2</sub>. The absorbance was then measured at 450 nm and a reference wavelength of 600 nm with the Promega GloMax® Discoverer (GM3000) microplate reader. Cytotoxicity was assessed by comparing the results of the experimental group to the control group to determine the IC<sub>50</sub> of the aqueous leaf extract of MO extract and ATRA. The respective IC<sub>50</sub> values were used for all downstream experiments.

### 3.3.5. Human HepG<sub>2</sub> cell experimental treatment groups

The cells were allocated to four experimental groups (three treatment groups and an untreated group), as described in Table 3.1. Cell treatments were conducted for 24 hours in 25 cm<sup>3</sup> cell culture flasks (T25) (SPL Life Sciences, 70025) and T75 cell culture flasks (see Appendix B for detailed treatment protocol).

**Table 3.1: Experimental groups**

Groups	Group description
1	24-hour Control group
2	24-hour MO treatment group (per the pre-determined IC <sub>50</sub> )
3	24-hour ATRA treatment group (per the pre-determined IC <sub>50</sub> )
4	24-hour (MO + ATRA) combination treatment group

### 3.3.6. Assessment of apoptosis markers

The activation of caspase-9 disrupts mitochondrial function, which initiates apoptosis in the affected cells (Brentnall et al., 2013; Li et al., 2015a). Once initiated, caspase-3 and/or caspase-7 execute apoptosis (Li et al., 2015a). These are key events in the process of apoptosis, resulting in the degradation of the mitochondria and the subsequent onset of cell death (Brentnall et al., 2013).

#### i. *Caspase-Glo 3/7 assay reagent*

In order to assess caspase-3/7, cells were treated in T75 cell culture flasks, according to their respective treatment groups, at ~ 80% confluency. The cells were exposed to various treatment compounds for 24 hours in a humidified incubator at 37°C with 5% CO<sub>2</sub>. The cells were trypsinized after treatment, and the cell suspension was removed. A cell count was then performed using a TC20™ Automated Cell Counter (Bio-Rad Laboratories, Inc., 145-0101) to determine the number of cells from each treatment flask (see Appendix B for detailed cell removal and cell count protocol). Cells from each treatment group were seeded into a white 96-well plate in triplicate (20 000 cells per well). Additional PBS was added to each well to ensure that each well had a 50 µL total volume of 20 000 cells suspended in PBS. The same volume of prepared

caspase 3/7 reagent was added to each well. The 96-well plate was then covered in foil, gently shaken, and incubated for 30 minutes away from light at RT. Following this, the luminescence of the plate was measured using the GloMax<sup>®</sup> multiplate reader at 560 nm.

ii. *Caspase-Glo 9 assay reagent*

The activity of caspase-9 was measured using the same procedure described for caspase-3/7. However, the Promega Caspase-Glo<sup>™</sup> 9 Assay Kit (G8210) was used, and the assay reagent was prepared per the manufacturer's instructions (Caspase-Glo<sup>®</sup> 9 Assay Technical Bulletin TB333).

3.3.7. Assessment of CMA markers

The binding of sequestered substrate proteins to the cytosolic tail of LAMP2A is defined as the rate-limiting step for CMA activity (Cuervo and Dice, 2000b; Juste and Cuervo, 2019). Therefore, LAMP2A expression is used as a surrogate marker for CMA activity (Juste and Cuervo, 2019). The HK2 proto-oncogenic protein plays a role in the sustained proliferation of various types of cancerous cells (Xia et al., 2015). More importantly, HK2 is also targeted for degradation through the CMA pathway, particularly in cancer cell lines, including HepG<sub>2</sub> (Galan-Acosta et al., 2015; Xia et al., 2015).

i. *ELISA – Quantification of LAMP2A expression*

Cultured cells were treated (see Table 3.1) and incubated for 24 hours in a humidified incubator at 37°C with 5% CO<sub>2</sub>. Following treatment, the treatment media was removed, transferred into 15 mL conical tubes, and stored at -20°C until the assay was

ready to be performed. The tubes were thawed at RT and centrifuged for 20 minutes (2000 rpm, RT) to pellet the cellular debris. The supernatant was then removed and centrifuged again under the same conditions. The ELISA was carried out using the Human LAMP2/CD10b ELISA Kit (ThermoFisher Scientific, EH295RB) to quantify the expression of LAMP2A. In preparation for this assay, 1X Washer Buffer, 1X Assay Diluent B, 1X Assay Diluent D, biotin conjugate, 1X Streptavidin-horseradish peroxidase (HRP) and standard solutions were prepared as per the manufacturer's instructions (EH295RB) (see Appendix for detailed preparation protocol).

The assay was performed in a 96-well plate as follows: 100  $\mu$ L of each standard was added to the appropriate wells in duplicate. The same volume of RT samples was added to the appropriate wells in triplicate. The plate was then covered with the provided adhesive plate cover and incubated for 2 and a half hours at RT with gentle shaking on the orbital shaker. After the incubation period, the solutions were removed. Each well was washed three times with 200  $\mu$ L 1X Wash Buffer by filling the wells with the wash buffer solution, gently shaking the plate and removing the wash buffer before repeating the steps 2 more times. After the wash buffer was removed following the final wash, the plate was inverted on a sterile paper towel and blotted to ensure the complete removal of the wash buffer, thus completing the washing procedure. Following this washing, 100  $\mu$ L of the biotin conjugate was added to each well. The plate was covered and incubated for one hour at RT with gentle shaking. Following the incubation, the biotin conjugate was removed from each well. The wells were washed using the 1X Wash Buffer as previously described, and 100  $\mu$ L of the prepared Streptavidin-HRP solution was added to each well. The plate was covered and incubated at RT for 45 minutes with gentle shaking. Following the incubation, the

Streptavidin-HRP solution was removed from each well. The wells were washed using the 1X Wash Buffer as previously described. Subsequently, 100 TMB Substrate was added to each well. The plate was then covered and incubated away from light for 30 minutes at RT with gentle shaking. Following the incubation, 50  $\mu$ L Stop Solution was added to each well. The plate was then tapped gently to mix the solutions. The absorbance was read at 450 nm using the GloMax<sup>®</sup> microplate reader.

ii. *Western blot – Quantification of LAMP2A, HSC90, HK2 protein expression*

Western blotting was performed to determine LAMP2A, HSC90, and HK2 protein expression. Following the respective cell treatments, protein isolation was performed, and the protein concentration was quantified using the bicinchoninic acid (BCA) assay, Pierce<sup>™</sup> BCA Protein Assay Kit (ThermoFisher Scientific, 25225). The BCA protein quantification assay was performed as follows: The HepG<sub>2</sub> liver cancer cells were cultured in 75 cm<sup>3</sup> cell culture flasks until 90% confluency. When at the desired confluency, the cells were treated and exposed for 24 hours to their respective treatment media. Following the 24 hours, the treatment media was removed and stored at -20°C. 5 mL of cold PBS was then added to each flask. The cap of each flask was replaced, and the flasks were swirled for 1 minute. Following the wash, the PBS was removed. Then, 500  $\mu$ L of cold cell lytic solution was added to each flask. The cell lytic solution was prepared as follows: in a 15 mL conical tube wrapped in aluminium foil, 5 mL of CellLytic<sup>™</sup> M (Sigma, C2978) and 50  $\mu$ L of Halt<sup>™</sup> Protease Inhibitor Cocktail, EDTA-Free (ThermoFisher, 78437) were added. Once the prepared cell lytic solution was added to the cell culture flask, the flasks incubated for 30 minutes at RT with gentle shaking, using an orbital shaker. Following the incubation, cell scrapers were used to lyse the cells. The cell lysates were added to microcentrifuge tubes and

centrifuged for 15 minutes at 12000 g at 4 °C. The supernatant of each cell lysate was then stored at -80°C until needed. To quantify the protein, a Pierce™ Bicinchoninic Acid (BCA) assay (ThermoFisher Scientific, 25225) was performed according to the manufacturer's instructions as follows: standards were prepared according to Table B1. The volume of BCA working reagent (WR) required was calculated as follows:

(number of standards + number of samples) + number of replicates +  
Volume of WR required per sample, where the number of standards was 9, the number of samples was 4 (4 experimental groups), the number of replicates was 3, and volume of WR required per sample was 200 µL.

The WR reagent was prepared by mixing 50 parts of Reagent A and 1 part of Reagent B in a 15 mL conical tube. The tube was wrapped in aluminium foil to keep it away from light. In a clear 96-well cell culture plate, 25 µL of the sample standards were added to their respective wells in triplicate. The protein lysate samples were thawed on ice. 25µL of each sample was added to each respective well in triplicate. Then, 200 µL of the prepared WR was added to each standard and sample well. The plate lid was then replaced before it was shaken gently on an orbital shaker for 30 seconds at RT, in the dark. The plate was then removed and incubated at 37°C for 30 minutes. Following the incubation, the plate was allowed to cool to RT before it the absorbance was measured at 560 nm using the GloMax plate reader. The average of the absorbance values of the standards were then normalized using the average Blank Standard absorbance values. The normalized averages were used to create a standard curve (see Figure B3 for example) which was used to extrapolate the concentration of the samples.

The western blot experiment was performed as follows: the cell lysate samples were thawed on ice and standardised to 687.28 µg/mL using the prepared cell lytic solution (see Appendix B for the cell lytic preparation protocol). An equal volume (14 µL) of the sample and Laemmli loading buffer (see Appendix B for the Laemmli loading buffer preparation protocol) were added to each pre-chilled microcentrifuge tube. The Laemmli loading buffer (composed of 2X Laemmli sample buffer and 2-Mercaptoethanol) was added to ensure efficient separation of proteins along the Sodium Dodecyl Sulfate-Polyacrylamide Gel Electrophoresis (SDS-PAGE) gels. The samples and loading buffer mixture were then heated at 100°C for 5 minutes using a digital heat block (Benchmark Scientific Inc, BSH1002-E). The 10% Precast Mini-Protein TGX Stain-Free Fast Cast SDS-PAGE gels (Bio-Rad Laboratories, Inc., 4561033) were placed in a Mini-PROTEAN Tetra System SDS-PAGE tank (Bio-Rad Laboratories, Inc.) and filled with cold SDS running buffer (see Appendix B for details regarding the running buffer preparation protocol), which was also added to the cassette inner chamber. Each gel's first and sixth lanes were loaded with 10 µL of the molecular weight marker (MWM), Precision Plus Protein™ (Bio-Rad Laboratories, Inc., 1610373). In total, 28 µL of the sample and loading buffer mixture was added to each lane of each gel well (the samples were loaded per treatment group; see Table 3.2). Once all samples were loaded, the appropriate amount of cold running buffer was added to the outer chambers of the SDS-PAGE tank and proteins were separated at 150 V for 70 minutes using a PowerPac™ Basic Power Supply (Bio-Rad Laboratories, Inc., 1645050) until the Laemmli loading buffer reached the bottom of the gel.

**Table 3.2: Precast gel arrangement of wells (loading sequence)**

Well Number	1	2	3	4	5	6	7	8	9	10
Sample Loaded	MWM	C	MO	ATRA	M + A	MWM	C	MO	ATRA	M + A

Abbreviations: MWM, Molecular weight marker; C, Control; MO, *Moringa oleifera*; ATRA, All-trans-retinoic acid; M+A, (MO+ATRA) combination

Following the electrophoresis, the stain-free function of the gel was activated on a ChemiDoc MP Imaging System (Bio-Rad Laboratories, Inc., 12003154). The activation step is an essential part of the staining process for Stain-Free TGX gels. During activation, a specific wavelength of UV light (usually 302 nm) is applied to the gel for a short period. The UV light activates a fluorescent compound incorporated into the gel matrix, covalently binding to tryptophan protein residues within the gel. Subsequently, the resolved proteins were electro-transferred onto Trans-Blot Turbo Transfer Pack (Bio-Rad Laboratories, Inc., 1704158) PVDF (Polyvinylidene fluoride) nitrocellulose membrane using a Trans-Blot® Turbo™ Transfer System (Bio-Rad Laboratories, Inc., 1704150) for three minutes at 2.5 A and 25 V. The PVDF membrane was then washed three times for 5 minutes as follows: using forceps, the membrane was placed in a flat bottom container with 15 mL 1X tris-buffered saline and Tween 20 (TBST) wash buffer (see Appendix B for detailed wash buffer preparation protocol). After each wash cycle, the wash buffer was replaced with fresh 1X TBST wash buffer. The PVDF membrane was then blocked with 5 mL EveryBlot Blocking Buffer (Bio-Rad Laboratories, Inc., 12010020) for 15 minutes with gentle shaking. Following this, the blocking buffer was removed. The PVDF membrane was then incubated with the first

primary (1°) antibody, the Anti-Hexokinase II antibody. The 1° antibodies were prepared (see Table 3.3), and the PVDF membrane was incubated at 4°C overnight with this 1° antibody. After the incubation period, the membrane was allowed to acclimatise to RT. The 1° antibody was then removed, and the membrane was washed three times using wash buffer as previously described. After the final wash step, the PVDF membrane was incubated with 5 mL of the anti-IgG, HRP-linked antibody, and secondary (2°) antibody at RT for 2 hours, with gentle shaking. The 2° antibody was prepared as outlined in Table 3.3.

The 2° antibody was removed, and the membrane was rinsed thrice with 1X TBST wash buffer. After the final wash step, the membrane was rinsed twice with dH<sub>2</sub>O for 5 minutes each time. After the final dH<sub>2</sub>O rinse, a stain-free image of the membrane was taken using the ChemiDoc MP Imaging System (Bio-Rad Laboratories, Inc., 12003154). The PVDF membrane was then exposed to 300 µL enhanced chemiluminescence Clarity™ Western ECL Substrate Chemiluminescence Reagent (Bio-Rad Laboratories, Inc.) utilising the Bio-Rad ChemiDoc™ imaging system to activate the protein signal. A 1:1 mixture of Clarity™ Western ECL Substrate Luminol/enhancer solution and Peroxide solution (Bio-Rad Laboratories Inc, 1705060) was prepared on the day of the imaging. The solution was kept away from light. Once the membrane was covered with the ECL substrate, a chemiluminescent image of the membrane was captured using the ChemiDoc System. Subsequently, the PVDF membrane was removed from the ChemiDoc System and placed in a flat bottom container containing 1X TBST wash buffer for 5 minutes with gentle shaking.

**Table 3.3: Primary antibody preparations**

Antibody	HK2 1° antibody	LAMP2A 1° antibody	Beta-actin ( $\beta$ - actin), biotin conjugate antibody	HRP-linked 2° antibody
Manufacturer	Sigma-Aldrich	ThermoFisher Scientific	Abcam	Abcam
Species produced in	Rabbit	Rabbit	Mouse	Goat
Catalogue #	SAB5700666	51-2200	ab173838	ab7074S
Dilution ratio: Antibody: EveryBlot blocking buffer	1:1000	2:1000	1:2000	1:5000
Volume of antibody added to 5 mL EveryBlot blocking buffer	5 $\mu$ L	10 $\mu$ L	2.5 $\mu$ L	1 $\mu$ L

*Membrane stripping and re-probing*

Following the final rinse step, the 1X TBST wash buffer was removed, and stripping buffer, which was prepared by mixing 2 mL of the Re-Blot Plus (Sigma-Aldrich, 2504) with 18 mL dH<sub>2</sub>O, was used to remove the first 1° antibody on the PVDF membrane. The membrane was incubated in 5 mL stripping buffer for 30 minutes at RT. The stripping buffer was discarded after the incubation period, and the PVDF membrane was blocked with EveryBlot blocking buffer as previously described. After blocking, the PVDF membrane was re-probed with the second 1° antibody (LAMP-2A Polyclonal Antibody (AMC2)) overnight at 4°C. The same steps were followed to obtain a chemiluminescent image of the membrane as described above after incubation with

the first 1° antibody. After capturing the image, the membrane was stripped as previously described. Following the blocking step, the membrane was incubated with horseradish peroxidase (HRP)-conjugated Anti-beta Actin antibody [BA3R] for one hour at RT with gentle shaking. In order to control for protein loading, all blots were probed for Beta-Actin protein. The Beta-actin antibody mixture was removed after the incubation period, and the membrane was rinsed twice with wash buffer for 5 minutes each time. Following the final rinse step, the membrane was rinsed twice with dH<sub>2</sub>O for 5 minutes each time before a stain-free image of the membrane was captured on the ChemiDoc. This was followed by adding ECL, as previously described. After obtaining the image, the membrane was rinsed once with a wash buffer for 5 minutes and probed for different target proteins as previously described.

#### *Quantification of protein band intensity*

The protein bands on the captured images were quantified using the Image Lab (Bio-Rad Laboratories, Inc., Version 6.1.0 build 7) software. They were refined in terms of their display use. The intensity values of the proteins of interest, measured in arbitrary units (a.u.), were normalised to the intensity value of their respective Beta-Actin loading control. These normalised protein intensity values were then exported to Microsoft Excel for additional processing before conducting statistical analysis using the appropriate tests. A minimum of three independent experiments were performed to ensure the reliability of the data.

### **3.4. Statistical analysis**

Statistical analyses were performed using the GraphPad Prism V9 software package (GraphPad Software, Inc., San Diego, CA). In order to ensure the reliability of the data, experiments were performed in triplicate and repeated three times. Data was recorded in spreadsheets and regularly backed up onto an external drive and a cloud-based system (Google Drive). All data sets were assessed for Gaussian distribution using the D'Agostino-Pearson normality test. Results were graphically presented as the mean  $\pm$  standard error of the mean of 3 independent experiments. The One-Way Analysis of Variance (ANOVA) was used to make pairwise comparisons between the means of multiple groups, and the Bonferroni Post Hoc Analysis was applied to reduce the risk of false positives in the statistical analysis. Results were considered statistically significant when  $p < 0.05$ . Statistical analysis was performed by the primary researcher in consultation with a biostatistician from the Department of Biostatistics at the UFS thus ensure rigorous oversight.

## CHAPTER 4

### RESULTS

#### 4.1. Introduction to results

In order to address the experimental questions, a comprehensive series of experiments were performed to determine the effects of ATRA and MO on cell viability. Additionally, the effects of simultaneous combination treatment with ATRA and MO, comparing that effect to the individual compounds (see Table 3.1), was investigated. In order to ensure the validity of the findings, various experimental protocols were performed. Furthermore, all experiments were conducted with a minimum of 3 independent experiments in triplicate to ensure reliability. All experimental treatments were maintained for 24 hours.

#### 4.2. Cell viability

To determine the  $IC_{50}$ , cultured human HepG<sub>2</sub> cancer cells were exposed to increasing concentrations of ATRA (0-500  $\mu$ M) and MO aqueous leaf extract (0-10000  $\mu$ g/mL) for 24 hours. Cell viability was assessed using a WST-1 reductive capacity assay following the treatment exposure time. This assay measured the ability of viable cells to reduce WST-1, providing a quantitative assessment of cell viability.

After 24 hours of exposure, the results revealed a concentration-dependent decline in cell viability following ATRA treatment exposure (Figure 4.2.1). At the lowest concentration of ATRA (100  $\mu$ M), the reductive capacity showed a slight increase (113.80%  $\pm$  0.1309%) compared to the control group. However, as the concentration of ATRA increased, a steady decline in reductive capacity was observed, with the 300

$\mu\text{M}$  treatment group demonstrating the lowest reductive capacity ( $69.42\% \pm 0.0744\%$ ) relative to the control group (Figure 4.2.1). The observed  $\text{IC}_{50}$  was  $1415 \mu\text{M}$ . The standard error of the mean (SEM) for all the concentrations is  $0.004021$ . In all subsequent experiments, HepG<sub>2</sub> cells were exposed to  $1415 \mu\text{M}$  ATRA treatment for 24 hours.

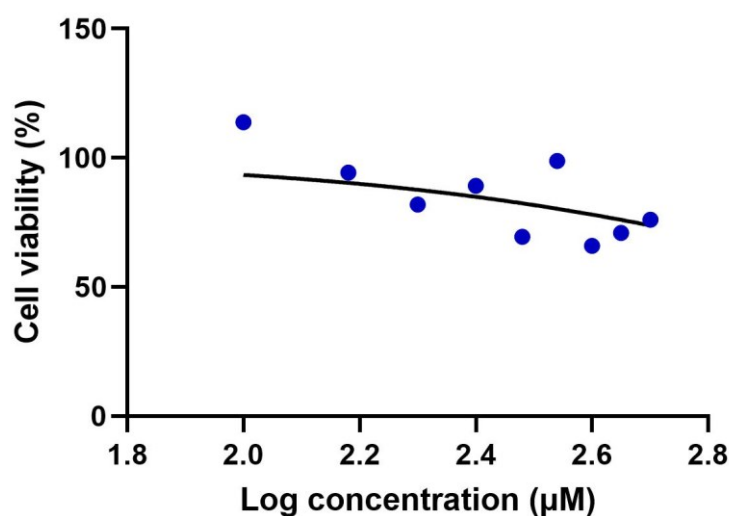


**Figure 4.2.1: The concentration-dependent effects of ATRA on HepG<sub>2</sub> cancer cell viability.** Cells were treated with 0-500  $\mu\text{M}$  ATRA for 24 hours. An  $\text{IC}_{50}$  of  $1415 \mu\text{M}$  was observed.

A similar trend was also observed following 24 hours of MO aqueous leaf extract treatment exposure. The reductive capacity slightly increased ( $110\% \pm 0.1906\%$ ) at the lowest ( $100 \mu\text{g/mL}$ ) MO aqueous leaf extract treatment concentration relative to the control (Figure 4.2.2).

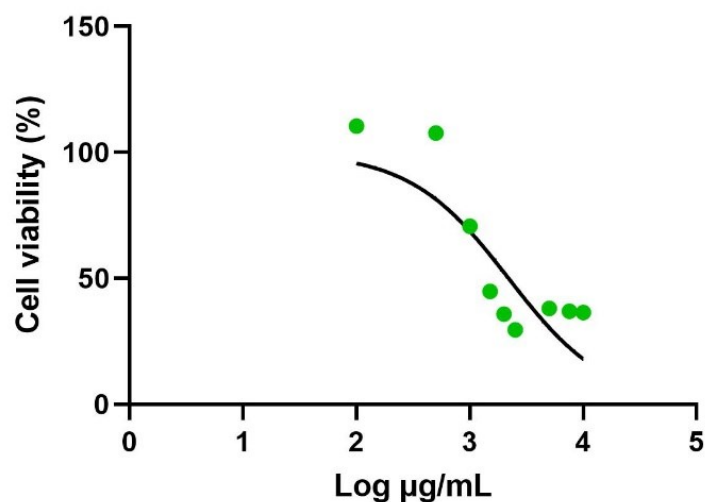


**Figure 4.2.2: The concentration-dependent effects of MO aqueous leaf extract on HepG<sub>2</sub> cancer cell viability.** Cells were treated with 0-10000  $\mu\text{g/mL}$  MO aqueous leaf extract for 24 hours. An  $\text{IC}_{50}$  of 2198 $\mu\text{g/mL}$  was observed.

Similar to the treatment effects of ATRA exposure, the reductive capacity continued to decline as the concentration of MO aqueous extract treatment increased. The group exposed to the highest concentration of MO aqueous extract (10000  $\mu\text{g/mL}$ ) showed a significant reduction in reductive capacity (36.40%  $\pm$  0.0040%) compared to the control group. The observed SEM for all the concentrations 0.00077. The observed  $\text{IC}_{50}$  was 2198  $\mu\text{g/mL}$ . In all subsequent experiments, HepG<sub>2</sub> cells were exposed to 2198  $\mu\text{g/mL}$  MO aqueous leaf extract treatment for 24 hours.

For all subsequent downstream experiments, the HepG<sub>2</sub> cells were allocated to four experimental groups, namely: (1) control, (2) ATRA treatment, (3) MO treatment, and (4) ATRA+MO combination treatment group.

### 4.3. The assessment of cell death markers

To assess the effects of treatment exposure (see Table 3.1) on HepG<sub>2</sub> cell death, apoptotic markers caspase-3/7 (effector caspases) and caspase-9 (initiator caspase) activity levels were measured. The level of caspase activity was measured as luminescence in relative light units (RLU).

A consistent decrease in caspase-9 activity was observed following 24-hour exposure to the respective treatments (see Table 3.1) relative to the control group (see Figure 4.3.1). The ATRA-treatment group revealed a 0.005 fold change ( $p < 0.0001$ ) in caspase-9 activity (RLU = 7556.3) relative to the control group (RLU = 1612667.0). The MO treatment group showed a 0.534 fold change ( $p < 0.0001$ ) in caspase-9 activity (RLU = 861200.0) compared to the control group. The ATRA+MO combination treatment group revealed a 0.005 fold change ( $p < 0.0001$ ) in caspase-9 activity (RLU = 8537.3) relative to the control group. The ATRA+MO combination treatment group also showed a significant decrease in caspase-9 activity (0.001 fold change,  $p < 0.0001$ ) compared to the MO treatment group. There was no significant difference between the ATRA and the ATRA+MO combination treatment group (Figure 4.3.1).

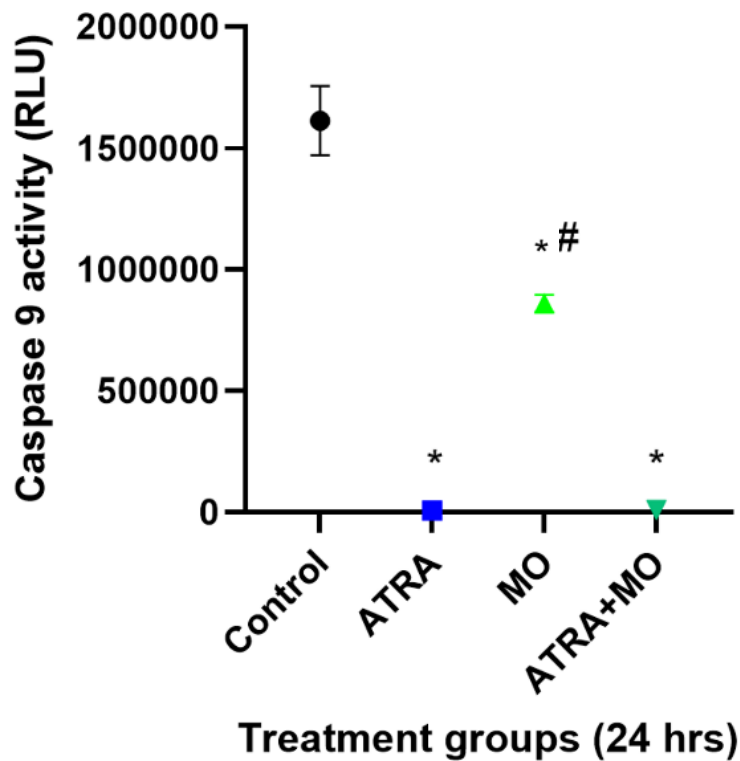


**Figure 4.3.1: Caspase-9 activity in HepG<sub>2</sub> cancer cells following treatment exposure to ATRA, MO and ATRA+MO combination treatment groups.** \* $p < 0.0001$  compared to the control group; # $p < 0.0001$  compared to the ATRA+MO combination treatment group.

The HepG<sub>2</sub> cells displayed changes in the downstream caspase-3/7 activity following 24-hour exposure to the respective treatments compared to the control group (Figure 4.3.2). The ATRA-exposed cells showed a significant decrease (0.242 fold change,  $p < 0.0001$ ) in caspase-3/7 activity (RLU = 3584.0) compared to the control (RLU = 14836.7) cells. Compared to the control cells, a decrease in caspase-3/7 activity was also seen following ATRA+MO combination treatment (RLU = 2971.0, 0.197 fold change,  $p < 0.0001$ ). MO exposure, however, resulted in a significant increase (1.468 fold change,  $p < 0.0013$ ) in caspase-3/7 activity (RLU = 21786.7) compared to the control cells. The ATRA + MO combination exposed cells showed a significant decrease (0.134 fold change,  $p < 0.0001$ ) in caspase-3/7 activity compared to the MO

treatment group. There was no significant difference between the ATRA and the ATRA + MO combination treatment group (Figure 4.3.2).

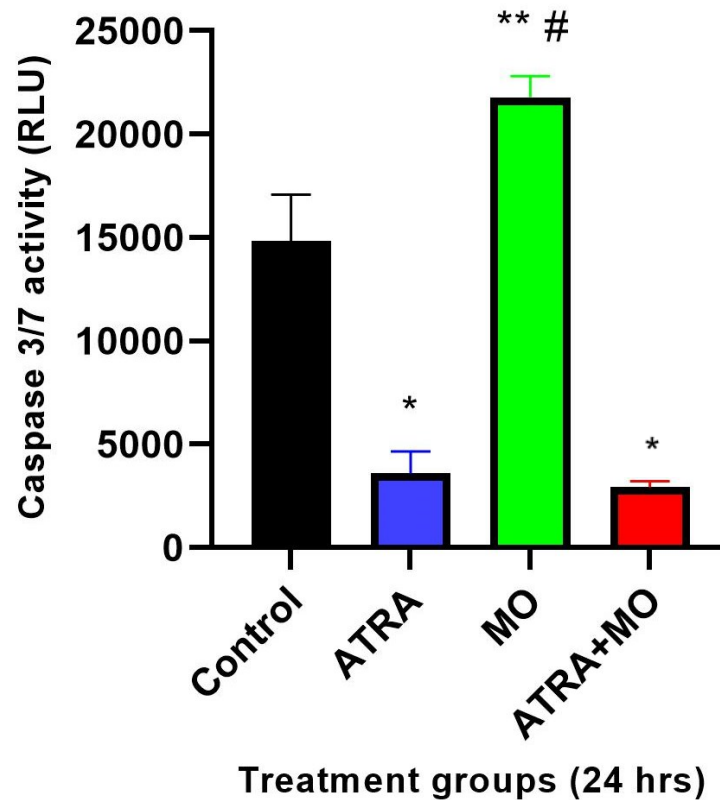


**Figure 4.3.2: Caspase-3/7 enzyme activity in HepG<sub>2</sub> cancer cells following treatment exposure to ATRA, MO and ATRA+MO combination treatment groups.** \*p<0.0001 compared to the control group; \*\*p<0.0013 compared to the control group; #p<0.0001 compared to the ATRA+MO combination treatment group.

#### 4.4. The evaluation of basal CMA activity

In order to assess the effect of ATRA and MO treatment exposure on basal CMA activity, LAMP2A expression was used as a marker of CMA activity following treatment exposure (see Table 3.1). A CMA-selective LAMP2A ELISA assay kit, a CMA-specific assay designed to measure the levels of LAMP2A isoform involved in CMA specifically, was used to quantify the level of CMA activity in response to 24-hour treatment exposure to ATRA, MO, and ATRA+MO combination treatment.

There were no significant differences in LAMP2A concentration observed following 24-hour treatment exposure (Figure 4.4)

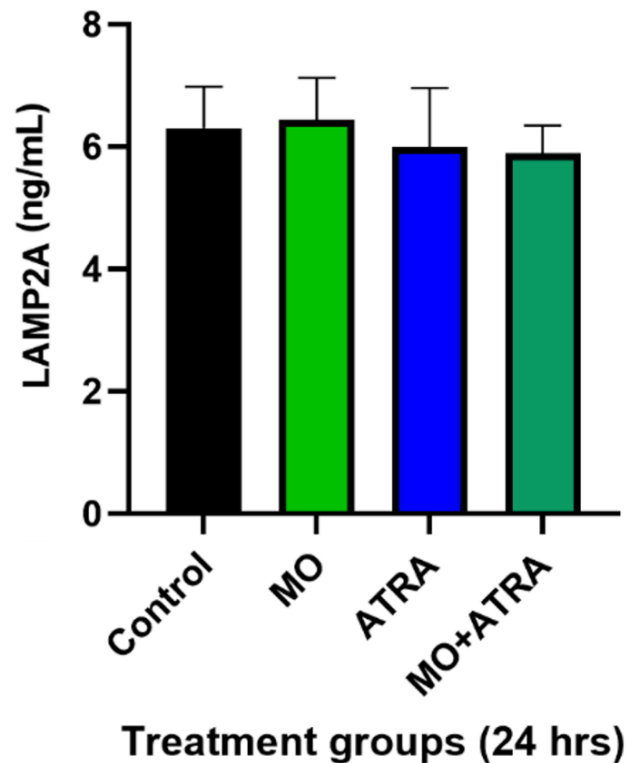


Figure 4.4: CMA-selective LAMP2A ELISA assay results. LAMP2A activity following 24-hour ATRA, MO, and ATRA+MO combination treatment ( $p > 0.05$ ).

#### 4.5. The assessment of CMA markers by western blotting

To further assess the effect of treatment exposure (see Table 3.1) on basal CMA activity, western blot analysis was performed using anti-LAMP2A and anti-HK2 antibodies (see Table 3.3). HK2 is a cargo protein involved in CMA, while LAMP2A is a specific receptor protein on the lysosomal membrane for CMA. Using western blot, the expression of these proteins was quantified as markers for CMA activity in response to 24-hour treatment exposure to ATRA, MO, and ATRA+MO combination treatment.

#### 4.5.1. *Preliminary western blot results*

The preliminary results revealed a decline in LAMP2A expression following MO treatment exposure (0.759 fold change) compared to the control. Similarly, a decline in LAMP2A expression was observed following ATRA treatment exposure (0.400 fold change) compared to the control. A decline in LAMP2A expression following ATRA+MO combination treatment exposure (0.212 fold change) compared to the control was also observed. In addition, the LAMP2A expression was lower following ATRA+MO combination treatment exposure compared to the MO treatment group (0.279 fold change) and compared to the ATRA treatment group (0.529 fold change) (Figure 4.5.1).

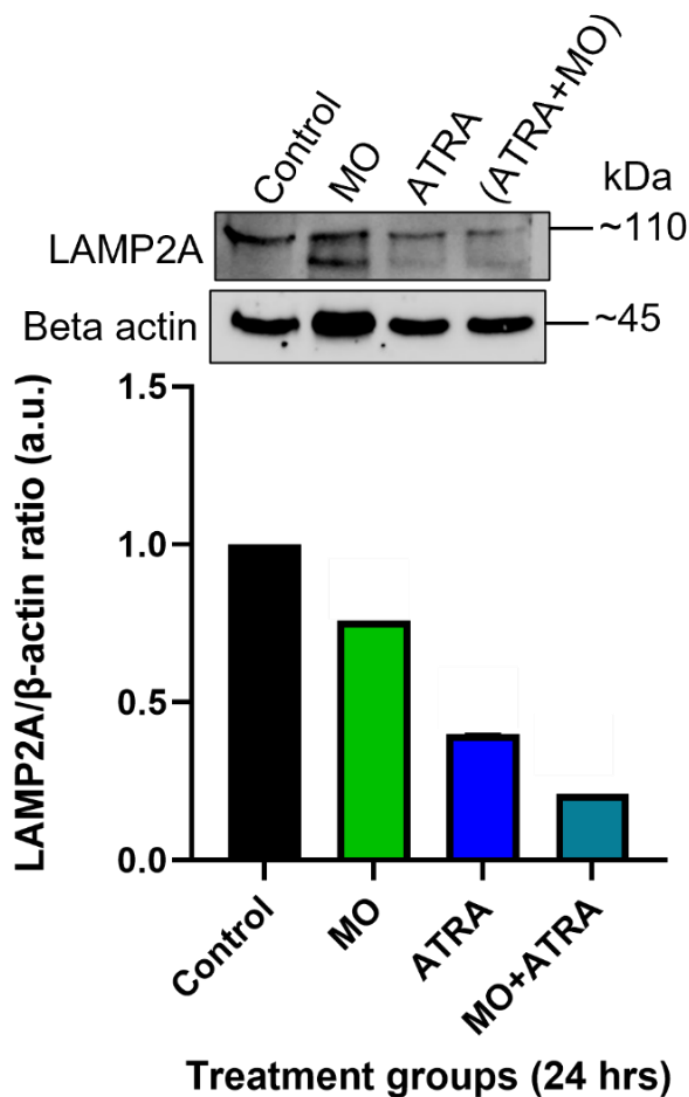


**Figure 4.5.1: LAMP2A expression in HepG<sub>2</sub> cancer cells following treatment exposure to ATRA, MO and ATRA+MO combination treatment groups.** Protein expression densitometric analysis (A) and representative western blot (B) for LAMP2A protein expression is shown. *n*=1

An increase in HK2 expression was observed following MO treatment exposure compared to the control (42.210 fold change). A more considerable increase in HK2 expression was observed following ATRA treatment exposure compared to the control (82.357 fold change). An even greater increase in HK2 expression following ATRA+MO combination treatment exposure was observed compared to the control (111.783 fold change). The HK2 expression was the highest in the ATRA+MO

combination treatment exposed HepG<sub>2</sub> cells with a 2.648 fold change compared to the HK2 expression in the MO treatment exposed cells. The increase in HK2 expression of the ATRA+MO combination treatment exposed cells was less severe when compared to the HK2 of the HepG<sub>2</sub> cells following ATRA treatment exposure (1.357 fold change) (Figure 4.5.2).

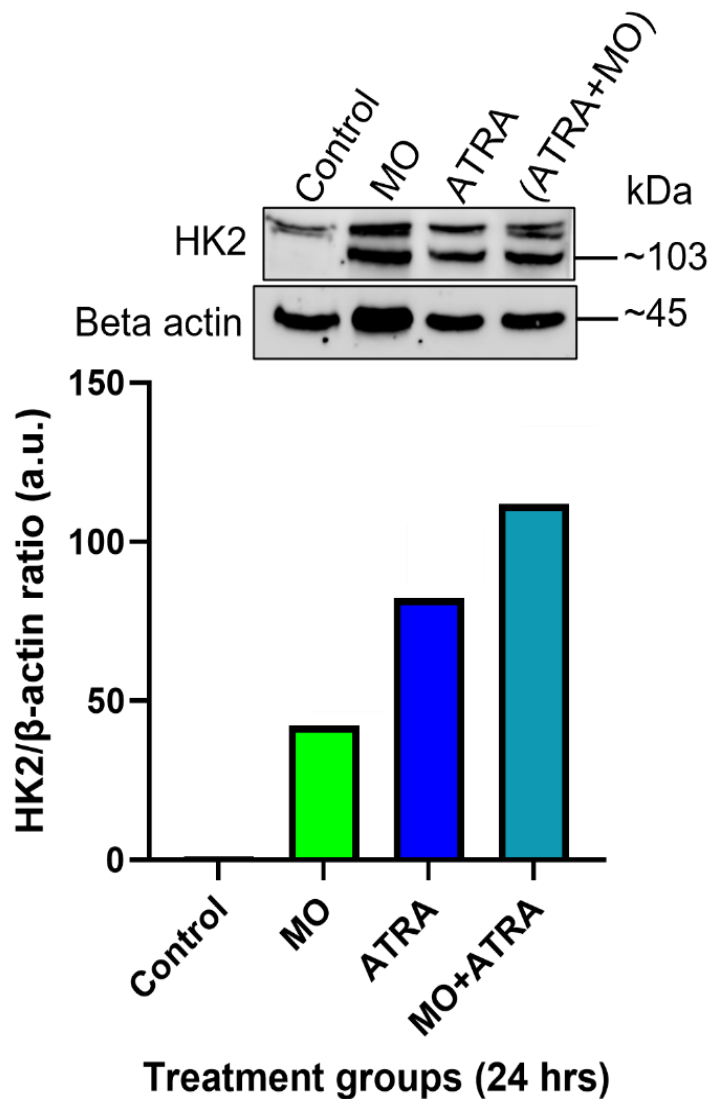


**Figure 4.5.2: HK2 expression in HepG<sub>2</sub> cancer cells following treatment exposure to ATRA, MO and ATRA+MO combination treatment groups.** Protein expression densitometric analysis relative to the control (A) and representative western blot (B) for LAMP2A protein expression is shown. *n*=1

## CHAPTER 5

### DISCUSSION

#### 5.1. Introduction to discussion

Hepatocellular carcinoma (HCC) is the most prevalent type of primary liver cancer and the second-highest contributor to global cancer-related deaths (McGlynn et al., 2021). Regionally, South Africa (SA) has one of the highest HCC prevalences. The high prevalence of HCC can be attributed, in part, to the increased incidence of prominent risk factors (Liu et al., 2015; Maponga et al., 2020; Waller et al., 2015). Among these risk factors, hepatitis B virus (HBV) infection accounts for up to 60% of HCC cases in developing countries, where HCC presents a significant threat (Kew, 2012; Maponga et al., 2020). Additionally, the high number of human immunodeficiency virus (HIV) cases in SA may further exacerbate the burden of HCC, as HIV is particularly prevalent within the country (Maponga et al., 2020; Randall, 2017).

SA has the fourteenth-highest prevalence of HCC; however, it is the seventh-largest contributor to global HCC-related deaths (Zakharia et al., 2018). This persistent healthcare challenge is compounded by socioeconomic factors and healthcare challenges, leading to an underestimation of the true epidemiology of this disease (Kew, 2013; Lemoine et al., 2013; Zakharia et al., 2018). Advancements have been made in treating HCC, including the FDA approval of Sorafenib – the only chemotherapeutic drug approved for the treatment of HCC (Chen et al., 2014; Gillman et al., 2021). However, the treatment of HCC remains a significant public healthcare challenge owing to its numerous limitations. These limitations include the occurrence of metastasis, the development of acquired resistance and the associated Sorafenib

treatment side effects, including cardiovascular, dermatological, renal and gastrointestinal complications (Li et al., 2015b; Oishi and Wang, 2011; Tang et al., 2020).

Although the precise molecular mechanisms underlying the development of HCC still need further clarification, several cell signalling pathways are increasingly investigated for their role in HCC progression (Alqahtani et al., 2019; Aravalli et al., 2008). Among these pathways, autophagy pathways have notably emerged as an area of intense research interest, as the dysregulation of selective autophagic pathways has been implicated in the progression of HCC (Bao et al., 2014; Kon et al., 2011; Saha et al., 2018). Specifically, chaperone-mediated autophagy (CMA), one of the three main autophagic pathways, has been demonstrated to play a significant role in HCC tumorigenesis (Ding et al., 2016; Guo et al., 2017; Kon et al., 2011). Although CMA is upregulated in numerous cancerous cells, including HCC, its precise contribution to HCC progression remains fully elucidated (Kon et al., 2011). Therefore, targeting CMA in HCC presents a promising avenue for potential adjuvant therapeutic strategies (Robert et al., 2019). Several studies have highlighted the anti-cancer properties of the medicinal plant, *Moringa oleifera* (MO), against several cancers, including HCC (Ahmed et al., 2020; Siddiqui et al., 2021; Sreelatha et al., 2011; Tiloke et al., 2019). The MO plant is saturated with phytochemical compounds which display anti-cancer properties, with the leaves having the highest abundance of these compounds (Ahmed et al., 2020; Khor et al., 2018). In light of these considerations, the present study aimed to investigate the effect of all-trans-retinoic acid (ATRA) and MO on CMA activity in HepG<sub>2</sub> cancer cells. ATRA has been identified as a CMA chemical modulator, making it a promising compound for studying the effects of CMA inhibition on the survival and

progression of HCC cells (Anguiano et al., 2013; Arias, 2015; Lee et al., 2017; Robert et al., 2019). Additionally, this study explored whether CMA activity influences the pro-death role of MO in HepG<sub>2</sub> cells by examining the possible interaction between CMA and the effects of ATRA and MO, using human HepG<sub>2</sub> cells as an *in vitro* model for HCC.

## 5.2. Discussion

Several studies that have investigated the cytotoxic effects of ATRA have highlighted its ability to reduce cell viability in numerous cancer cell lines, including melanoma cell lines, Hep3B, and HepG<sub>2</sub> cells (Liu et al., 2016; Schmidt-Mende et al., 2006; Zhang et al., 2003; Zhu et al., 2019).

In this study, a concentration-dependent decline in the reductive capacity of HepG<sub>2</sub> cells was observed following 24-hour exposure to ATRA. This was observed as a reduction in HepG<sub>2</sub> cell viability as the ATRA concentration was increased, as shown in Figure 4.2.1. Similar findings were reported by Wu and colleagues who observed ATRA treatment inhibited the proliferation and migration of SMMC-7721 hepatocarcinoma cells in a concentration- and time-dependent manner (Wu et al., 2006). Consistent with these findings, a study by Arce and colleagues showed that 72-hour ATRA (50 µg/ml) exposure significantly reduced the cell viability of HepG<sub>2</sub> cells (Arce et al., 2005). Hep<sub>3</sub>B liver cancer cells were more susceptible to ATRA treatment, with an observed ±50% drop in cell viability following 72-hour 10 µg/mL ATRA treatment exposure (Arce et al., 2005). Interestingly, in the current study, a slight increase in reductive capacity was observed at the lowest concentration of ATRA (100 µM), which is consistent with previous findings where low concentrations of ATRA (10–

50  $\mu\text{M}$ ) initially increased reductive capacity, followed by a decline at higher concentrations (100–1000  $\mu\text{M}$ ) (Al-Sheddi et al., 2015). Similarly, Arce and colleagues also reported little to no effect on the cell viability of HepG<sub>2</sub> cells following exposure to low concentrations (0-50  $\mu\text{M}$ ) of ATRA with the lethal concentration of 50 of 130  $\mu\text{M}$  (Arce et al., 2005). These findings strongly support the concentration-dependent inhibitory effect of ATRA on the viability of HepG<sub>2</sub> cancer cells.

The current study demonstrated a concentration-dependent decline in cell reductive capacity following 24-hour MO aqueous leaf extract treatment exposure (Figure 4.2.2). These findings align with previous research conducted by Sreelatha and colleagues demonstrating a concentration-dependent decline in human epithelial carcinoma cells upon exposure to MO aqueous leaf extract treatment (Sreelatha et al., 2011). Tiloke and colleagues also reported a similar concentration-dependent decline in HepG<sub>2</sub> cell viability following 24-hour MO aqueous leaf extract exposure (Tiloke et al., 2019). These consistent results indicate that MO treatment leads to a concentration-dependent reduction in the viability of HepG<sub>2</sub> cells. Similar, to ATRA, these findings suggest that both MO and ATRA can potentially negatively affect the survival of HepG<sub>2</sub> cells.

Excessive proliferation and the avoidance of apoptosis are one of the hallmarks of tumorigenesis and have therefore been the focus of various chemotherapeutic approaches (Blank and Shiloh, 2007; Fabregat, 2009; Rathore et al., 2017). MO leaves contain antioxidative phytochemicals that have been shown to induce apoptosis in numerous cases (Adebayo et al., 2017; Ahmed et al., 2020; Tiloke et al., 2018). Various studies have also reported on ATRA's ability to induce apoptosis in

cancerous cells, including HepG<sub>2</sub> cells (Arce et al., 2005; Mangiarotti et al., 1996; Toma et al., 1997). Apoptosis is a controlled process regulated by caspase proteins and the Bcl-2 family of proteins (Blank and Shiloh, 2007). Activating these caspases is an integral part of apoptosis, making caspase activity closely associated with the level of apoptosis (Blank and Shiloh, 2007; Brentnall et al., 2013; Shi, 2004).

This study found a significant decline in caspase-9 activity, as shown in Figure 4.3.1 and caspase-3/7 (Figure 4.3.2), following ATRA exposure compared to the control. The induction of apoptosis following ATRA treatment exposure has been shown to be hallmarked by the release of cytochrome c into the cell's cytosol (Schmidt-Mende et al., 2006). Cytochrome c is a mitochondria-bound protein which triggers the caspase cascade – and ultimately apoptosis, upon release into the cytosol (Kalpage et al., 2019; Korshunov et al., 1999; Santucci et al., 2019). The release of cytochrome c is followed by caspase-9 activation, which in turn activates the downstream caspases (caspase-3 and -7) and ultimately leads to onset apoptosis (Boatright and Salvesen, 2003; Hongmei, 2012; Li and Yuan, 2008; Schmidt-Mende et al., 2006). In contradiction to the results observed in this study, previous research has reported different effects of ATRA exposure on caspase activity and apoptosis in various cell types. Yao and colleagues observed a significant increase in caspase-9 activity in mouse embryonic palatal mesenchymal (MEPM) cells following 48-hour ATRA exposure (Yao et al., 2011). Similarly, Schmidt-Mende and colleagues observed a time- and concentration-dependent increase in caspase-3-like activity following ATRA treatment of myelomonocytic P39 cells for up to 96 hours (Schmidt-Mende et al., 2006). These results were further supported by Yu and colleagues, who reported that ATRA-induced apoptosis is dependent on caspase activation (Yu et al., 2006). The

study observed a concentration-dependent increase in caspase-3 and -9 activity in MEPM cells following 24-hour ATRA exposure, with the highest concentration of ATRA (5  $\mu$ M) showing the highest level of caspase activation (Yu et al., 2006). To confirm the role of these caspases in ATRA-induced apoptosis, Yu and colleagues inhibited caspase-3 and -9 in the MEPM cells before being treated with ATRA for 24 hours. The authors observed that ATRA could not induce DNA fragmentation, which leads to apoptosis, of the MEPM cells when caspase-3 and -9 were inhibited (Yu et al., 2006). In a separate study, Schmidt-Mende and colleagues observed that ATRA induced apoptosis of myelomonocytic P39 cells (Schmidt-Mende et al., 2006). However, they reported that the induction of apoptosis was only observed after 72 hours of ATRA treatment exposure, following cell differentiation observed in the earlier hours (Schmidt-Mende et al., 2006). In another study where MCF-7 breast cancer cells were exposed to ATRA for 24 to 240 hours, an interruption of the cell's cycle was observed by a reduction of S-phase DNA contents (Mangiarotti et al., 1996). Interestingly, ATRA-induced apoptosis was also observed after 72 hours in this study (Mangiarotti et al., 1996).

The present study observed significant reductions in caspase-9 activity (Figure 4.3.1) and caspase-3/7 expression levels (Figure 4.3.2) after 24 hours of ATRA exposure compared to the control. However, the severe reduction in cell confluency and drastic change in cell morphology of the ATRA-treated cells compared to the control (see Appendix C, Figure C1 and Figure C2) suggest the occurrence of cellular changes that extend beyond caspase-dependent apoptosis. These observations raise the possibility of alternative forms of cell death involved in ATRA exposure. The notion of alternative cell death pathways is supported by previous research conducted by Arce

and colleagues, who reported caspase-independent HepG<sub>2</sub> apoptosis following ATRA treatment exposure (Arce et al., 2005b). This suggests that ATRA can potentially induce cell death through caspase-independent pathways or alternative mechanisms altogether (Arce et al., 2005). Interestingly, a significant increase in caspase-3/7 expression following 24 hours of MO treatment exposure was observed (Figure 4.3.2). This observation aligns with findings from previous studies. Tiloke and colleagues reported a significant increase in caspase-3/7 activity in HepG<sub>2</sub> cells exposed to MO crude aqueous leaf extract (Tiloke et al., 2019). Subsequently, Do and colleagues also reported heightened caspase-3/7 activity following treatment with MO aqueous extract in human melanoma cells (Do et al., 2020b). Moreover, their study revealed that MO induces mitochondria-related caspase-independent apoptosis of the melanoma cells (Do et al., 2020b). In a separated study, Do and colleagues noted that the MO phenolic extract can induce apoptosis in human melanoma cells through a caspase-independent mechanism (Do et al., 2020a). These findings raise the possibility of a caspase-independent mechanism of cell death which could potentially explain the decrease in caspase-9 activity observed in the current study. However, further extensive research would be needed to explore this possibility in greater depth.

Studies have shown that cell death can occur, despite the inhibition of the apoptotic family of proteins, suggesting that cells may employ other mechanisms of cell death (Shimizu et al., 2014). One such identified non-apoptotic cell death mechanism is autophagy-dependent cell death (ADCDC) (also known as Type II programmed cell death to distinguish it from apoptosis or Type I programmed cell death) (Blank and Shiloh, 2007; Shimizu et al., 2014). ADCDC refers to cell death through the activation of autophagy (also known as macroautophagy) as opposed to the autophagy-related

death that occurs under normal physiological conditions (Shimizu et al., 2014). Unlike apoptosis, which relies upon the activation of caspases and subsequent cleaving of numerous downstream target proteins, ADCD is characterised by the presence of abundant autophagosomes and the absence of caspase activation in dying cells (Lin and Baehrecke, 2015; Lüthi and Martin, 2007; Schnaith et al., 2007; Tsujimoto and Shimizu, 2005). However, there is an ongoing debate on whether autophagy itself induces cell death or is upregulated in response to cellular demise (Fulda and Kögel, 2015; Lin and Baehrecke, 2015). To definitively determine the induction of ADCD, the rate of cell death in the presence of autophagy can be compared to the rate of cell death when autophagy is selectively inhibited (Fulda and Kögel, 2015; Shimizu et al., 2014). Autophagy can play a pro-cell survival or pro-death role (Shi et al., 2017); however, the overstimulation of autophagy can result in cell death (Fulda and Kögel, 2015; Shi et al., 2017).

Previous studies have shown that ATRA treatment exposure leads to the upregulation of autophagy, resulting in the subsequent onset of ADCD, as observed in HepG<sub>2</sub> cells (Fang et al., 2020). Another form of cell death associated with ATRA treatment exposure is ferroptosis. Ferroptosis is a recently recognised form of programmed cell death characterised by the intracellular accumulation of iron ions and reactive oxygen species induced by lipid peroxidation (Sun et al., 2022; Xie et al., 2016). This is often accompanied by mitochondrial morphological changes, such as the condensation of mitochondrial cristae (Xie et al., 2016). Sun and colleagues found that the onset of ferroptosis in HepG<sub>2</sub> cells increased after ATRA treatment exposure (Sun et al., 2022).

These findings highlight the existence of alternative pathways of cell death induced by ATRA, including ADCD and ferroptosis. Further investigations are needed to unravel the precise molecular mechanisms underlying these cell death pathways and their significance in the context of ATRA treatment. Understanding the diverse modes of cell death activated by ATRA will contribute to a comprehensive understanding of its therapeutic potential and provide insights into its multifaceted actions in the present study's cellular contexts.

Lysosome-associated membrane protein type 2A (LAMP2A), a receptor protein found on the lysosomal membrane, plays an integral part in the CMA pathway (Kaushik and Cuervo, 2018; Majeski and Dice, 2004; Parzych and Klionsky, 2014). It forms a complex with chaperone proteins (HSC70, HSP40, HSP90, hip, hop, and bag-1) to facilitate the translocation of damaged or excess proteins translocated across the lysosomal membrane for subsequent enzymatic degradation (Bejarano and Cuervo, 2010; Dash et al., 2019; Kaushik and Cuervo, 2018). The level of CMA activity is directly influenced by the binding rate between the LAMP2A cytosolic tail and the substrate protein (Arias, 2015; Dash et al., 2019). This binding event is considered to be the rate-limiting step for CMA activity in both physiological and pathological conditions, making LAMP2A expression a reliable measure of CMA activity in numerous cell lines (Arias, 2015; Cuervo and Dice, 2000a, 2000b; Ding et al., 2016).

The LAMP2A ELISA results observed in the present study showed no significant difference in LAMP2A expression in all treatment groups compared to the control group observed, as shown in Figure 4.4. However, ATRA has been previously shown to inhibit the expression of LAMP2A by activating the retinoic acid receptor alpha

(RAR $\alpha$ ) (Hubert et al., 2022; Molina et al., 2020). The inhibition of LAMP2A translates as the reduction of CMA activity (Molina et al., 2020; Wang and Lu, 2022). Rafiq and colleagues reported reduced CMA activity in acute promyelocytic leukaemia following ATRA treatment (Rafiq et al., 2022). The authors observed a reduction in LAMP2A-HSC70 colocalization in response to ATRA treatment (Rafiq et al., 2022). In line with these findings, the present study's Hownary western blot results also showed a decline in LAMP2A expression following 24-hour ATRA exposure (Figure 4.5.1). In order to confirm these results, the expression of hexokinase 2 (HK2) was also assessed using western blot analysis. HK2 is a glycolytic protein cleared through the CMA pathway (Arias and Cuervo, 2020; Galan-Acosta et al., 2015). A correlating increase in HK2 was observed following 24-hour ATRA exposure (Figure 4.5.2). Due to the HK2 protein being cleared through the CMA pathway, the increase of this protein supports the decrease in LAMP2A expression observed, translating to an observed decline in CMA activity. Increasing CMA activity has been proposed to increase HK2 degradation in cancer cells (Arias and Cuervo, 2020). Xia and colleagues found that the activation of CMA above baseline levels increased HK2 degradation (Xia et al., 2015). These reports highlight the potential of ATRA to alter CMA activity, which is observed as changes in LAMP2A expression. However, to establish the validity and reliability of the results obtained from the western blot analysis, it is critical to repeat the experiment multiple times ( $n>1$ ) to enhance the robustness of the findings by minimising the impact of random variations and providing a more comprehensive assessment of the results' consistency and reproducibility.

To the researcher's knowledge, no studies have investigated the effects of MO on LAMP2A or CMA activity. However, Tiloke and colleagues showed that MO extract

could increase oxidative stress in lung cancer cells (Tiloke et al., 2013). In a later study, Tiloke and colleagues also observed an increase in reactive oxygen species (ROS) – which induces oxidative stress – in oesophageal and liver cancer cells (Tiloke et al., 2013, 2016, 2019). Madi and colleagues acknowledged an increase in oxidative stress upon MO extract treatment of human lung adenocarcinoma cells (Madi et al., 2016). In another study, Guon and Chung reported increased ROS upon MO extract of human melanoma cells (Guon and Chung, 2017). Despite basal levels of CMA observed in numerous cells, oxidative stress is known to be a potent inducer of CMA, which has previously been shown to translate into increased LAMP2A levels (Bejarano and Cuervo, 2010; Catarino et al., 2017; Dash et al., 2019). In contradiction, a decrease in LAMP2A expression was observed following 24-hour MO exposure, compared to the control, in this study (Figure 4.5.1). This observation was supported by an increase in HK2 expression following 24-hour MO exposure compared to the control. These observations suggest a MO-induced decline in CMA activity. The CMA-inhibitory effects of ATRA and MO were compounded in the ATRA+MO combination treatment group, where the LAMP2A expression (Figure 4.5.1) was observed along with the corresponding highest HK2 expression (Figure 4.5.2). These findings indicate that MO, alone or in combination with ATRA, may have inhibitory effects on CMA in an *in vitro* model of HCC. It has been shown that CMA supports tumour growth and progression of various cancers, including HCC.

Consequently, the inhibition of CMA has been shown to affect tumour development and progression. Targeting CMA, MO, and ATRA may disrupt crucial cellular processes that contribute to HCC development and potentially enhance the efficacy of HCC treatment modalities. Therefore, the inhibitory effects of MO on CMA,

especially when combined with ATRA, could hold therapeutic promise in the treatment of HCC. Further investigations are warranted to elucidate the underlying mechanisms of MO's inhibitory effects on CMA in HCC and to evaluate the therapeutic implications of targeting CMA as a treatment strategy for HCC. These findings opened avenues for future research and the development of novel adjuvant therapeutic approaches for HCC patients.

## CHAPTER 6

### Study conclusions, limitations, and future recommendations

#### 6.1. Introduction

The prevalence of hepatocellular carcinoma (HCC), its poor prognosis and the existing limitations with current HCC therapeutics remain a significant healthcare challenge to developing countries such as South Africa. These challenges necessitate the investigation of alternative treatment options. The cellular survival mechanism, autophagy, has been shown to play a role in the development and progression of HCC. Amongst the autophagy pathways, the upregulation of the chaperone-mediated autophagy (CMA) pathway has been prominently described in numerous cancers such as HCC. Due to consistent reports of its contribution to the development of HCC, CMA serves as a promising target for alternative adjuvant HCC therapeutic options. Bioactive compounds found in medicinal plants, such as *Moringa oleifera* (MO), have shown anti-cancer properties which could be exploited for their potential efficacy against HCC. Despite all parts of the MO plant containing these bioactive compounds, the leaves have the greatest abundance of bioactive compounds with anti-cancer properties. Considering the cancer-supportive role of CMA and the cancer-suppressive role of MO, this study aimed to investigate the effects of MO aqueous leaf extract on CMA activity in human HepG<sub>2</sub> cancer cells.

#### 6.2 Conclusion

This study showed MO's ability to reduce HepG<sub>2</sub> cell reductive capacity. All-trans-retinoic acid (ATRA) was used in this study as it has been reported to inhibit CMA activity. MO treatment reduced HepG<sub>2</sub> cell reductive capacity, suggesting a negative

impact on cell viability. Similarly, ATRA, known for its inhibitory effect on chaperone-mediated autophagy (CMA) activity, also showed the ability to reduce the reductive capacity of HepG<sub>2</sub> cancer cells. Both these compounds reduced HepG<sub>2</sub> liver cancer cell proliferation and cell viability in a concentration-dependent manner. These observations highlighted the potential of both MO and ATRA as therapeutic agents in modulating HCC cell health by compromising cellular function and viability.

Based on the morphological observations, both MO and ATRA induced significant alterations in the morphology of HepG<sub>2</sub> cells and led to a substantial reduction in cell confluency (as depicted in Appendix C, Figure C1 and Figure C2). Notably, the negative effects of these compounds on cell survival were independent of caspase activity, suggesting the involvement of alternative mechanisms in the observed cell death. Therefore, further investigations must aim to explore and elucidate the specific pathways and molecular mechanisms through which MO and ATRA induce cell death in HepG<sub>2</sub> cells. By uncovering the precise mechanisms of cell death, valuable insights can be obtained, aiding in developing more targeted and effective therapeutic strategies for HCC.

Several studies have previously reported on the CMA inhibitory potential of ATRA. This study found a reduction in LAMP2A expression following ATRA treatment exposure. To reinforce this, the expression of the CMA cargo protein, Hexokinase II (HK2) increased. Together, these results reveal that ATRA inhibits CMA activity in HepG<sub>2</sub> cells. To the researcher's knowledge, no previous studies have reported MO's effects on CMA activity in an *in vitro* model of HCC. Also, this study found a decrease in LAMP2A expression. Similarly, there was a corresponding decrease in HK2

expression. These results show that MO has an inhibitory effect on CMA. The observed effects of MO and ATRA combined exposure on CMA activity were greater than MO or ATRA alone. An even greater reduction in CMA activity was observed following combined treatment.

These results show that MO and ATRA negatively affect the viability of HCC cells. These compounds also show an ability to induce HepG<sub>2</sub> cell death. However, the mechanism through which cell death occurs requires further elucidation. The results also suggest that MO can reduce CMA activity. ATRA also showed an inhibitory potential on CMA activity in the HepG<sub>2</sub> cells (see Figure 6 for a depiction of the study's main findings). Combining the two compounds has an even greater inhibitory effect on CMA activity than each of the individual compounds alone. Therefore, it is plausible that the anti-cancer effects of MO may occur through its inhibitory effects on CMA activity.

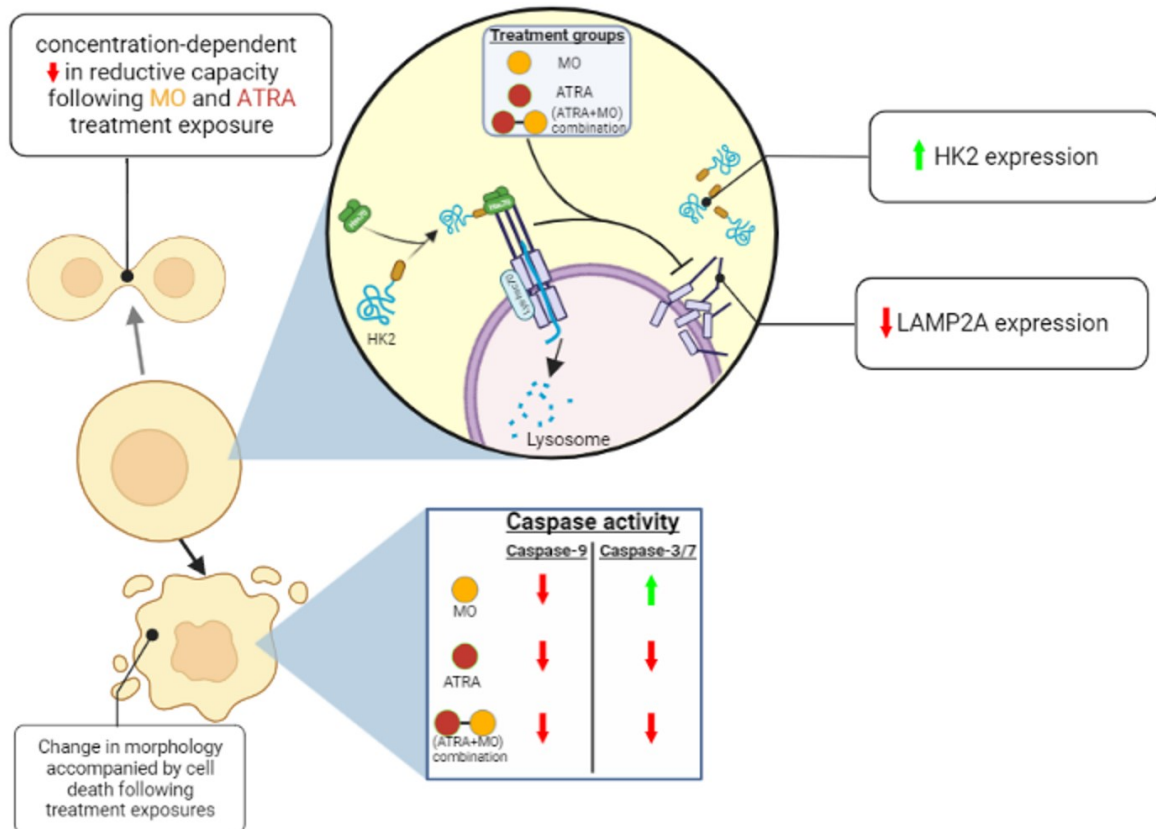


**Figure 6: Diagram depicting this study's main findings.** Abbreviations: ATRA, all-trans-retinoic acid; HK2, hexokinase II; LAMP2A, lysosome-associated membrane protein type 2A; MO, *Moringa oleifera*

### 6.3 Recommendations

*In vitro* HCC models contribute significantly to understanding the molecular mechanisms involved in developing HCC. However, there are limitations to these *in vitro* models, such as the lack of intra-tumour and inter-tumour representation. Using purchased cell lines sourced from a single source also provides a level of homogeneity that does not represent the heterogeneity observed in patient tumours. While this study provided valuable insights into the effects of ATRA and MO on the HCC cells, it would be valuable to investigate these effects in an *in vivo* model to determine how these results translate to a more physiologically relevant setting. Transitioning to an *in vivo* model would allow for a better understanding of how the observed results

translate to a complex biological environment. This would further clarify these effects and provide insight into how the interaction between other cell types and physiological events influence the observations seen in this study.

When the cell morphology was assessed following treatment, there were significant changes in cell morphology (see Appendix C, Figure C1) and live cell count (see Figure C2) following ATRA, MO, and MO+ATRA combination treatment. However, the caspase-mediated apoptosis results did not represent these changes. Therefore, future studies will have to explore the possible assessment of caspase-independent forms of cell death, as morphologically observed in this study.

The MO leaves have numerous bioactive compounds that have anti-cancer potential. Thus, it would be beneficial to isolate the bioactive compounds and test them individually to determine which compounds are responsible for the observations made in this study.

Although it has been reported that CMA activity is significantly increased in numerous cancerous cells including HCC cells, future studies could benefit from having a positive control for CMA activity. This will allow for a better assessment of the function of CMA activity within the HepG<sub>2</sub> cells. This could also improve observations on the effect of MO and ATRA on CMA activity, by assessing their effect on CMA activity that is confirmed to be stimulated.

Repetition of experiments increases the reliability of the results. Therefore, reducing financial constraints may enable more comprehensive optimisation of the various

assays, which would benefit future studies. Comprehensive optimisation of assays can help refine experimental protocols, enhance assay sensitivity, minimise variability, and improve the overall quality of data generated. This optimisation may involve fine-tuning experimental conditions, standardising protocols, utilising appropriate controls, and implementing rigorous quality control measures.

#### **6.4. Limitations**

While valuable insights on the effects of MO on CMA were obtained from this study, it is important to acknowledge its limitations. One of the limitations faced was finances. Due to financial constraints, certain reagents were purchased at low quantities and could not be replaced. This prevented the robust optimisation of various assays. A prominent example was using the heat shock protein 90 (HSP90) antibody for western blot. The choice of the antibody required more optimisation than initially anticipated. However, due to the high antibody working concentration required (antibody to diluent ratio is 1:125-1:250) and the limited volume of the commercially acquired antibody (25  $\mu$ L), the optimisation could not be performed to determine the ideal concentration. Three repeats were performed; however, the concentration was not ideal as the protein bands could not be determined. Unfortunately, the volume and dilution of the HSP90 did not allow the antibody concentration to be optimised.

The optimization of LAMP2A and HK2 antibodies proved to be more time-consuming than initially anticipated. While these optimizations were ultimately successful, financial and time constraints precluded the repeated conducting of additional repetitions of the western blot procedure to achieve an n=3 result. Nevertheless, the

preliminary results (n=1) obtained provide valuable insights into the effects of MO, ATRA, and the combination on CMA activity in HepG<sub>2</sub> cells.

Additionally, an unforeseen obstacle arose when supplier backlogs disrupted the continuity of the study, rendering the previously prepared HSP90 antibody unusable. Due to the small volume, the new antibody solution could not be prepared for subsequent exposures and troubleshooting. Therefore, the antibody could not be assessed further in the study.

Another limitation faced was time constraints. Delays from manufacturers resulted in reduced time to perform some experiments and an extended time to complete the studies. Despite the setbacks encountered, it is essential to acknowledge the limitations imposed by these external factors and maintain transparency in reporting the circumstances that influenced the course and outcomes of the study.

## REFERENCES

- Abd-Rabou, A.A., Abdalla, A.M., Ali, N.A. and Zoheir, K.M.A. (2017) 'Moringa oleifera root induces cancer apoptosis more effectively than leave nanocomposites and its free counterpart', *Asian Pacific Journal of Cancer Prevention*, 18, pp. 2141–2149.
- Adebayo, I.A., Balogun, W.G. and Arsad, H. (2017) 'Moringa oleifera: An apoptosis inducer in cancer cells', *Tropical Journal of Pharmaceutical Research*, 16(9) University of Benin, pp. 2289–2296.
- Ahmed, W.A., Kashwaa, F.A.A.-B., Hameed, O.H.M.A. el and Elhefny, M.A. (2020) 'Potential role of Moringa oleifera on different cell lines and experimental animal model', *Cancer Biology*, 10(3), pp. 63–69.
- Al-Asmari, A.K., Albalawi, S.M., Athar, M.T., Khan, A.Q., Al-Shahrani, H. and Islam, M. (2015) 'Moringa oleifera as an anti-cancer agent against breast and colorectal cancer cell lines', *PLoS ONE*, 10(8) Public Library of Science, pp. 1–14.
- Alqahtani, A., Khan, Z., Alloghbi, A., Ahmed, T.S.S., Ashraf, M. and Hammouda, D.M. (2019) 'Hepatocellular carcinoma: Molecular mechanisms and targeted therapies', *Medicina (Lithuania)*, 55(9) MDPI AG, pp. 1–22.
- Al-Qassab, Y., Grassilli, S., Brugnoli, F., Vezzali, F., Capitani, S. and Bertagnolo, V. (2018) 'Protective role of all-trans retinoic acid (ATRA) against hypoxia-induced malignant potential of non-invasive breast tumor derived cells', *BMC Cancer*, 18(1) BioMed Central Ltd, pp. 1-13.
- Al-Sheddi, E.S., Al-Oqail, M.M., Saquib, Q., Siddiqui, M.A., Musarrat, J., Al-Khedhairi, A.A. and Farshori, N.N. (2015) 'Novel all trans-retinoic acid derivatives: Cytotoxicity, inhibition of cell cycle progression and induction of apoptosis in human cancer cell lines', *Molecules*, 20(5) MDPI AG, pp. 8181–8197.

Anand, K., Gengan, R.M., Phulukdaree, A. and Chuturgoon, A. (2015) 'Agroforestry waste *Moringa oleifera* petals mediated green synthesis of gold nanoparticles and their anti-cancer and catalytic activity', *Journal of Industrial and Engineering Chemistry*, 21 The Korean Society of Industrial and Engineering Chemistry, pp. 1105–1111.

Anguiano, J., Garner, T.P., Mahalingam, M., Das, B.C., Gavathiotis, E. and Cuervo, A.M. (2013) 'Chemical modulation of chaperone-mediated autophagy by retinoic acid derivatives', *Nature Chemical Biology*, 9(6), pp. 374–382.

Anwanwan, D., Singh, S.K., Singh, S., Saikam, V. and Singh, R. (2020) 'Challenges in liver cancer and possible treatment approaches', *Biochimica et Biophysica Acta - Reviews on Cancer*, 1873(1) Elsevier, p. 188314.

Aravalli, R.N., Steer, C.J. and Cressman, E.N.K. (2008) 'Molecular mechanisms of hepatocellular carcinoma', *Hepatology*, 48(6), pp. 2047–2063.

Arce, F., Gätjens-Boniche, O., Vargas, E., Valverde, B. and Díaz, C. (2005a) 'Apoptotic events induced by naturally occurring retinoids ATRA and 13-cis retinoic acid on human hepatoma cell lines Hep3B and HepG2', *Cancer Letters*, 229(2), pp. 271–281.

Arias, E. (2015) 'Lysosomal mTORC2/PHLPP1/Akt axis: a new point of control of chaperone-mediated autophagy', *Oncotarget*, 6(34), pp. 35147–35148.

Arias, E. and Cuervo, A.M. (2020) Pros and Cons of Chaperone-Mediated Autophagy in Cancer Biology, *Trends in Endocrinology and Metabolism*, 31(1) Elsevier Inc., pp. 53-66

Arias, E., Koga, H., Diaz, A., Mocholi, E., Patel, B. and Cuervo, A.M. (2015) 'Lysosomal mTORC2/PHLPP1/Akt Regulate Chaperone-Mediated Autophagy', *Molecular Cell*, 59(2) Cell Press, pp. 270–284.

- Bandyopadhyay, U., Sridhar, S., Kaushik, S., Kiffin, R. and Cuervo, A.M. (2010) 'Identification of Regulators of Chaperone-Mediated Autophagy', *Molecular Cell*, 39(4), pp. 535–547.
- Bao, L., Chandra, P.K., Moroz, K., Zhang, X., Thung, S.N., Wu, T. and Dash, S. (2014) 'Impaired autophagy response in human hepatocellular carcinoma', *Experimental and Molecular Pathology*, 96(2), pp. 149–154.
- Barhoi, D., Upadhaya, P., Barbhuiya, S.N., Giri, A. and Giri, S. (2021) 'Aqueous Extract of Moringa oleifera Exhibit Potential Anticancer Activity and can be Used as a Possible Cancer Therapeutic Agent: A Study Involving In Vitro and In Vivo Approach', *Journal of the American College of Nutrition*, 40(1) Routledge, pp. 70–85.
- Bejarano, E. and Cuervo, A.M. (2010) 'Chaperone-mediated autophagy', *Proceedings of the American Thoracic Society*, 7(1), pp. 29–39.
- Berkovich, L., Earon, G., Ron, I., Rimmon, A., Vexler, A. and Lev-Ari, S. (2013) 'Moringa Oleifera aqueous leaf extract down-regulates nuclear factor-kappaB and increases cytotoxic effect of chemotherapy in pancreatic cancer cells', *BMC Complementary and Alternative Medicine*, 13(212), pp. 1-7.
- Blank, M. and Shiloh, Y. (2007) 'Programs for cell death: Apoptosis is only one way to go', *Cell Cycle*, 6(6) Taylor and Francis Inc., pp. 686–695.
- Boatright, K.M. and Salvesen, G.S. (2003) 'Mechanisms of caspase activation', *Current Opinion in Cell Biology*, 15(6) Elsevier Ltd, pp. 725-731.
- Bold, R.J., Termuhlen, P.M. and Mcconkey, D.J. (1997) 'Apoptosis, cancer and cancer therapy', *Surgical Oncology*, 6(3), pp. 133–142.
- Bonhoure, A., Vallentin, A., Martin, M., Senff-Ribeiro, A., Amson, R., Telerman, A. and Vidal, M. (2017) 'Acetylation of translationally controlled tumor protein promotes its

degradation through chaperone-mediated autophagy', *European Journal of Cell Biology*, 96(2) Elsevier GmbH., pp. 83–98.

Boukes, G.J., Koekemoer, T.C., van de Venter, M. and Govender, S. (2017) 'Cytotoxicity of thirteen South African macrofungal species against five cancer cell lines', *South African Journal of Botany*, 113 SAAB, pp. 62–67.

Brentnall, M., Rodriguez-Menocal, L., Ladron De Guevara, R., Cepero, E. and Boise<sup>1</sup>, L.H. (2013) 'Caspase-9, caspase-3 and caspase-7 have distinct roles during intrinsic apoptosis', *BMC Cell Biology*, 14, pp. 32–40.

Bruix, J., Han, K., Gores, G., Llovet, J.M. and Mazzaferro, V. (2015) 'Liver cancer: Approaching a personalized care', *Journal of Hepatology*, 62(1) European Association for the Study of the Liver, pp. S144–S156.

Burley, M.R. and Roth, C.M. (2007) 'Effects of Retinoic Acid on Proliferation and Differentiation of HepG2 Cells', *The Open Biotechnology Journal*, 1, pp. 47–51.

Catarino, S., Pereira, P. and Girao, H. (2017) 'Molecular control of chaperone-mediated autophagy', *Essays in Biochemistry*, 61(6) Portland Press Ltd, pp.663-674.

Cescon, M., Cucchetti, A., Ravaioli, M. and Pinna, A.D. (2013) 'Hepatocellular carcinoma locoregional therapies for patients in the waiting list. Impact on transplantability and recurrence rate', *Journal of Hepatology*, 58(3) European Association for the Study of the Liver, pp. 609–618.

Charoensin, S. (2014) 'Antioxidant and anticancer activities of *Moringa oleifera* leaves', *Journal of Medicinal Plant Research*, 8(7), pp. 318–325.

Chava, S., Lee, C., Aydin, Y., Chandra, P.K., Dash, A., Chedid, M., Thung, S.N., Moroz, K., Wu, T. and Nayak, N.C. (2017) 'Chaperone-mediated autophagy compensates for impaired macroautophagy in the cirrhotic liver to promote hepatocellular carcinoma', *Oncotarget*, 8(25), pp. 40019–40036.

Chen, X., Liu, H., Li, M. and Qiao, L. (2014) 'Advances in non-surgical management of primary liver cancer', *World Journal of Gastroenterology*, 20(44), pp. 16630–16638.

Choi, K.S. (2012) 'Autophagy and cancer', *Experimental and Molecular Medicine*, 44(2), pp. 109–120.

Ciscato, F., Filadi, R., Masgras, I., Pizzi, M., Marin, O., Damiano, N., Pizzo, P., Gori, A., Frezzato, F., Chiara, F., Trentin, L., Bernardi, P. and Rasola, A. (2020) 'Hexokinase 2 displacement from mitochondria-associated membranes prompts Ca<sup>2+</sup>-dependent death of cancer cells', *EMBO reports*, 21(7) EMBO, pp. 1–13.

Cuervo, A.M. (2009) 'Chaperone-mediated autophagy: selectivity pays off', *Trends in Endocrinology and Metabolism*, 21(3), pp. 142–150.

Cuervo, A.M. and Dice, J.F. (2000a) 'Unique properties of LAMP2A compared to other LAMP2 isoforms', *Journal of Cell Science*, 113, pp. 4441–4450.

Cuervo, A.M. and Dice, J.F. (2000b) 'Regulation of LAMP2A Levels in the lysosomal membrane', *Traffic*, 1, pp. 570–583.

Dash, S., Aydin, Y. and Moroz, K. (2019) 'Chaperone-Mediated Autophagy in the Liver: Good or Bad?', *Cells*, 8(11) NLM (Medline), pp. 1-31.

Ding, Z., Fu, X., Shi, Y., Zhou, J. and Peng, Y. (2016) 'Lamp2a is required for tumor growth and promotes tumor recurrence of hepatocellular carcinoma', *International Journal of Oncology*, 49, pp. 2367–2376.

Ding, Z., Shi, Y., Zhou, J., Qiu, S., Xu, Y., Dai, Z., Shi, G., Wang, X., Ke, A., Wu, B. and Fan, J. (2008) 'Association of autophagy defect with a malignant phenotype and poor prognosis of hepatocellular carcinoma', *Cancer Research*, 68(22), pp. 9167–9176.

Do, B.H., Hoang, N.S., Nguyen, T.P.T., Ho, N.Q.C., Le, T.L. and Doan, C.C. (2020a) 'Phenolic Extraction of Moringa Oleifera Leaves Induces Caspase-Dependent and

Caspase-Independent Apoptosis through the Generation of Reactive Oxygen Species and the Activation of Intrinsic Mitochondrial Pathway in Human Melanoma Cells', *Nutrition and Cancer*, 73(5) Routledge, pp. 869–888.

Do, B.H., Nguyen, T.P.T., Ho, N.Q.C., Le, T.L., Hoang, N.S. and Doan, C.C. (2020b) 'Mitochondria-mediated Caspase-dependent and Caspase-independent apoptosis induced by aqueous extract from *Moringa oleifera* leaves in human melanoma cells', *Molecular Biology Reports*, 47(5) Springer, pp. 3675–3689.

Elsayed, E.A., Sharaf-Eldin, M.A. and Wadaan, M. (2015) 'In vitro evaluation of cytotoxic activities of essential oil from *Moringa oleifera* seeds on HeLa, HepG2, MCF-7, CACO-2 and L929 cell lines', *Asian Pacific Journal of Cancer Prevention*, 16(11), pp. 4671–4675.

Fabregat, I. (2009) 'Dysregulation of apoptosis in hepatocellular carcinoma cells', *World Journal of Gastroenterology*, 15(5) Baishideng Publishing Group Co, pp. 513–520.

Fang, S., Hu, C., Xu, L., Cui, J., Tao, L., Gong, M., Wang, Y., He, Y., He, T. and Bi, Y. (2020) 'All-trans-retinoic acid inhibits the malignant behaviors of hepatocarcinoma cells by regulating autophagy', *Am J Transl Res*, 12(10), pp. 6793–6810.

Fattovich, G., Stroffolini, T., Zagni, I. and Donato, F. (2004) 'Hepatocellular Carcinoma in Cirrhosis: Incidence and Risk Factors', *Gastroenterology*, 127(5), pp. 35–50.

Franco-Juárez, B., Coronel-Cruz, C., Hernández-Ochoa, B., Gómez-Manzo, S., Cárdenas-Rodríguez, N., Arreguin-Espinosa, R., Bandala, C., Canseco-Ávila, L.M. and Ortega-Cuellar, D. (2022) 'TFEB; beyond its role as an autophagy and lysosomes regulator', *Cells*, 11(3153), pp. 1-20.

Fu, W. and Hall, M.N. (2020) 'Regulation of MTORC2 signaling', *Genes*, 11(9) MDPI AG, pp. 1-19.

- Fuchs, Y. and Steller, H. (2011) 'Programmed cell death in animal development and disease', *Cell*, 147(4), pp. 742–758.
- Fulda, S. and Debatin, K.M. (2006) 'Extrinsic versus intrinsic apoptosis pathways in anticancer chemotherapy', *Oncogene*, 25(34), pp. 4798–4811.
- Fulda, S. and Kögel, D. (2015) 'Cell death by autophagy: Emerging molecular mechanisms and implications for cancer therapy', *Oncogene*, 34(40) Nature Publishing Group, pp. 5105–5113.
- Galan-Acosta, L., Xia, H., Yuan, J. and Vakifahmetoglu-Norberg, H. (2015) 'Activation of chaperone-mediated autophagy as a potential anticancer therapy', *Autophagic Punctum*, 11(12), pp. 2370–2371.
- Galluzzi, L., Baehrecke, E.H., Ballabio, A., Boya, P., Manuel, J., Pedro, B.-S., Cecconi, F., Choi, A.M., Chu, C.T. and Codogno, P. (2017) 'Molecular definitions of autophagy and related processes', *The EMBO Journal*, 36(13), pp. 1811–1836.
- Garancini, M., Pinotti, E., Nespoli, S., Romano, F., Gianotti, L. and Giardini, V. (2016) 'Hepatic resection beyond barcelona clinic liver cancer indication: When and how', *World Journal of Hepatology*, 8(11), pp. 513–519.
- García-Beltrán, J.M., Mansour, A.T., Alsaqufi, A.S., Ali, H.M. and Esteban, M.Á. (2020) 'Effects of aqueous and ethanolic leaf extracts from drumstick tree (*Moringa oleifera*) on gilthead seabream (*Sparus aurata* L.) leucocytes, and their cytotoxic, antitumor, bactericidal and antioxidant activities', *Fish and Shellfish Immunology*, 106 Academic Press, pp. 44–55.
- Ghafouri-Fard, S., Tamizkar, H.K., Hussien, B.M. and Taheri, M. (2021) 'MicroRNA signature in liver cancer', *Pathology Research and Practice*, 219 Elsevier GmbH., p. 153369.

Gillman, R., Floro, K.L., Wankell, M. and Hebbard, L. (2021) 'The role of DNA damage and repair in liver cancer', *BBA - Reviews on Cancer*, 1875(1) Elsevier B.V., p. 188493.

Glick, D., Barth, S. and Macleod, K.F. (2010) 'Autophagy: Cellular and molecular mechanisms', *Journal of Pathology*, 221(1), pp. 3–12.

Gomes, L.R., Menck, C.F.M. and Cuervo, A.M. (2017) 'Chaperone-mediated autophagy prevents cellular transformation by regulating MYC proteasomal degradation', *Autophagy*, 13(5) Taylor & Francis, pp. 928–940.

Gunduz, C., Basoglu, O.K., Kvamme, J.A., Verbraecken, J., Anttalainen, U., Marrone, O., Steiropoulos, P., Roisman, G., Joppa, P., Hein, H., Trakada, G., Hedner, J., Grote, L., Steiropoulos, P., Verbraecken, J., Petiet, E., Trakada, G., Montserrat, J.M., Fietze, I., Penzel, T., Ludka, O., Rodenstein, D., Masa, J.F., Bouloukaki, I., Schiza, S., Kent, B., McNicholas, W.T., Ryan, S., Riha, R.L., Kvamme, J.A., Hein, H., Schulz, R., Grote, L., Hedner, J., Zou, D., Pépin, J.L., Levy, P., Bailly, S., Lavie, L., Lavie, P., Basoglu, O.K., Tasbakan, M.S., Varoneckas, G., Joppa, P., Tkacova, R., Staats, R., Barbé, F., Lombardi, C., Parati, G., Drummond, M., van Zeller, M., Bonsignore, M.R., Petitjean, M., Roisman, G., Pretl, M., Vitols, A., Dogas, Z., Galic, T., Pataka, A., Anttalainen, U., Saaresranta, T., Plywaczewski, R., Sliwinski, P. and Bielicki, P. (2020) 'Long-term positive airway pressure therapy is associated with reduced total cholesterol levels in patients with obstructive sleep apnea: data from the European Sleep Apnea Database (ESADA)', *Sleep Medicine*, 75, pp. 201–209.

Guo, B., Li, L., Guo, J., Liu, A., Wu, J., Wang, H., Shi, J., Pang, D. and Cao, Q. (2017) 'M2 tumor-associated macrophages produce interleukin-17 to suppress oxaliplatin-induced apoptosis in hepatocellular carcinoma', *Oncotarget*, 8(27), pp. 44465–44476.

Guo, W., Qiu, Z., Wang, Z., Wang, Q., Tan, N., Chen, T., Chen, Z., Huang, S., Gu, J., Li, J., Yao, M., Zhao, Y. and He, X. (2015) 'MiR-199a-5p Is Negatively Associated With

Malignancies and Regulates Glycolysis and Lactate Production by Targeting Hexokinase 2 in Liver Cancer', *Hepatology*, 62(4), pp. 1132–1144.

Guon, T.E. and Chung, H.S. (2017) 'Moringa oleifera fruit induce apoptosis via reactive oxygen species-dependent activation of mitogen-activated protein kinases in human melanoma A2058 cells', *Oncology Letters*, 14(2) Spandidos Publications, pp. 1703–1710.

He, S. and Tang, S. (2020) 'WNT /  $\beta$  -catenin signaling in the development of liver cancers', *Biomedicine & Pharmacotherapy*, 132(August) Elsevier Masson SAS, p. 110851.

Herceg, Z. and Paliwal, A. (2011) 'Epigenetic mechanisms in hepatocellular carcinoma: How environmental factors influence the epigenome', *Mutation Research - Reviews in Mutation Research*, 727(3), pp. 55–61.

Hollenstein, D.M. and Kraft, C. (2020) 'Autophagosomes are formed at a distinct cellular structure', *Current Opinion in Cell Biology*, 65 Elsevier Ltd, pp. 50–57.

Hongmei, Z. (2012) 'Extrinsic and Intrinsic Apoptosis Signal Pathway Review', in *Apoptosis and Medicine*. InTech., chptr 1.

Hotchkiss, R.S., Strasser, A., Mcdunn, J.E. and Swanson, P.E. (2009) 'Cell Death', *The New England Journal of Medicine*, 361(16), pp. 1570–83.

Hu, L., Lau, S.H., Tzang, C.H., Wen, J.M., Wang, W., Xie, D., Huang, M., Wang, Y., Wu, M.C., Huang, J.F., Zeng, W.F., Sham, J.S.T., Yang, M. and Guan, X.Y. (2004) 'Association of Vimentin overexpression and hepatocellular carcinoma metastasis', *Oncogene*, 23(1) Nature Publishing Group, pp. 298–302.

Hubert, V., Weiss, S., Rees, A.J. and Kain, R. (2022) 'Modulating Chaperone-Mediated Autophagy and Its Clinical Applications in Cancer', *Cells*, 11(16) MDPI, pp. 1–19.

Hwang, S., Lee, Y.-J., Kim, K.-H., Ahn, C.-S., Moon, D.-B., Ha, T.-Y., Song, G.-W., Jung, D.-H. and Lee, S.-G. (2015) 'The impact of tumor size on long-term survival outcomes after resection of solitary hepatocellular carcinoma: single-institution experience with 2558 patients', *Journal of Gastrointestinal Surgery*, 19, pp. 1281–1290.

Janser, F.A., Tschan, M.P. and Langer, R. (2019) 'The role of autophagy in HER2-targeted therapy', *Swiss Medical Weekly*, 149(October), pp. 1–13.

Jewkes, R., Sikweyiya, Y., Morrell, R. and Dunkle, K. (2009) 'Understanding men's health and use of violence: Interface of rape and HIV in South Africa', *South African Medical Research Council*.

Jung, I.L. (2014) 'Soluble extract from *Moringa oleifera* leaves with a new anticancer activity', *PLoS ONE*, 9(4), pp. 1–10.

Juste, Y.R. and Cuervo, A.M. (2019) 'Analysis of chaperone-mediated autophagy', *Methods of Molecular Biology*, 1880, pp. 703–727.

Kalpage, H.A., Bazyljanska, V., Recanati, M.A., Fite, A., Liu, J., Wan, J., Mantena, N., Malek, M.H., Podgorski, I., Heath, E.I., Vaishnav, A., Edwards, B.F., Grossman, L.I., Sanderson, T.H., Lee, I. and Huttemann, M. (2019) 'Tissue-specific regulation of cytochrome c by post-translational modifications: respiration, the mitochondrial membrane potential, ROS, and apoptosis', *The FASEB Journal*, 33(2) Wiley, pp. 1540–1553.

Kane, R.C., Farrell, A.T., Saber, H., Tang, S., Williams, G., Jee, J.M., Liang, C., Booth, B., Chidambaram, N., Morse, D., Sridhara, R., Garvey, P., Justice, R. and Pazdur, R. (2006) 'Report from FDA sorafenib for the T treatment of advanced renal cell carcinoma', *Clinical Cancer Research*, 12(24), pp. 7271–7279.

- Karim, N.A.A., Ibrahim, M.D., Kntayya, S.B., Rukayadi, Y., Hamid, H.A. and Razis, A.F.A. (2016) 'Moringa oleifera Lam: Targeting chemoprevention', *Asian Pacific Journal of Cancer Prevention*, 17(8) Asian Pacific Organization for Cancer Prevention, pp. 3675–3686.
- Kaushik, S., Bandyopadhyay, U., Sridhar, S., Kiffin, R., Martinez-Vicente, M., Kon, M., Orenstein, S.J., Wong, E. and Cuervo, A.M. (2011) 'Chaperone-mediated autophagy at a glance', *Journal of Cell Science*, 124(4), pp. 495–499.
- Kaushik, S. and Cuervo, A.M. (2018) 'The coming of age of chaperone-mediated autophagy', *Nature Reviews Molecular Cell Biology*, 19(6) Nature Publishing Group, pp. 365–381.
- Kerdsomboon, K., Chumsawat, W. and Auesukaree, C. (2020) 'Chemosphere effects of Moringa oleifera leaf extracts and its bioactive compound gallic acid on reducing toxicities of heavy metals and metalloid in *Saccharomyces cerevisiae*', *Chemosphere*, 270 Elsevier Ltd, pp. 128659–128669.
- Kew, M.C. (2013) 'Epidemiology of hepatocellular carcinoma in sub-Saharan Africa', *Annals of Hepatology*, 12(2) Elsevier, pp. 173–182.
- Kew, M.C. (2012) 'Hepatocellular carcinoma in developing countries: Prevention, diagnosis and treatment', *World Journal of Hepatology*, 4(3), pp. 99–104.
- Khalafalla, M.M., Abdellatef, E., Dafalla, H.M., Nassrallah, A.A., Aboul-Enein, K.M., Lightfoot, D.A., El-Deeb, F.E. and El-Shemy, H.A. (2010) 'Active principle from Moringa oleifera Lam leaves effective against two leukemias and a hepatocarcinoma', *African Journal of Biotechnology*, 9(49), pp. 8467–8471.
- Khatun, S., Ashraduzzman, M., Absar, N., Pervin, F., Ali, M.A., Bari, L., Karima, M.R. and Hassan, P. (2007) 'Purification and characterization of three galactose specific

lectins from Sajna (*Moringa oleifera* L.) leaves', *Journal of the Chinese Chemical Society*, 54(2), pp. 357–364.

Khor, K.Z., Lim, V., Moses, E.J. and Abdul Samad, N. (2018) 'The in vitro and in vivo anticancer properties of *Moringa oleifera*', *Evidence-based Complementary and Alternative Medicine*, 2018, pp. 1–14.

Kimmelman, A.C. (2011) 'The dynamic nature of autophagy in cancer', *Genes & Development*, 25, pp. 1999–2010.

Kon, M., Kiffin, R., Koga, H., Chapochnick, J., Macian, F., Varticovski, L. and Cuervo, A.M. (2011) 'Chaperone-mediated autophagy is required for tumor growth', *Science Translational Medicine*, 3(109), pp. 1–30.

Korshunov, S.S., Krasnikov, B.F., Pereverzev, M.O. and Skulachev, V.P. (1999) 'The antioxidant functions of cytochrome c', *FEBS Letters*, 462(1–2), pp. 192–198.

Kwee, S.A., Hernandez, B., Chan, O. and Wong, L. (2012) 'Choline Kinase Alpha and Hexokinase-2 Protein Expression in Hepatocellular Carcinoma: Association with Survival', *PLoS ONE*, 7(10), pp. 1–8.

Lee, M.W., Raman, S.S., Asvadi, N.H., Siripongsakun, S., Hicks, R.M., Chen, J., Worakitsitatorn, A., McWilliams, J., Tong, M.J., Finn, R.S., Agopian, V.G., Busuttil, R.W. and Lu, D.S.K. (2017) 'Radiofrequency ablation of hepatocellular carcinoma as bridge therapy to liver transplantation: A 10-year intention-to-treat analysis', *Hepatology*, 65(6), pp. 1979–1990.

Lemoine, M., Nayagam, S. and Thursz, M. (2013) 'Viral hepatitis in resource-limited countries and access to antiviral therapies: Current and future challenges', *Future Virology*, 8(4), pp. 371–380.

Levine, B. and Kroemer, G. (2008) 'Autophagy in the pathogenesis of disease', *Cell*, 132(1), pp. 27–42.

- Levy, J.M.M., Towers, C.G. and Thorburn, A. (2017) 'Targeting autophagy in cancer', *Nature Reviews Cancer*, 17(9) Nature Publishing Group, pp. 528–542.
- Li, D., Kang, J., Golas, B.J., Yeung, V.W. and Madoff, D.C. (2014) 'Minimally invasive local therapies for liver cancer', *Cancer Biology & Medicine*, 11, pp. 217–236.
- Li, J. and Yuan, J. (2008) 'Caspases in apoptosis and beyond' *Oncogene*, 27(48) Macmillan Publishers Limited, pp. 6194-6206.
- Li, W., Yang, Q. and Mao, Z. (2011) 'Chaperone-mediated autophagy: Machinery, regulation and biological consequences', *Cellular and Molecular Life Sciences*, 68(5), pp. 749–763.
- Li, X., Ma, J. and Wang, J. (2015a) 'Cytotoxicity, oxidative stress, and apoptosis in HepG2 cells induced by ionic liquid 1-methyl-3-octylimidazolium bromide', *Ecotoxicology and Environmental Safety*, 120 Elsevier, pp. 342–348.
- Li, Y., Gao, Z. and Qu, X. (2015b) 'The adverse effects of sorafenib in patients with advanced cancers', *Basic & Clinical Pharmacology & Toxicology*, 116, pp. 216–221.
- Li, Y., Lu, L., Luo, N., Wang, Y.Q. and Gao, H.M. (2017) 'Inhibition of PI3K/Akt/mTOR signaling pathway protects against D-galactosamine/lipopolysaccharide-induced acute liver failure by chaperone-mediated autophagy in rats', *Biomedicine and Pharmacotherapy*, 92 Elsevier Masson SAS, pp. 544–553.
- Liao, Z., Wang, B., Liu, W., Xu, Q., Hou, L., Song, J., Guo, Q. and Li, N. (2021) 'Dysfunction of chaperone - mediated autophagy in human diseases', *Molecular and Cellular Biochemistry*, 476(3) Springer US, pp. 1439–1454.
- Lin, L. and Baehrecke, E.H. (2015) 'Autophagy, cell death, and cancer', *Molecular and Cellular Oncology*, 2(3) Taylor and Francis Ltd., pp. 1–8.
- Liu, C.Y., Chen, K.F. and Chen, P.J. (2015) 'Treatment of liver cancer', *Cold Spring Harbor Perspectives in Medicine*, 5(9), pp. 1–17.

- Liu, H., Chen, F., Zhang, L., Zhou, Q., Gui, S. and Wang, Y. (2016) 'A novel all-trans retinoic acid derivative 4-amino-2-trifluoromethyl-phenyl retinate inhibits the proliferation of human hepatocellular carcinoma HepG2 cells by inducing G0/G1 cell cycle arrest and apoptosis via upregulation of p53 and ASPP1 and downregulation of iASPP', *Oncology Reports*, 36(1) Spandidos Publications, pp. 333–341.
- Lu, T., Huang, G.-J., Wang, H.-J., Chen, J.-L., Hsu, H.-P. and Lu, T.-J. (2010) 'Hispolon promotes MDM2 downregulation through chaperone-mediated autophagy', *Biochemical and Biophysical Research Communications*, 398(1) Elsevier Inc., pp. 26–31.
- Lu, Y. and Cederbaum, A.I. (2008) 'CYP2E1 and Oxidative Liver Injury by Alcohol', *Free Radical Biology and Medicine*, 44(5), pp. 723–738.
- Lüthi, A.U. and Martin, S.J. (2007) 'The CASBAH: A searchable database of caspase substrates', *Cell Death and Differentiation*, 14(4), pp. 641–650.
- Madi, N., Dany, M., Abdoun, S. and Usta, J. (2016) 'Moringa oleifera's Nutritious Aqueous Leaf Extract Has Anticancerous Effects by Compromising Mitochondrial Viability in an ROS-Dependent Manner', *Journal of the American College of Nutrition*, 35(7) Routledge, pp. 604–613.
- Mahfuz, S. and Piao, X.S. (2019) 'Application of Moringa (Moringa oleifera) as natural', *Animals*, 9(431), pp. 1–19.
- Majeski, A.E. and Dice, J.F. (2004) 'Mechanisms of chaperone-mediated autophagy', *The International Journal of Biochemistry & Cell Biology*, 36, pp. 2435–2444.
- Mangiarotti, R., Danova, M., Alberici, R. and Pellicciari, C. (1996) 'All-trans retinoic acid (ATRA)-induced apoptosis is preceded by G1 arrest in human MCF-7 breast cancer cells', *British Journal of Cancer*, 77(2), pp. 186–191.

Maponga, T.G., Glashoff, R.H., Vermeulen, H., Robertson, B., Burmeister, S., Bernon, M., Omoshoro-Jones, J., Ruff, P., Neugut, A.I., Jacobson, J.S., Preiser, W. and Andersson, M.I. (2020) 'Hepatitis B virus-associated hepatocellular carcinoma in South Africa in the era of HIV', *BMC Gastroenterology*, 20(1) BioMed Central, pp. 1–9.

Martín-Renedo, J., Mauriz, J.L., Jorquera, F., Ruiz-Andrés, O., González, P. and González-Gallego, J. (2008) 'Melatonin induces cell cycle arrest and apoptosis in hepatocarcinoma HepG2 cell line', *Journal of Pineal Research*, 45, pp. 532–540.

McGlynn, K.A., Petrick, J.L. and El-Serag, H.B. (2021) 'Epidemiology of Hepatocellular Carcinom'a *Hepatology*. 73(S1) John Wiley and Sons Inc, pp. 4-13.

Mizushima, N. (2018) 'A brief history of autophagy from cell biology to physiology and disease', *Nature Cell Biology*, 20(5) Nature Publishing Group, pp. 521–527.

Mizushima, N. and Komatsu, M. (2011) 'Autophagy: Renovation of cells and tissues', *Cell*, 147(4) Elsevier Inc., pp. 728–741.

Molina, M.L., García-Bernal, D., Martínez, S. and Valdor, R. (2020) 'Autophagy in the immunosuppressive perivascular microenvironment of glioblastoma' *Cancers*, 12(1) MDPI AG, pp. 1-20.

Morishita, H. and Mizushima, N. (2019) 'Diverse Cellular Roles of Autophagy', *Annual Review of Cell and Developmental Biology*, 35(23), pp. 3.1-3.23.

Mowers, E.E., Sharifi, M.N. and Macleod, K.F. (2017) 'Autophagy in cancer metastasis', *Oncogene*, 36, pp. 1619–1630.

Ndom, P. (2019) 'Cancer prevention in Africa: liver cancer', *eCancerMedical Science*, (Table 2), pp. 1–8.

Nguyen, C.H., Bauer, K., Hackl, H., Schlerka, A., Koller, E., Hladik, A., Stoiber, D., Zuber, J., Staber, P.B., Hoelbl-kovacic, A., Purton, L.E., Grebien, F. and Wieser, R.

(2019) 'All-trans retinoic acid enhances, and a pan-RAR antagonist counteracts, the stem cell promoting activity of EVI1 in acute myeloid leukemia', *Cell Death and Disease*, 10 Springer US, pp. 944–960.

Ni, X., Hu, G. and Cai, X. (2019) 'The success and the challenge of all-trans retinoic acid in the treatment of cancer', *Critical reviews in food science and nutrition*, 59(sup1) NLM (Medline), pp. S71–S80.

Oishi, N. and Wang, X.W. (2011) 'Novel therapeutic strategies for targeting liver cancer stem cells', *International Journal of Biological Sciences*, 7(5), pp. 517–535.

Park, M.Y., Kim, K.R., Park, H.S., Park, B.-H., Choi, H.N., Jang, K.Y., Chung, M.J., Kang, M.J., Lee, D.G. and Moon, W.S. (2007) 'Expression of the serum response factor in hepatocellular carcinoma: Implications for epithelial-mesenchymal transition', *International Journal of Oncology*, 31, pp. 1309–1315.

Parzych, K.R. and Klionsky, D.J. (2014) 'An overview of autophagy: morphology, mechanism, and regulation', *Antioxidants & Redox Signaling*, 20(3), pp. 460–473.

Patel, B. and Cuervo, A.M. (2015) 'Methods to study chaperone-mediated autophagy', *Methods*, 75 Academic Press Inc., pp. 133–140.

Patel, V.P., Pande, V.V. and Devendra Borawake, D. (2018) 'Screening of Moringa oleifera leaf extract on various human cancerous Cell line using microtiter plate-based assay', *International Journal of Bioengineering & Biotechnology*, 3(2), pp. 8–13.

Patra, K.C. and Hay, N. (2013) 'Hexokinase 2 as oncotarget', *Oncotarget*, 4(11), pp. 1862–1863.

Peskin, A. V and Winterbourn, C.C. (2000) 'A microtiter plate assay for superoxide dismutase using a water-soluble tetrazolium salt (WST-1)', *Clinica Chimica Acta*, 293, pp. 157–166.

Peter, M.E. and Krammer, P.H. (2003) 'The CD95(APO-1/Fas) DISC and beyond' *Cell Death and Differentiation*, 10(1), pp. 26-35

Pfeffer, C.M. and Singh, A.T.K. (2018) 'Apoptosis: A target for anticancer therapy', *International Journal of Molecular Sciences*, 19(2), pp. 1-10.

Pinheiro, P.S., Callahan, K.E., Jones, P.D., Morris, C., Ransdell, J.M., Kwon, D., Brown, C.P. and Kobetz, E.N. (2019) 'Liver cancer: A leading cause of cancer death in the United States and the role of the 1945–1965 birth cohort by ethnicity', *JHEP Reports*, 1(3) Elsevier, pp. 162–169.

Porter, A.G. and Jänicke, R.U. (1999) 'Emerging roles of caspase-3 in apoptosis', *Cell Death and Differentiation*, 6, pp. 99–104.

Qin, X., Suzuki, H., Honda, M., Okada, H., Kaneko, S., Inoue, I., Ebisui, E., Hashimoto, K., Caminci, P., Kanki, K., Tatsukawa, H., Ishibashi, N., Masaki, T., Matsuura, T., Kagechika, H., Toriguchi, K., Hatano, E., Shirakami, Y., Shiota, G., Shimizu, M., Moriwaki, H. and Kojima, S. (2018) 'Prevention of hepatocellular carcinoma by targeting MYCN-positive liver cancer stem cells with acyclic retinoid', *Proceedings of the National Academy of Sciences of the United States of America*, 115(19), pp. 4969–4974.

Rafiq, S., Mungure, I., Niklaus, N.J., Müller, S., Jacquel, A., Robert, G., Auberger, P., Torbett, B.E., Muller, S. and Humbert, M. (2022) 'HSPA8 chaperone complex drives chaperone-mediated autophagy regulation in acute promyelocytic leukemia differentiation', *Biorxiv*, pp. 1-33.

Randall, S. (2017) *South African national HIV prevalence, incidence, behaviour and communication survey, 2017: towards achieving the UNAIDS 90-90-90 targets*.

Ranke, J., Mölter, K., Stock, F., Bottin-weber, U., Poczobutt, J., Hoffmann, J., Ondruschka, B., Filser, J. and Jastorff, B. (2004) 'Biological effects of imidazolium ionic

liquids with varying chain lengths in acute *Vibrio fischeri* and WST-1 cell viability assays', *Ecotoxicology and Environmental Safety*, 58, pp. 396–404.

Rathore, R., McCallum, J.E., Varghese, E., Florea, A.M. and Büsselberg, D. (2017) 'Overcoming chemotherapy drug resistance by targeting inhibitors of apoptosis proteins (IAPs)', *Apoptosis*, 22(7) Springer New York LLC, pp. 898–919.

Robert, G., Jacquelin, A. and Auberger, P. (2019) 'Chaperone-Mediated Autophagy and Its Emerging Role in Hematological Malignancies', *Cells*, 8(1260), pp. 1–19.

Rodriguez-Navarro, J.A., Kaushik, S., Koga, H., Dall'Armi, C., Shui, G., Wenk, M.R., di Paolo, G. and Cuervo, A.M. (2012) 'Inhibitory effect of dietary lipids on chaperone-mediated autophagy', *Proceedings of the National Academy of Sciences of the United States of America*, 109(12), pp. E705-E714.

Saha, S., Panigrahi, D.P., Patil, S. and Bhutia, S.K. (2018) 'Autophagy in health and disease: A comprehensive review' *Biomedicine and Pharmacotherapy*. 104(2018) Elsevier Masson SAS, pp. 485-495.

Sakamoto, M. (2009) 'Early HCC: diagnosis and molecular markers', *Journal of Gastroenterology*, 44(Suppl XIX), pp. 108–111.

Salvesen, G.S. and Dixit, V.M. (1997) 'Caspases: Intracellular signaling by proteolysis', *Cell*, 91, pp. 443–446.

Santucci, R., Sinibaldi, F., Cozza, P., Polticelli, F. and Fiorucci, L. (2019) 'Cytochrome c: An extreme multifunctional protein with a key role in cell fate', *International Journal of Biological Macromolecules*. Elsevier B.V., pp. 1-39.

Schenk, T., Stengel, S. and Zelent, A. (2014) 'Unlocking the potential of retinoic acid in anticancer therapy' *British Journal of Cancer*, 111(11) Nature Publishing Group, pp. 2029-2045.

- Schmidt-Mende, J., Gogvadze, V., Hellström-Lindberg, E. and Zhivotovsky, B. (2006) 'Early mitochondrial alterations in ATRA-induced cell death', *Cell Death and Differentiation*, 13(1), pp. 119–128.
- Schnaith, A., Kashkar, H., Leggio, S.A., Addicks, K., Krönke, M. and Krut, O. (2007) 'Staphylococcus aureus subvert autophagy for induction of caspase-independent host cell death', *Journal of Biological Chemistry*, 282(4), pp. 2695–2706.
- Shi, L., Li, H. and Zhan, Y. (2017) 'All-trans retinoic acid enhances temozolomide-induced autophagy in human glioma cells U251 via targeting Keap1/Nrf2/ARE signaling pathway', *Oncology Letters*, 14(3) Spandidos Publications, pp. 2709–2714.
- Shi, Y. (2004) 'Caspase activation, inhibition, and reactivation: A mechanistic view', *Protein Science*, 13(8), pp. 1979–1987.
- Shimizu, S., Yoshida, T., Tsujioka, M. and Arakawa, S. (2014) 'Autophagic cell death and cancer *International*', *Journal of Molecular Sciences*, 15(Suppl.) Molecular Diversity Preservation International, pp. D84-D90.
- Shintani, T. and Klionsky, D.J. (2004) 'Autophagy in health and disease: a double-edged sword', *Science*, 306(5698), pp. 990–995.
- Siddiqui, S., Upadhyay, S., Ahmad, I., Hussain, A. and Ahamed, M. (2021) 'Cytotoxicity of Moringa oleifera fruits on human liver cancer and molecular docking analysis of bioactive constituents against caspase-3 enzyme', *Journal of Food Biochemistry*, 45(5) Blackwell Publishing Ltd, pp. 1–13.
- Sreelatha, S., Jeyachitra, A. and Padma, P.R. (2011) 'Antiproliferation and induction of apoptosis by Moringa oleifera leaf extract on human cancer cells', *Food and Chemical Toxicology*, 49(6), pp. 1270–1275.

- Sun, Y., He, Y., Tong, J., Liu, D., Zhang, H., He, T. and Bi, Y. (2022) 'All-trans retinoic acid inhibits the malignant behaviors of hepatocarcinoma cells by regulating ferroptosis', *Genes and Diseases*, 9(6) Chongqing University, pp. 1742–1756.
- Sung, H., Ferlay, J., Siegel, R.L., Laversanne, M., Soerjomataram, I., Jemal, A. and Bray, F. (2021) 'Global cancer statistics 2020: GLOBOCAN estimates of incidence and mortality worldwide for 36 cancers in 185 countries', *CA: A Cancer Journal for Clinicians*, 0(0), pp. 1–41.
- Susanto, H., Yunisa, D.T., Taufiq, A., Putra, W.E., Jannah, N.R., Putri, S.A., Dewi, I.A., Febriyanti, Q.D.A. and Mufidah, I.N. (2021) 'Anti fibrogenesis effect of green materials Moringa oleifera leaf powder (MOLP) on the progression of hepatocellular carcinoma', *AIP Conference Proceedings*. American Institute of Physics Inc., Vol.2353.
- Suzuki, J., Nakajima, W., Suzuki, H., Asano, Y. and Tanaka, N. (2017) 'Chaperone-mediated autophagy promotes lung cancer cell survival through selective stabilization of the pro-survival protein, MCL1', *Biochemical and Biophysical Research Communications*, 482(4) Elsevier B.V., pp. 1334–1340.
- Tabboon, P., Sripanidkulchai, B. and Sripanidkulchai, K. (2016) 'Hypocholesterolemic mechanism of phenolics-enriched extract from Moringa oleifera leaves in HepG2 cell lines', *Songklanakarin Journal of Scientific Technology*, 38(2), pp. 155–161.
- Tang, A., Hallouch, O., Chernyak, V., Kamaya, A. and Sirlin, C.B. (2018) 'Epidemiology of hepatocellular carcinoma: target population for surveillance and diagnosis', *Abdominal Radiology*, 43(1) Springer US, pp. 13–25.
- Tang, W., Chen, Z., Zhang, W., Cheng, Y., Zhang, B., Wu, F., Wang, Q., Reiter, F.P., Toni, E.N. De and Wang, X. (2020) 'The mechanisms of sorafenib resistance in

hepatocellular carcinoma: theoretical basis and therapeutic aspects', *Signal Transduction and Targeted Therapy*, 5 Springer US, pp. 87–101.

Tang, Y., Wang, X.-W., Liu, Z.-H., Sun, Y.-M. and Tang, Y.-X. (2017) 'Chaperone-mediated autophagy substrate proteins in cancer', *Oncotarget*, 8(31), pp. 51970–51985.

Tiloke, C., Anand, K., Gengan, R.M. and Chuturgoon, A.A. (2018) 'Moringa oleifera and their phytonanoparticles: Potential antiproliferative agents against cancer', *Biomedicine & Pharmacotherapy*, 108(September) Elsevier, pp. 457–466.

Tiloke, C., Phulukdaree, A. and Chuturgoon, A.A. (2013) 'The antiproliferative effect of Moringa oleifera crude aqueous leaf extract on cancerous human alveolar epithelial cells', *BMC Complementary and Alternative Medicine*, 13(1) BMC Complementary and Alternative Medicine, pp. 226–233.

Tiloke, C., Phulukdaree, A. and Chuturgoon, A.A. (2016) 'The Antiproliferative Effect of Moringa oleifera Crude Aqueous Leaf Extract on Human Esophageal Cancer Cells', *Journal of Medicinal Food*, 19(4) Mary Ann Liebert Inc., pp. 398–403.

Tiloke, C., Phulukdaree, A., Gengan, R.M. and Chuturgoon, A.A. (2019) 'Moringa oleifera aqueous leaf extract induces cell-cycle arrest and apoptosis in human liver hepatocellular carcinoma cells', *Nutrition and Cancer*, Taylor & Francis, pp. 1–10.

Tolba, R., Kraus, T., Liedtke, C., Schwarz, M. and Weiskirchen, R. (2015) 'Diethylnitrosamine (DEN)-induced carcinogenic liver injury in mice', *Laboratory Animals*, 49, pp. 59–69.

Toma, S., Isnardi, L., Raffo, P., Dastoli, G., de Francisci, E., Riccardi, L., Palumbo, R. and Bollag, W. (1997) 'Effects of all-trans-retinoic acid and 13-cis-retinoic acid on breast-cancer cell lines: growth inhibition and apoptosis induction', *International Journal of Cancer*, 70 Wiley-Liss, Inc, pp. 619–627.

- Tsujimoto, Y. and Shimizu, S. (2005) 'Another way to die: Autophagic programmed cell death', *Cell Death and Differentiation*, 12, pp. 1528–1534.
- Twilley, D., Rademan, S. and Lall, N. (2020) 'A review on traditionally used South African medicinal plants, their secondary metabolites and their potential development into anticancer agents', *Journal of Ethnopharmacology*, 261 Elsevier Ireland Ltd, p. 113101.
- Villani, R., Vendemiale, G. and Serviddio, G. (2019) 'Molecular mechanisms involved in HCC recurrence after direct-acting antiviral therapy', *International Journal of Molecular Sciences*, 20(49), pp. 1–16.
- Waller, L.P., Deshpande, V. and Pysopoulos, N. (2015) 'Hepatocellular carcinoma: A comprehensive review', *World Journal of Hepatology*, 7(26), pp. 2648–2663.
- Wang, W., Xu, G., Ding, C.L., Zhao, L.J., Zhao, P., Ren, H. and Qi, Z.T. (2013) 'All-trans retinoic acid protects hepatocellular carcinoma cells against serum-starvation-induced cell death by upregulating collagen 8A2', *FEBS Journal*, 280(5), pp. 1308–1319.
- Wang, Y.T. and Lu, J.H. (2022) 'Chaperone-Mediated Autophagy in Neurodegenerative Diseases: Molecular Mechanisms and Pharmacological Opportunities', *Cells*, 11(14) MDPI, pp. 1-18.
- Wei, J., Ye, C., Liu, F. and Wang, W. (2014) 'All-trans retinoic acid and arsenic trioxide induce apoptosis and modulate intracellular concentrations of calcium in hepatocellular carcinoma cells', *Journal of Chemotherapy*, 26(6) Maney Publishing, pp. 348–352.
- Wong, R.S. (2011) 'Apoptosis in cancer: from pathogenesis to treatment', *Journal of Experimental and Clinical Cancer Research*, 30(1), pp. 1–14.

- Wu, L., Li, L., Chen, S., Wang, L. and Lin, X. (2020) 'Deep eutectic solvent-based ultrasonic-assisted extraction of phenolic compounds from *Moringa oleifera* L. leaves: Optimization, comparison and antioxidant activity', *Separation and Purification Technology*, 247(2020) Elsevier B.V., pp. 1–11.
- Wu, N., Zhang, W., Yang, Y., Liang, Y.L., Wang, L.Y., Jin, J.W., Cai, X.M. and Zha, X.L. (2006) 'Profilin 1 obtained by proteomic analysis in a 11-trans retinoic acid-treated hepatocarcinoma cell lines is involved in inhibition of cell proliferation and migration', *Proteomics*, 6(22), pp. 6095–6106.
- Wu, Q., Dawson, M.I., Zheng, Y.U.N., Hobbs, P.D., Agadir, A., Jong, L., Li, Y.I.N., Liu, R.U., Lin, B. and Zhang, X. (1997) 'Inhibition of trans -retinoic acid-resistant human breast cancer cell growth by retinoid X receptor-selective retinoids', *Molecular and Cellular Biology*, 17(11), pp. 6598–6608.
- Xia, H.-G., Najafov, A., Geng, J., Galan-Acosta, L., Han, X., Guo, Y., Shan, B., Zhang, Y., Norberg, E., Zhang, T., Pan, L., Liu, J., Coloff, J.L., Ofengeim, D., Zhu, H., Wu, K., Cai, Y., Yates, J.R., Zhu, Z., Yuan, J. and Vakifahmetoglu-Norberg, H. (2015) 'Degradation of HK2 by chaperone-mediated autophagy promotes metabolic catastrophe and cell death', *The Journal of Cell Biology*, 210(5), pp. 705–716.
- Xie, Y., Hou, W., Song, X., Yu, Y., Huang, J., Sun, X., Kang, R. and Tang, D. (2016) 'Ferroptosis: Process and function' *Cell Death and Differentiation*, 23 Nature Publishing Group, pp. 369-379.
- Xu, Y., Chen, G. and Guo, M. (2020) 'Correlations between phytochemical fingerprints of *Moringa oleifera* leaf extracts and their antioxidant activities revealed by chemometric analysis', *Phytochemical Analysis*, 32(5) John Wiley and Sons Ltd, pp. 698–709.

- Yang, C. and Wang, X. (2021) 'Lysosome biogenesis: Regulation and functions', *Journal of Cell Biology*, 220(6), Rockefeller University Press, pp. 1-15.
- Yang, S., Yang, L., Li, X., Li, B., Li, Y., Zhang, X., Ma, Y., Peng, X., Jin, H. and Li, H. (2019) 'New insights into autophagy in hepatocellular carcinoma: mechanisms and therapeutic strategies', *American Journal of Cancer Research*, 9(7), pp. 1329–1353.
- Yao, Z., Chen, D., Wang, A., Ding, X., Liu, Z., Ling, L., He, Q. and Zhao, T. (2011) 'Folic acid rescue of ATRA-induced cleft palate by restoring the TGF- $\beta$  signal and inhibiting apoptosis', *Journal of Oral Pathology and Medicine*, 40(5), pp. 433–439.
- Yoon, W.H., Song, I.S., Lee, B.H., Jung, Y.J., Kim, T.D., Li, G., Lee, T.G., Park, H.D., Lim, K. and Hwang, B.D. (2004) 'Differential regulation of vimentin mRNA by 12-O-tetradecanoylphorbol 13-acetate and all-trans-retinoic acid correlates with motility of Hep 3B human hepatocellular carcinoma cells', *Cancer Letters*, 203(1) Elsevier Ireland Ltd, pp. 99–105.
- Yu, Z., Han, J., Lin, J., Xiao, Y., Zhang, X. and Li, Y. (2006) 'Apoptosis induced by atRA in MEPM cells is mediated through activation of caspase and RAR', *Toxicological Sciences*, 89(2), pp. 504–509.
- Zakharia, K., Luther, C.A., Alsabbak, H. and Roberts, L.R. (2018) 'Hepatocellular carcinoma: Epidemiology, pathogenesis and surveillance - implications for sub-Saharan Africa', *South African Medical Journal*, 108, pp. S35-40.
- Zhang, C. and Cuervo, A.M. (2008) 'Restoration of chaperone-mediated autophagy in aging liver improves cellular maintenance and hepatic function', *Nature Medicine*, 14(9), pp. 959–965.
- Zhang, H., Satyamoorthy, K., Herlyn, M. and Rosdahl, I. (2003) 'All-trans retinoic acid (atRA) differentially induces apoptosis in matched primary and metastatic melanoma

cells-a speculation on damage effect of atRA via mitochondrial dysfunction and cell cycle redistribution', *Carcinogenesis*, 24(2), pp. 185–191.

Zhang, X., Hoffmann, B., Tran, P.B.-V., Graupner, G. and Pfahl, M. (1992) 'Retinoid X receptor is an auxiliary protein for thyroid hormone and retinoic acid receptors', *Nature*, 355(August), pp. 441–446.

Zhang, W., Li, X., Wang, S., Chen, Y. and Liu, H. (2020) 'Regulation of TFEB activity and its potential as a therapeutic target against kidney diseases', *Cell Death Discovery*, 6(32), pp. 1-10.

Zhu, Y.H., Ye, N., Tang, X.F., Khan, M.I., Liu, H.L., Shi, N. and Hang, L.F. (2019) 'Synergistic effect of retinoic acid polymeric micelles and prodrug for the pharmacodynamic evaluation of tumor suppression', *Frontiers in Pharmacology*, 10(MAY) Frontiers Media S.A., pp. 1–11.

Zhu, Y.J., Zheng, B., Wang, H.Y. and Chen, L. (2017) 'New knowledge of the mechanisms of sorafenib resistance in liver cancer', *Acta Pharmacologica Sinica*, 38(5) Nature Publishing Group, pp. 614–622.

# APPENDICES

## Appendix A



Health Sciences Research Ethics Committee

09-Dec-2021

Dear Mr Matlola Bopape

Ethics Clearance: The in vitro effects of Moringa oleifera on chaperone-mediated autophagy in human HepG2 liver cancer cells

Principal Investigator: Mr Matlola Bopape

Department: Basic Medical Sciences Department (Bloemfontein Campus)

[Submission Page](#)

**APPLICATION APPROVED**

Please ensure that you read the whole document

With reference to your application for ethical clearance with the Faculty of Health Sciences, I am pleased to inform you on behalf of the Health Sciences Research Ethics Committee that you have been granted ethical clearance for your project.

Your ethical clearance number, to be used in all correspondence is: UFS-HSD2021/1629/2501

The ethical clearance number is valid for research conducted for one year from issuance. Should you require more time to complete this research, please apply for an extension.

We request that any changes that may take place during the course of your research project be submitted to the HSREC for approval to ensure we are kept up to date with your progress and any ethical implications that may arise. This includes any serious adverse events and/or termination of the study.

A progress report should be submitted within one year of approval, and annually for long term studies. A final report should be submitted at the completion of the study.

**Research conducted in any Department of Health facility:** Researchers are required to sign and return the HSREC approval letters to the provincial Department of Health where they applied. It is also a requirement for researchers to submit electronic copies of their final research findings, and/or make a presentation of their findings and recommendations at departmental research days when and where indicated.

The HSREC functions in compliance with, but not limited to, the following documents and guidelines: The SA National Health Act, No. 61 of 2003; Ethics in Health Research: Principles, Structures and Processes (2015); SA GCP(2006); Declaration of Helsinki; The Belmont Report; The US Office of Human Research Protections 45 CFR 461 (for non-exempt research with human participants conducted or supported by the US Department of Health and Human Services- (HHS), 21 CFR 50, 21 CFR 56; CIOMS; ICH-GCP-E6 Sections 1-4; International Council for Harmonisation (ICH) Harmonised Guideline, Integrated Addendum to ICH E6(R1), Guideline for Good Clinical Practice (GCP) E6(R2), 2016, SAHPRA Guidelines as well as Laws and Regulations with regard to the Control of Medicines, Constitution of the HSREC of the Faculty of Health Sciences.

For any questions or concerns, please feel free to contact HSREC Administration: 051-4017794/5 or email [EthicsFHS@ufs.ac.za](mailto:EthicsFHS@ufs.ac.za).

Thank you for submitting this proposal for ethical clearance and we wish you every success with your research.

Yours Sincerely

Prof. A. Sherriff

Chairperson: Health Sciences Research Ethics Committee

Health Sciences Research Ethics Committee

Office of the Dean: Health Sciences:

T: +27 (0)51 401 7795/7794 | E: [ethics@ufs.ac.za](mailto:ethics@ufs.ac.za)

IRB 00011992; REC 230408-011; IORG 0010596; FWA 00027947

Block D, Dean's Division, Room D104 | P.O. Box/Poebus 339 (Internal Post Box G40) | Bloemfontein 9300 | South Africa  
[www.ufs.ac.za](http://www.ufs.ac.za)



**Figure A1: Initial ethical clearance letter.**

04-Mar-2022

Prof. A. Sherriff  
Chairperson : Health Sciences Research Ethics Committee

Health Sciences Research Ethics Committee  
Office of the Dean: Health Sciences

T: +27 (0)51 401 7795/7794 | E: ethics@ufs.ac.za  
IRB 00011992; REC 230408-011; IORG 0010096; FWA 00027947

Block D, Dean's Division, Room D104 | P.O. Box/Postbus 339 (Internal Post Box G40) | Bloemfontein 9300 | South Africa  
www.ufs.ac.za



Dear Mr Matlola Bopape

Ethics Number: UFS-HSD2021/1629-0003

Ethics Clearance: The in vitro effects of *Moringa oleifera* on chaperone-mediated autophagy in human HepG2 liver cancer cells

Principal Investigator: Mr Matlola Bopape

Department: Basic Medical Sciences Department (Bloemfontein Campus)

[Submission Page](#)

SUBSEQUENT SUBMISSION APPROVED

With reference to your recent submission for ethical clearance from the Health Sciences Research Ethics Committee, I am pleased to inform you on behalf of the HSREC that you have been granted ethical clearance for your request as stipulated below:

- The HepG2 cell line to be used in this study will be acquired from the Department of Medical Biochemistry and Chemical Pathology at the University of KwaZulu-Natal:
  - The Department of Basic Medical Sciences has acquired the HepG2 cells from Merck/Sigma, however, there is a delay in permit approval from the Department of Health as well as a delay in the availability of stock of the cell line. To prevent a delay in the study, the Department of Medical Biochemistry and Chemical Pathology at the University of KwaZulu-Natal has agreed to provide the HepG2 cell line.
- The Protocol states that the cells are acquired from the University of KwaZulu-Natal as well on page 19.
- Kindly note: There is no change in the cell line nor is there any change in the protocol. The only change is the source of the cells.

The HSREC functions in compliance with, but not limited to, the following documents and guidelines: The SA National Health Act No. 61 of 2003; Ethics in Health Research: Principles, Structures and Processes (2015); SA GCP(2020); Declaration of Helsinki; The Belmont Report; The US Office of Human Research Protections 45 CFR 461 (for non-exempt research with human participants conducted or supported by the US Department of Health and Human Services- (HHS), 21 CFR 50, 21 CFR 56; CIOMS; ICH-GCP-E6 Sections 1-4; International Council for Harmonisation (ICH) Harmonised Guideline, Integrated Addendum to ICH E6(R1), Guideline for Good Clinical Practice (GCP) E6(R2), 2016, SAHPRA Guidelines as well as Laws and Regulations with regard to the Control of Medicines, Constitution of the HSREC of the Faculty of Health Sciences.

For any questions or concerns, please feel free to contact HSREC Administration: 051-4017794/5 or email [EthicsFHS@ufs.ac.za](mailto:EthicsFHS@ufs.ac.za).

Thank you for submitting this request for ethical clearance and we wish you continued success with your research.

Yours Sincerely

**Figure A2: Subsequent ethical clearance letter following the request to obtain the human HepG<sub>2</sub> cancer cells from the University of KwaZulu-Natal.**



Health Sciences Research Ethics Committee

12-Jan-2023

Dear Mr Matlola Bopape

Ethics Number: UFS-HSD2021/1629-0004

Ethics Clearance: **The in vitro effects of Moringa oleifera on chaperone-mediated autophagy in human HepG2 liver cancer cells**

Principal Investigator: Mr Matlola Bopape

Department: Basic Medical Sciences Department (Bloemfontein Campus)

[Submission Page](#)

**SUBSEQUENT SUBMISSION APPROVED**

With reference to your recent submission for ethical clearance from the Health Sciences Research Ethics Committee. I am pleased to inform you on behalf of the HSREC that you have been granted ethical clearance for your request as stipulated below:

Continuation Report: This project's ethics clearance is extended until 11 January 2024.

The HSREC functions in compliance with, but not limited to, the following documents and guidelines: The SA National Health Act. No. 61 of 2003; Ethics in Health Research: Principles, Structures and Processes (2015); SA GCP(2020); Declaration of Helsinki; The Belmont Report; The US Office of Human Research Protections 45 CFR 461 (for non-exempt research with human participants conducted or supported by the US Department of Health and Human Services- (HHS), 21 CFR 50, 21 CFR 56; CIOMS; ICH-GCP-E6 Sections 1-4; International Council for Harmonisation (ICH) Harmonised Guideline, Integrated Addendum to ICH E6(R1), Guideline for Good Clinical Practice (GCP) E6(R2), 2016, SAHPRA Guidelines as well as Laws and Regulations with regard to the Control of Medicines, Constitution of the HSREC of the Faculty of Health Sciences.

The Principal Investigator (PI) bears final responsibility for the RIMS application. In the event of any misconduct or improper activities perpetrated by a third party, the PI will be held vicariously liable. The HSREC will bear no responsibility or liability for any actions of a PI and/or third party or breach of confidentiality caused by the PI and/or third party.

For any questions or concerns, please feel free to contact HSREC Administration: 051-4017794/5 or email [EthicsFHS@ufs.ac.za](mailto:EthicsFHS@ufs.ac.za).

Thank you for submitting this request for ethical clearance and we wish you continued success with your research.

Yours Sincerely

Prof. A. Sherriff

Chairperson : Health Sciences Research Ethics Committee

Health Sciences Research Ethics Committee

Office of the Dean: Health Sciences

T: +27 (0)51 401 7793/7794 | E: [ethicsfhs@ufs.ac.za](mailto:ethicsfhs@ufs.ac.za)

IRB 00011992; REC 230408-011; IORG 0010096; FWA 00027947

Block D, Dean's Division, Room D104 | P.O. Box/Posbus 339 (Internal Post Box G40) | Bloemfontein 9300 | South Africa

[www.ufs.ac.za](http://www.ufs.ac.za)



Figure A3: Ethical clearance extension letter for 2023.

Ref: **Plant Identification Dispatch List** 19 January 2022

**Client:** Dr Charlette Tiloke  
**Address:** Staff No. 0890138  
 University of the Free State  
 Department of Basic Medical Science

**Tel:**  
**Cell:** 0845251340  
**Email:** Tilokec@ufs.ac.za

**ID CODES:**

0 = No challenges  
 1 = Specimen too poor to ID  
 2 = Label information inadequate  
 3 = Cannot match specimen in herbarium  
 4 = Specialist not available to do ID  
 5 = Genus requiring/under revision  
 6 = Specimen closest to name listed (cf)  
 7 = Please send more material  
 8 = Please refer to attached note/letter  
 9 = New record

**FATE:**

K = specimen kept for herbarium  
 R = specimen returned  
 S = specimen scrapped

Collector	No.	Plant Name	Det. By	Det. Notes	ID Code	Fate
1 C. Tiloke	2	<i>Moringa oleifera</i> Lam.	Ngwenya, A.M. 19/1/2022			

Curator  
 KwaZulu-Natal Herbarium (NH)

Please note a handling fee is charged for each specimen received for identification.

1

**Figure A4: *Moringa oleifera* certificate of authenticity issued by the KwaZulu-Natal Herbarium (NH)**

## Appendix B

**The percentage of DMSO:** The ATRA stock solution was prepared using 100% DMSO (see Materials and methods). Treatment solutions of ATRA were derived from the prepared ATRA stock solution. To prepare the treatment solution of ATRA (1415  $\mu\text{M}$ ), the stock solution was diluted in CCM. The percentage of DMSO in the working solution (calculated using the 10 mL final volume as an example, which was the treating volume 75  $\text{cm}^3$  flasks) was:

$$\text{Percentage of DMSO} = \frac{\text{Volume of DMSO}}{\text{Total volume}} \times 100\%$$

$$\text{Percentage of DMSO} = \frac{283 \mu\text{L}}{10\,000 \mu\text{L}} \times 100\%$$

$$\text{Percentage of DMSO} = 2.83\%$$

**Table B1: DMSO Percentages for ATRA Concentration Range Used to Determine the IC<sub>50</sub>**

Column	Concentration of treatment solution ( $\mu\text{M}$ )	Volume of DMSO used to prepare the treatment solution ( $\mu\text{L}$ )	Volume of CCM used to prepare the treatment solution ( $\mu\text{L}$ )	% of DMSO in working solution
1	0	0	1000	0
2	100	2	998	0.2
3	150	3	997	0.3
4	200	4	996	0.4
5	250	5	995	0.5
6	300	6	994	0.6
7	350	7	993	0.7
8	400	8	992	0.8
9	450	9	991	0.9
10	500	10	990	1.0

**Treatment of cells for experiments:** The cells were cultured and treated in 25  $\text{cm}^3$  cell culture flasks (SPL Life Sciences, 70025) using 5 mL treatment media, unless stated otherwise. The treatment media was prepared in 15 mL conical tubes on the day of treatment. For MO, new stock was prepared and filtered before diluted to the

IC<sub>50</sub> MO aqueous leaf extract on the day of treatment, then diluted in fresh pre-warmed CCM to create a 5 mL solution of the IC<sub>50</sub>. For ATRA, a 2 mL microcentrifuge tube of 50 mM stock was thawed at RT in the dark. Once thawed, the microcentrifuge was vortexed and diluted to form a 5 mL solution of the IC<sub>50</sub>. For the (MO+ATRA) combination group, the same volumes of ATRA stock and MO stock as the volumes added for the respective groups, were added to the 15 mL tube. An appropriate volume of CCM was then added to create a 5 mL treatment solution. For treatment in a 75 cm<sup>3</sup> cell culture flask, all volumes were doubled to create 10 mL treatment solutions. The conical tubes containing ATRA were covered with aluminium foil to keep them away from light.

**The enzyme-linked immunosorbent assay (ELISA):** To prepare the 1X Wash buffer, RT Wash Buffer Concentrate (20X) was mixed to precipitate the salts. 20 mL of the Wash Buffer Concentrate was dissolved in 380 mL deionized water (dH<sub>2</sub>O) to create 1X Wash Buffer.

To prepare the 1X Assay Diluent B and 1X Assay Diluent D, 5 mL each of 5X Assay Diluent B and 5X Assay Diluent D were diluted in 20 mL dH<sub>2</sub>O each.

To prepare the biotin conjugate, a vial of Human LAMP2 Biotin Conjugate was vortexed before 100 µL of the prepared 1X Assay Diluent B was added to the vial to create the biotin conjugate concentrate. The mixture was then mixed gently. 100 µL of the biotin conjugate concentrate was then dissolved in 7900 µL of 1X Assay Diluent B.

To prepare the standards, one vial of Human LAMP2 Standard, recombinant human LAMP2 was vortexed briefly before adding 600  $\mu\text{L}$  of the prepared 1X Assay Diluent D to create a 75 ng/mL standard solution. The solution was mixed thoroughly to ensure that the powder is completely dissolved. Seven microtubes were prepared each with 300  $\mu\text{L}$  of the prepared 1X Assay diluent D. The different concentrations of standard solution were prepared via serial dilution as indicated below: the first standard prepared (75 ng/mL) was considered as standard 1. Following the complete dissolving of the powder, 200  $\mu\text{L}$  of the solution was added to the first microtube containing the 300  $\mu\text{L}$  of 1X Assay Diluent D. The solution was mixed thoroughly and labelled as standard 2. 200  $\mu\text{L}$  of standard 2 was then transferred to the next microtube containing the 300  $\mu\text{L}$  of 1X Assay Diluent D. The solution was mixed thoroughly and labelled standard 3. This serial dilution was repeated 4 more times until there were 7 standards. The last microtube containing the 300  $\mu\text{L}$  of 1X Assay Diluent D was left as the blank standard. This resulted in a total of 8 standards where standard 1 was the reconstituted 75 ng/mL standard solution, standard 2 was 30 ng/mL, standard 3 was 12 ng/mL, standard 4 was 4.8 ng/mL, standard 5 was 1.920 ng/mL, standard 6 was 0.768 ng/mL, standard 7 was 0.307 ng/mL and the final tube contained only the 300  $\mu\text{L}$  of 1X Assay Diluent D that was added initially (Figure B1).

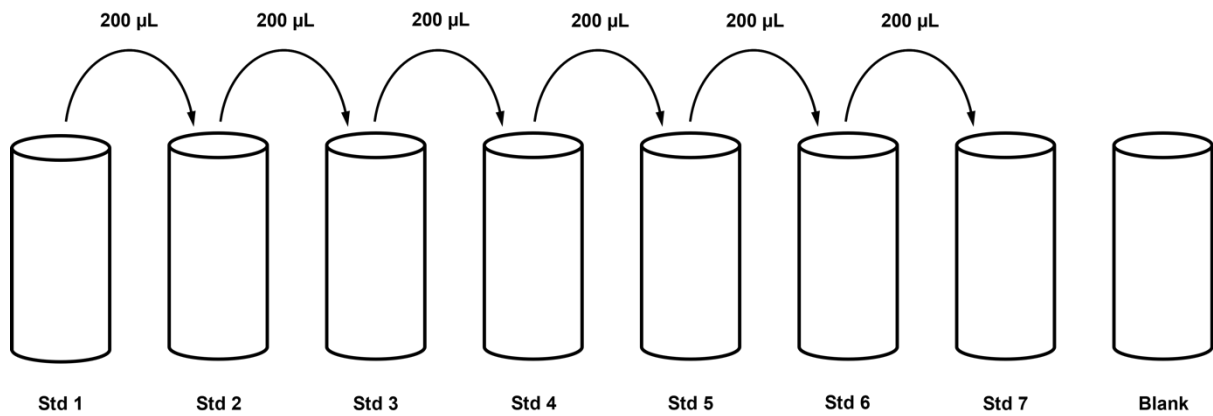


**Figure B1: Illustration of the preparation of the Human LAMP2 ELISA standards serial dilution. Std, Standard**

The Streptavidin-HRP solution was prepared within 15 minutes of being used as follows: the 150X Streptavidin-HRP vial was briefly gently mixed to ensure all precipitates are dissolved. In a 15 mL conical tube 60 µL of the 150X Streptavidin-HRP was dissolved in 8940 µL of 1X Assay Diluent B.

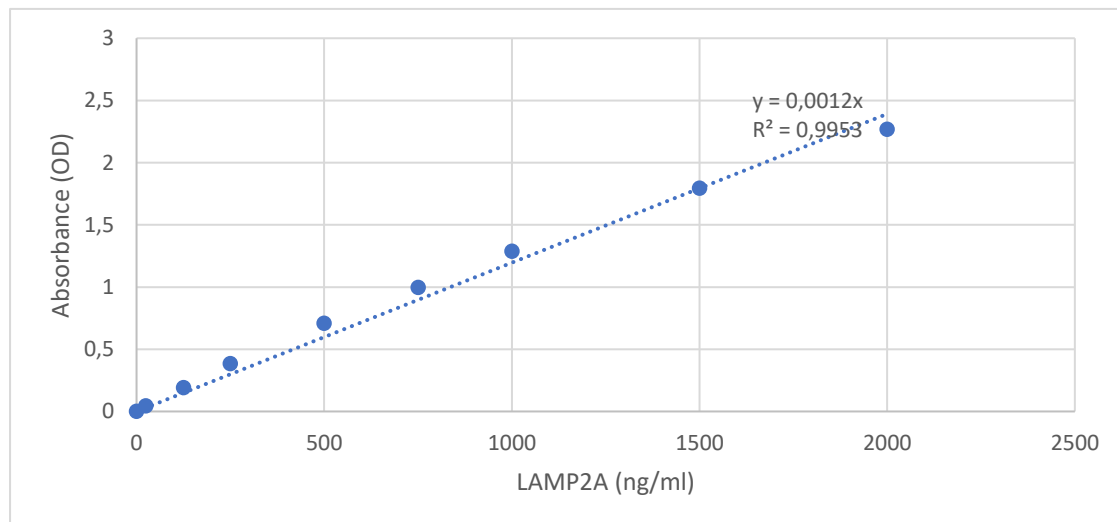


**Figure B2: Standard curve of collated repeats for LAMP2A ELISA**

**The bicinchoninic assay (BCA):** The BCA standards were prepared as shown in Table B1

**Table B1: Dilution Scheme for Standard Test Tube Protocol adapted from manufacturer's protocol (ThermoFisher Scientific, Pierce™ BCA Protein Assay Kit, 23225)**

Vial	Volume of Diluent (PBS) (μL)	Volume and Source of BSA (μL)	Final BSA Concentration (μg/mL)
A	0	300 of Stock	2000
B	125	375 of Stock	1500
C	325	325 of Stock	1000
D	175	175 of vial B dilution	750
E	325	325 of vial C dilution	500
F	325	325 of vial E dilution	250
G	325	325 of vial F dilution	125
H	400	100 of vial G dilution	25
I	400	0	0 = Blank

The average of the were used optical density values of the standards were used to create a standard curve (see Figure B2 for example). This was used to extrapolate the concentrations of the samples.

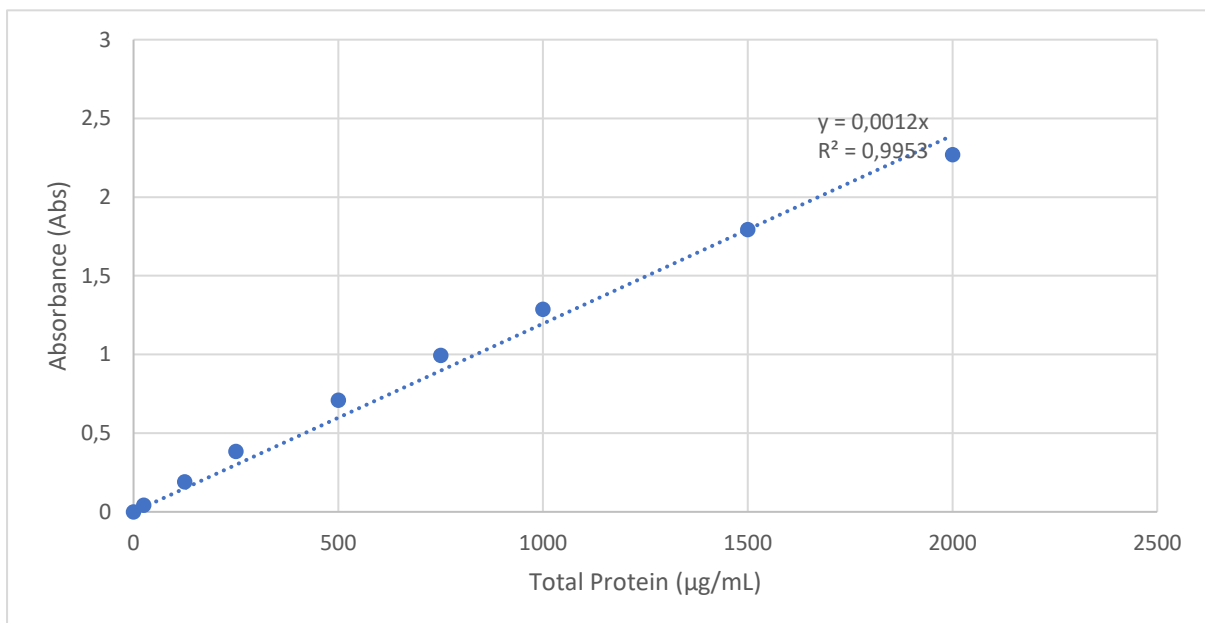


**Figure B3: Standard curve of collated repeats for BCA protein quantification assay**

**Western blot:** The loading buffer was prepared on the day as follows: 1000  $\mu$ L of 2X Laemmli's Sample Buffer (Bio-Rad Laboratories Inc, 1610737) and 5% of 2-Mercaptoethanol (Bio-Rad Laboratories Inc, 1610710) was added to a microcentrifuge tube.

To prepare the running buffer, 100 mL 10X Tris/Glycine/SDS Buffer (Bio-Rad Laboratories Inc, 1610732) and 900 mL dH<sub>2</sub>O were added to a clean 1000 mL beaker. The solution was mixed well using a magnetic stirrer and chilled at 4°C on the day of the experiment.

To prepare the wash buffer, 100 mL 10X Tris/Glycine Buffer (Bio-Rad Laboratories Inc, 1610734), 1 mL 10% Tween 20 Solution (Bio-Rad Laboratories Inc, 1610781) and 900 mL dH<sub>2</sub>O were mixed in a 1000 mL beaker.

**Caspase-Glo apoptosis assay:** To remove the cells from the treatment flask, the flask surface was washed 3 times with 5 mL pre-warmed PBS. 6 mL of 0.05% trypsin was added to each flask to detach the cells from the flask surface. The flasks were then incubated for 25 minutes in a humidified incubator at 37°C and 5% CO<sub>2</sub>. Following this incubation, 10 mL of pre-warmed CCM was added to each flask to neutralize the trypsin. The contents of the flask containing the cells in suspension were removed and added to a 50 mL conical tube (each flask's contents were added to a different tube and the tubes were clearly labelled). The conical tubes were then centrifuged at 2000 rpm for 20 minutes at RT, to pellet the cells. The supernatant of each tube was removed before 2 mL of pre-warmed PBS was added to each tube. The tubes were then centrifuged a second time with the same conditions as described above. The

supernatant of each tube was removed before adding 2 mL of pre-warmed PBS to each tube. Each tube was then then vortexed to dislodge the cell pellet allowing the cells to be in suspension. 10 µL of each cell suspension was then added to a new microtube and the tubes were labelled clearly. The same volume of trypan blue was added to each microtube. The cell suspension was then trypan blue were mixed together before adding 10 µL of each trypan blue-cell suspension mixture to each side of an automatic cell counter slide. The cell count of each of the cell suspensions were performed using an automatic cell counter and the average of each side of the cell counter slide was considered as the cell count using this equation:

$$\frac{\text{Live cell count (Side A)} + \text{Live cell count (Side B)}}{2}$$

## Appendix C

The morphological characteristics of human HepG<sub>2</sub> cancer cells were examined pre- and post-treatment. The morphological characteristics post-treatment is depicted in Figure C1.

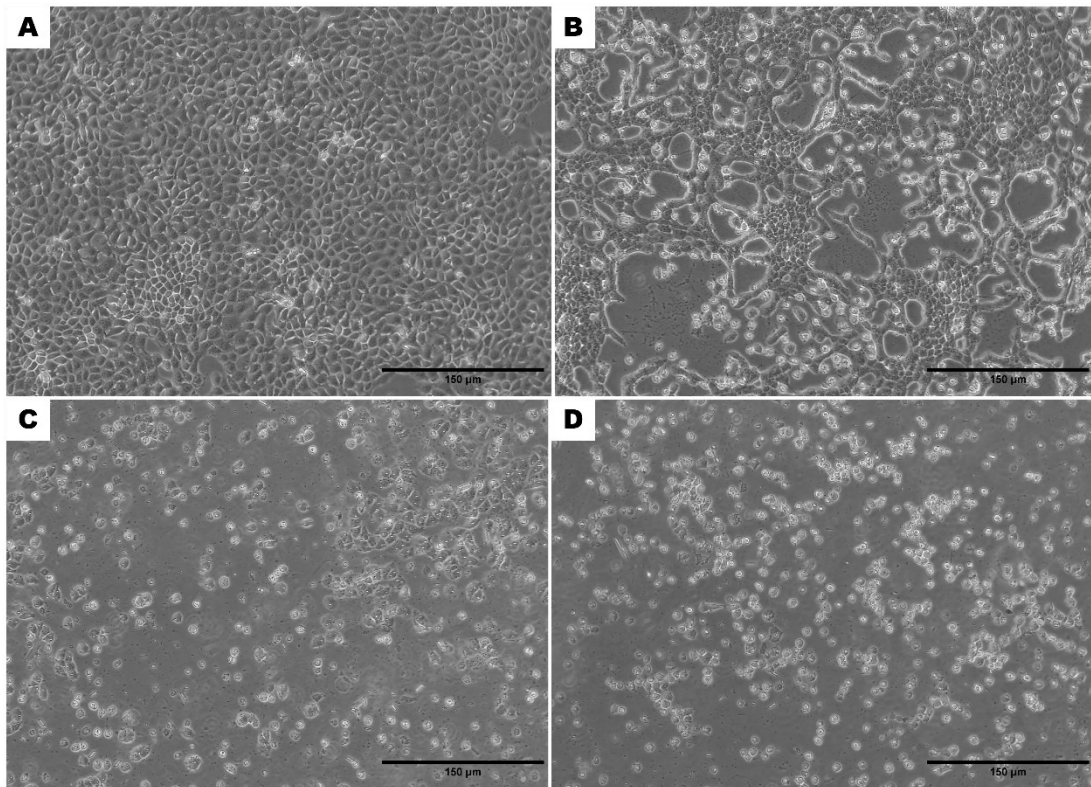


**Figure C1: Morphological characterization of human HepG<sub>2</sub> cells in response to 24-hour treatment.** A = Control group; B = MO treated group; C = ATRA treated group; D = ATRA+MO combination treatment group. 100X Magnification.

Cell counts were conducted to observe the changes in total human HepG<sub>2</sub> cancer cell count compared to the live cells post treatment as depicted in Figure C2.

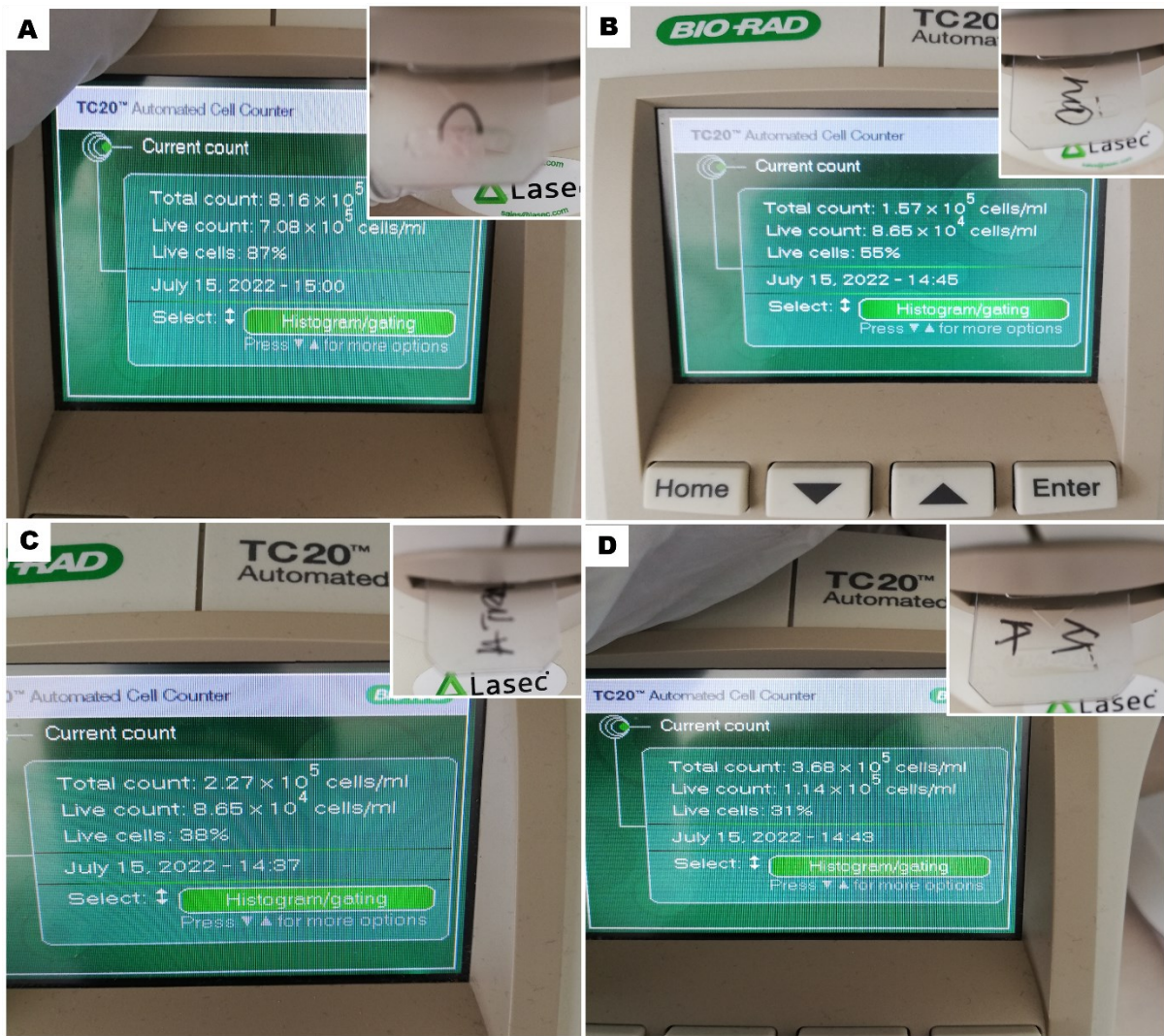


**Figure C2: Cell count and viability of human HepG<sub>2</sub> cells in response to 24-hour treatment.** A = Control group; B = MO treated group; C = ATRA treated group; D = ATRA+MO combination treatment group.

## Appendix D

Hoechst stain procedure was conducted to assess the presence of mycoplasma in the HepG<sub>2</sub> cancer cells used (Figure D). This was conducted to ensure that the cells lacked contamination and were therefore suitable for use in this study. The Hoechst stain procedure was conducted as following:

**Cell culturing:** A single glass microscope slide coverslip was added into each well of a clear six-well microplate. Cultured HepG<sub>2</sub> cancer cells were seeded onto each coverslip as follows: twenty thousand cells suspended in 500  $\mu$ L of pre-warmed CCM. The culture plate along with the cells was then incubated in a humidified atmosphere at 37°C and 5% CO<sub>2</sub> for 24-hours to allow the cells to adhere to the microscope slide coverslip. Following the incubation, CCM was aspirated from each well. Each well was then rinsed with 500  $\mu$ L pre-warmed PBS. The PBS was then aspirated from each well.

**Preparation of the 4% paraformaldehyde (PFA):** To prepare 400 mL of the PFA solution, 400 mL of pre-warmed PBS along with 20 g of Paraformaldehyde (Sigma-Aldrich, 158127) powder were added to a glass beaker. The beaker was then placed on the magnetic stirrer and the mixture was stirred for 1 hour at 37 °C, to completely dissolve the PFA powder. The PFA solution was then allowed to cool for 1 hour at room temperature (RT). The PFA was then filtered as follows: using a syringe attached to a filter, the PFA solution was filtered in 5 mL intervals into a 15 mL conical tube (only 15 mL of the PFA solution was filtered).

**Cell fixation onto the microscope slide coverslip:** Following the PBS rinse, 500  $\mu$ L of pre-warmed CCM and the same volume of PFA were added to each coverslip within the wells. The plate was then incubated for 1 hour at 37°C. The CCM and PFA mixture was then aspirated from each well and 500  $\mu$ L of pre-warmed PBS was added to each well. With gentle shaking, the coverslips were rinsed 3 times (5 minutes each time), replacing the PBS with fresh pre-warmed PBS each time.

**Hoechst staining of the HepG<sub>2</sub> cancer cells:** After the last rinse, the PBS was aspirated before 50  $\mu$ L of Hoechst 33342, trihydrochloride, trihydrate (ThermoFisher Scientific, H3570) was added to each coverslip. The plate was then covered with aluminium foil, to keep it away from light, and incubated at RT for 10 minutes. The coverslips were then rinsed 3 times with 500  $\mu$ L PBS (5 minutes each time), replacing the PBS with fresh pre-warmed PBS each time.

**Mounting the microscope slide coverslips on the microscope slides:** A drop of Fluorescence Mounting Medium (Dako<sup>®</sup>, S3023) was added to each microscope slide and the cell-containing cover slip was mounted in an inverted manner onto each microscope slide (inverted to ensure the cells are between the microscope slide and coverslip). Each microscope slide was then incubated for 1 hour at RT in the dark, to allow the mounting media to dry. The slides were then viewed using the Axio Observer 7 for LSM confocal microscope (Carl Zeiss Microscopy GmbH) attached to a Colibri 7 light module (Carl Zeiss Microscopy GmbH, 5438001088). The images were obtained and processed using the Zeiss Zen Blue (blue edition) imaging software.

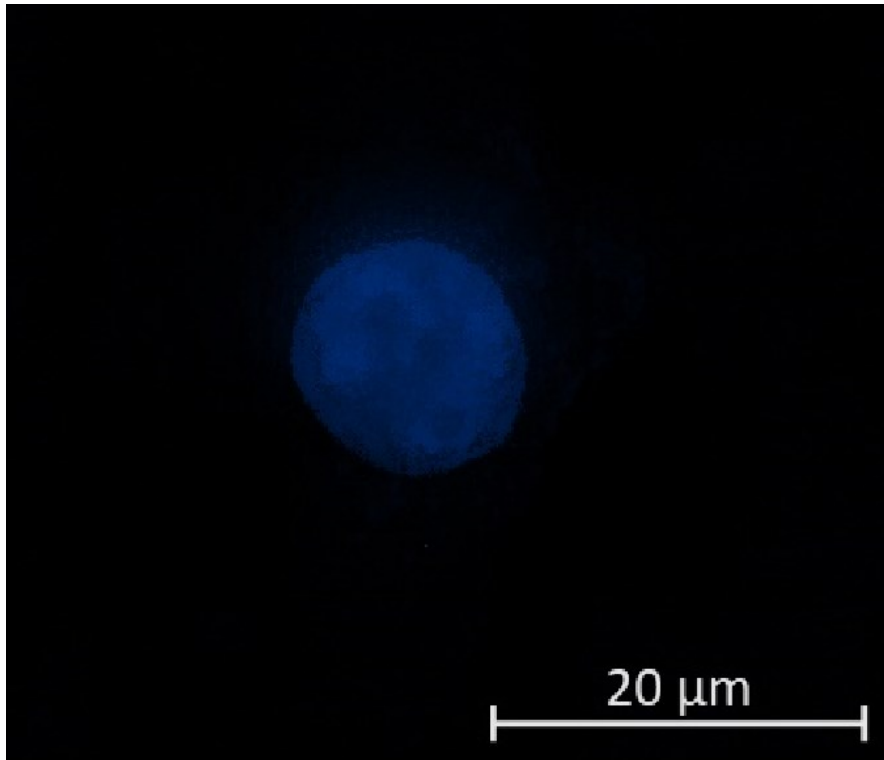


**Figure D: Fluorescent micrograph confirming the absence of mycoplasma in the human HepG<sub>2</sub> cells used for this study. 400X magnification.**

## Appendix E

### LANGUAGE PRACTITIONER: Anneke-Jean Diesel

BA Communication Science (Corporate and Marketing Communications)\*  
BA Hons Communication Science (Corporate and Marketing Communications)\*  
\* Cum Laude

17A Innes Avenue  
Waverley, Bloemfontein

Tel: 084 244 8961  
[annekedenobili@gmail.com](mailto:annekedenobili@gmail.com)

July 2023

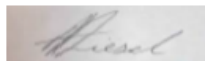
#### DECLARATION

I, Anneke-Jean Diesel, hereby declare that I did the language editing of the research of Matlola Abel Bopape (title: *The in vitro effects of Moringa oleifera on chaperone-mediated autophagy in human HepG2 liver cancer cells*). This research is submitted in fulfilment of the requirements of the degree Master of Medical Science (Physiology) in the Department of Basic Medical Sciences, School of Biomedical Sciences, Faculty of Health Sciences at the University of the Free State. All the suggested changes, including the implementation thereof, were left to the discretion of the student.

#### Please note:

The language editing did not include reference editing/checking or formatting. Also, the editor will not be held accountable for any later additions or changes to the document that the editor did not edit, nor if the student rejects/ignores any of the changes, suggestions or queries, which he/she is free to do. It remains the student's responsibility to ensure that the similarity index is according to the University's regulations. The editor can also not be held responsible for errors in the content of the document or whether or not the student passes or fails. It is the student's responsibility to review the edited document before submitting it for evaluation.

Sincerely



SATI Registration #: 1003466

**Figure E1: Declaration from language practitioner**

# Mr MA Bopape Turnitin Summary Report

---

## ORIGINALITY REPORT

---

<b>9%</b> SIMILARITY INDEX	<b>7%</b> INTERNET SOURCES	<b>5%</b> PUBLICATIONS	<b>3%</b> STUDENT PAPERS
-------------------------------	-------------------------------	---------------------------	-----------------------------

---

## MATCH ALL SOURCES (ONLY SELECTED SOURCE PRINTED)

---

1%

★ cora.ucc.ie

Internet Source

---

Exclude quotes On

Exclude matches < 10 words

Exclude bibliography On

**Figure E2: Turnitin similarity summary report**

# Appendix F

**From:** [Nutrition and Cancer](#)  
**To:** [Mildred Adano](#)  
**Subject:** Nutrition and Cancer - Decision on Manuscript ID NNC-11-23-6324-84  
**Date:** Wednesday, August 23, 2023 9:52:27 PM

23-Aug-2023

Dear Dr. Ntapi:

The review of the final revision of your manuscript entitled "Morings oleiferus and autophagy: Evidence from in vitro studies on chaperone-mediated autophagy in HepG2 cancer cells" is now complete. I am pleased to accept your manuscript for publication in Nutrition and Cancer. The comments of the reviewer(s) if any who reviewed your manuscript are included at the foot of this letter. We will let you know when your manuscript is assigned to an issue.

Thank you for your fine contribution to Nutrition and Cancer. I hope you will consider the journal as an outlet for your work in the future.

Please read the following text to familiarize yourself with the procedures that will be implemented to publish your article.

Keeping in Touch

The Editor of the journal is your primary source of information and advice. However, if you have a question the Editor is unable to answer, feel free to contact the Taylor and Francis Production Editor for the journal or the Taylor and Francis Electronic Journal Publishing Manager. (The Editor can put you in touch with both people.)

The journal is on a tight production schedule, so . . .

1. If you move or are away for an extended period during the time your manuscript is in production, let the Editor and Production Editor know where you can be reached (postal and e-mail addresses, telephone and fax numbers). You can imagine the delays that occur when the Production Editor e-mails typeset proofs to an address or phones a contributor with an important question, only to learn that the contributor is on sabbatical and did not leave forwarding information.
2. Contact the Production Editor if you are unable to return page proofs corrections within 7 days.

Understanding the Publication Process

1. You have now submitted your accepted manuscript to the journal. The first and most important task for authors after their manuscript is transferred to production will be to complete an online author agreement form. Please make sure you complete it as soon as you receive the publisher notice about it. Also, if you have not already done so, please e-mail (a) disclosure of interest form, and (b) any permissions to adapt or reprint tables, figures, and quotations to Mildred Adano at [HNUC-peerreview@journals.tandf.co.uk](mailto:HNUC-peerreview@journals.tandf.co.uk). Please go to [https://urldefense.com/v3/\\_http://mc.manuscriptcentral.com/nc\\_/\\_/11R1d1M/EHOJomBn7wON0zYgVplKf61pKSH1L0\\_B\\_0aRcBjKQh.qB1V5q4VQcCH530zQarKa-0T7p93AdfHk-pok\\_PFXkldg](https://urldefense.com/v3/_http://mc.manuscriptcentral.com/nc_/_/11R1d1M/EHOJomBn7wON0zYgVplKf61pKSH1L0_B_0aRcBjKQh.qB1V5q4VQcCH530zQarKa-0T7p93AdfHk-pok_PFXkldg) and click on the Instructions and Forms link to access the forms.
2. The Editor compiles an issue of manuscripts from several contributors and provides the Taylor and Francis Production Editor with the issue.
3. The Production Editor reviews the files. If your manuscript is not prepared correctly (see the Instructions for Authors link at [http://www.tandfonline.com/action/authorSubmissions?journalCode=nncc20&page=instructions\\_/\\_/11R1d1M/EHOJomBn7wON0zYgVplKf61pKSH1L0\\_B\\_0aRcBjKQh.qB1V5q4VQcCH530zQarKa-0T7p93AdfHk-pok\\_PFXkldg](https://urldefense.com/v3/_http://www.tandfonline.com/action/authorSubmissions?journalCode=nncc20&page=instructions_/_/11R1d1M/EHOJomBn7wON0zYgVplKf61pKSH1L0_B_0aRcBjKQh.qB1V5q4VQcCH530zQarKa-0T7p93AdfHk-pok_PFXkldg)), the Production Editor notifies the Editor so you can revise it. (Production on the issue is suspended until all manuscripts are ready.)
4. When all manuscripts are ready, the Production Editor oversees copyediting and typesetting of the issue and sends via e-mail to each contributor the PDF files of (a) the page proofs of the respective article, (b) a list of queries concerning the article, and (c) a reprint request form.
5. You proofread the typeset article, record any changes, and return to the Production Editor your responses to the queries, any other corrections, and the reprint request form (with payment if ordering reprints).
6. The Production Editor finalizes the issue and sends it to the printer.

We are pleased that you have considered Nutrition and Cancer for the publication of your work. If you have any questions, please contact the Managing Editor, Mildred Adano, at [HNUC-peerreview@journals.tandf.co.uk](mailto:HNUC-peerreview@journals.tandf.co.uk).

On behalf of the Editors of Nutrition and Cancer, we look forward to your continued contributions to the Journal.

Sincerely,

David C. Montrose, Ph.D.  
Editor-in-Chief, Nutrition and Cancer  
[davidmontrose@stonybrookmedicine.edu](mailto:davidmontrose@stonybrookmedicine.edu)

Reviewer(s) Comments to Author:

Have you considered open access?

When you complete your Author Publishing Agreement you will be asked whether you wish to publish your article open access via our Open Select publishing program. Open access offers greater accessibility, visibility and impact for your research. Articles published open access with Taylor & Francis Open Select typically receive 58% more citations\* and 6 times as many downloads\*\* compared to those that are not published open access.

If you select the option to make your article open access you will receive an invoice for the article publishing charge (APC). Some funders mandate open access publishing, and your research funder or institution may be able to cover the cost of the APC.

Visit our Author Services website at [https://urldefense.com/v3/\\_https://authorservices.taylorandfrancis.com/publishing-open-access/utm\\_source=broadcast&utm\\_medium=email&utm\\_campaign=REG29543\\_/\\_/11R1d1M/EHOJomBn7wON0zYgVplKf61pKSH1L0\\_B\\_0aRcBjKQh.qB1V5q4VQcCH530zQarKa-0T7p93AdfHk-pok\\_PFXkldg](https://urldefense.com/v3/_https://authorservices.taylorandfrancis.com/publishing-open-access/utm_source=broadcast&utm_medium=email&utm_campaign=REG29543_/_/11R1d1M/EHOJomBn7wON0zYgVplKf61pKSH1L0_B_0aRcBjKQh.qB1V5q4VQcCH530zQarKa-0T7p93AdfHk-pok_PFXkldg) to find out more about open access policies and to view the APC for this journal. Please also read our guide to sharing different versions of your article available at [https://urldefense.com/v3/\\_https://authorservices.taylorandfrancis.com/research-impact/sharing-versions-of-journal-articles\\_/\\_/11R1d1M/EHOJomBn7wON0zYgVplKf61pKSH1L0\\_B\\_0aRcBjKQh.qB1V5q4VQcCH530zQarKa-0T7p93AdfHk-pok\\_PFXkldg](https://urldefense.com/v3/_https://authorservices.taylorandfrancis.com/research-impact/sharing-versions-of-journal-articles_/_/11R1d1M/EHOJomBn7wON0zYgVplKf61pKSH1L0_B_0aRcBjKQh.qB1V5q4VQcCH530zQarKa-0T7p93AdfHk-pok_PFXkldg). Note that an embargo period usually applies if you want to deposit your Accepted Manuscript (the version of your article that's been accepted for publication) in a repository. We recommend that you keep a copy of your Accepted Manuscript for this purpose.

\* Citations received up to 10th June 2022 for articles published in 2017-2021. Data obtained from Digital Science's Dimensions platform.

\*\* Usage in 2018-2021 for articles published in 2017-2021.

**Figure F: Manuscript confirmation of acceptance email from the Journal of Nutrition and Cancer.**